European Journal of Medicinal Chemistry 218 (2021) 113397

Contents lists available at ScienceDirect

European Journal of Medicinal Chemistry

journal homepage: http://www.elsevier.com/locate/ejmech

Discovery of multifunctional anti-Alzheimer's agents with a unique mechanism of action including inhibition of the enzyme butyrylcholinesterase and γ-aminobutyric acid transporters

Anna Pasieka [a, 1], Dawid Panek [a, 1], Jakub Jończyk [a], Justyna Godyń [a], Natalia Szałaj [a], Gniewomir Latacz [b], Julia Tabor [a], Eva Mezeiova [c], Fabien Chantegreil [d], José Dias [d], Damijan Knez [e], Junfeng Lu [f], Rongbiao Pi [f], Jan Korabecny [c], Xavier Brazzolotto [d], Stanislav Gobec [e], Georg Höfner [g], Klaus Wanner [g], Anna Więckowska [a], Barbara Malawska [a, *]

[a] Department of Physicochemical Drug Analysis, Faculty of Pharmacy, Jagiellonian University Medical College, Medyczna 9, 30-688, Kraków, Poland
[b] Department of Technology and Biotechnology of Drugs, Faculty of Pharmacy, Jagiellonian University Medical College, Medyczna 9, 30-688, Kraków, Poland
[c] Biomedical Research Centre, University Hospital Hradec Kralove, Sokolska 581, 500 05, Hradec Kralove, Czech Republic
[d] Département de Toxicologie et Risques Chimiques, Institut de Recherche Biomédicale des Armées, 91223, Brétigny sur Orge, France
[e] Faculty of Pharmacy, University of Ljubljana, Askerceva 7, 1000, Ljubljana, Slovenia
[f] Department of Pharmacology & Toxicology, School of Pharmaceutical Sciences, Sun Yat-Sen University, Guangzhou, 510006, China
[g] Department of Pharmacy - Center for Drug Research, Ludwig-Maximilians-Universität München, Butenandtstr, 5-13, 81377, Munich, Germany

ARTICLE INFO

Article history:
Received 26 February 2021
Received in revised form
17 March 2021
Accepted 18 March 2021
Available online 31 March 2021

Keywords:
Alzheimer's disease
Multifunctional ligands
Inhibitors
Butyrylcholinesterase
BACE1
GABA transporters
Aβ aggregation

ABSTRACT

Looking for an effective anti-Alzheimer's agent is very challenging; however, a multifunctional ligand strategy may be a promising solution for the treatment of this complex disease. We herein present the design, synthesis and biological evaluation of novel hydroxyethylamine derivatives displaying unique, multiple properties that have not been previously reported. The original mechanism of action combines inhibitory activity against disease-modifying targets: β-secretase enzyme (BACE1) and amyloid β (Aβ) aggregation, along with an effect on targets associated with symptom relief - inhibition of butyrylcholinesterase (BuChE) and γ-aminobutyric acid transporters (GATs). Among the obtained molecules, compound **36** exhibited the most balanced and broad activity profile (*ee*AChE IC_{50} = 2.86 μM; *eq*BuChE IC_{50} = 60 nM; *h*BuChE IC_{50} = 20 nM; *h*BACE1 IC_{50} = 5.9 μM; inhibition of Aβ aggregation = 57.9% at 10 μM; *m*GAT1 IC_{50} = 10.96 μM; and *m*GAT2 IC_{50} = 19.05 μM). Moreover, we also identified **31** as the most potent *m*GAT4 and *h*GAT3 inhibitor (IC_{50} = 5.01 μM and IC_{50} = 2.95 μM, respectively), with high selectivity over other subtypes. Compounds **36** and **31** represent new anti-Alzheimer agents that can ameliorate cognitive decline and modify the progress of disease.

© 2021 Elsevier Masson SAS. All rights reserved.

1. Introduction

The discovery of new drug for Alzheimer's disease (AD) is one of the biggest challenges in modern medicinal chemistry. Although we have broadened the knowledge about its etiopathogenesis since AD was first described, effective pharmacotherapy still does not exist. Current treatments include only four symptomatic drugs (donepezil, galantamine, rivastigmine and memantine) and one fixed-dose combination of donepezil and memantine, which was approved in 2014 [1–3]. Marketed drugs are indicated for mild to severe Alzheimer's dementia, but they alleviate cognitive and behavioral symptoms for only a limited period of time (typically a few months after the start of treatment) [1]. Moreover, when reading the news about clinical trials for AD, only one word comes to mind: "failure" [4–6]. However, a series of setbacks have not discouraged pharmaceutical companies or academic units from pursuing the goal of a new, innovative therapy for AD. This is not unusual, considering how great the need is, especially when we reflect on the facts and figures that describe this disease:

* Corresponding author.
E-mail address: mfmalaws@cyf-kr.edu.pl (B. Malawska).
[1] These authors contributed equally to this work.

https://doi.org/10.1016/j.ejmech.2021.113397
0223-5234/© 2021 Elsevier Masson SAS. All rights reserved.

approximately 50 million cases of dementia currently (including 60–70% with AD), predictions of tripling that number by 2050, aging societies, extremely unpleasant symptoms that rob patients of their dignity, and finally, the awareness that this disease can affect anyone of us [7,8].

AD has a very complex pathogenesis with two main primary pathological hallmarks: neurofibrillary tangles (NFTs) and amyloid beta (Aβ) plagues that are results of misfolding, aggregation and accumulation of certain proteins, namely tau and amyloid beta. The accumulation of these plagues and tangles lead to neuronal damage, major synaptic changes, progressive neurodegeneration, neuronal death, and finally to dementia [9–13]. Dementia is mainly related to impaired cholinergic neurotransmission and thus, anti-AD drugs work as inhibitors of acetylcholinesterase (AChE) and/or butyrylcholinesterase (BuChE) - enzymes that hydrolyze acetylcholine (ACh) in neuron synapses [14,15]. It is worth noting that in the healthy brain, AChE hydrolyzes the main pool of acetylcholine with BuChE playing an additional role, but during the progression of AD, BuChE takes over the role of AChE and is responsible for almost 80% of the cholinesterase activity. This indicates that BuChE should be more desirable biological target aiming at cholinergic neurotransmission in the search for palliative therapies [16–18].

AD is associated not only with dementia and memory impairment related to cholinergic neurotransmission but also with clinical symptoms, including depression, hallucinations, speech disorders, motor disabilities, and aggressive behavior [19–21] related to impairment of serotoninergic, excitatory amino acid, or γ-aminobutyric acid (GABA) neurotransmission [22–24]. Although the role of the GABAergic system in AD was recognized earlier, from the observation that GABA neurotransmission is progressively reduced in AD, the results of recent studies have produced large amounts of new and interesting data [25–28]. GABAergic system regulate excitatory neurons in brain through GABA release and is involved in the processes of learning and memory. GABA transporters (GATs) play an important role in the regulation of GABAergic activity in different brain regions, and changes in their expression can potentially disrupt the excitatory/inhibitory balance, contributing to the pathogenesis of AD. It seems particularly valuable to show GATs as important molecular targets in the search for new anti-AD agents [29–31]. Until now four GATs have been identified and designated *h*GAT1, *h*BGT1, *h*GAT2, and *h*GAT3 (corresponding to *m*GAT1, *m*GAT2, *m*GAT3, and *m*GAT4 in mice) [32,33]. Individual types of transporters differ in their structure and occurrence, and their roles in the CNS have not yet been fully understood [34,35]. Both GAT1 and GAT3 subtypes are highly expressed in the CNS in different regions of the brain [36–38], in contrast to GAT2 and BGT1. It has been found *h*GAT3/*m*GAT4 transporter, known as the astrocyte-specific GABA transporter is significantly increased in both human and mouse AD brains [39]. Studies in a transgenic mouse model for AD (5xFAD) and in brain samples from human AD patients showed the GAT-4 inhibitor SNAP-5114 significantly attenuated tonic GABA currents and reversed the long-term potentiation impairment and rescued memory deficits [39]. Moreover, altered expression of GATs in the human AD brain and the complexity of the changes in their functions over the course of the disease have been shown and thus, targeting GABA transporters may be a promising solution in AD treatment [40,41]. GABA transporters inhibitors belong to different classes of chemical compounds, however, non-amino acid derivatives contain common structural elements (Fig. 1) [31].

Tau tangles, Aβ plaques and their production have also become an attractive biological processes for the development of new anti-AD drugs [45–47]. The focus is placed on reducing these hallmarks formation, aggregation or inducing their clearance. Regarding the Aβ, its most aggregable $Aβ_{1-40}$ and $Aβ_{1-42}$ fragments are produced by subsequent cutting of an amyloid precursor protein (APP) by enzymes β-secretase (BACE1) and γ-secretase [48–50]. Since their crucial roles in the etiopathogenesis of AD were discovered, BACE1 and γ-secretase have become targets of numerous research projects aiming to develop inhibitors or modulators [51,52]. Some of these compounds have entered clinical trials and were tested in patients at early and mild to moderate stages of AD with fully developed Aβ pathology [53–55]. However, due to the complexity of AD, it is important to focus not only on disease-modifying targets and to search for new drugs that alleviate dementia and the accompanying behavioral and psychological symptoms of dementia as well.

Taking into consideration the multifactorial nature of the disease, a combination therapy, especially a multitarget strategy, can be a great perspective [56,57]. The multitarget-directed ligand (MTDL) approach has been developed as an answer to the inefficiency of selective compounds in complex diseases such cancers, infections, and cardiovascular diseases [58,59]. Currently, multifunctional agents have also been successful in the field of CNS diseases, e.g., in the treatment of Parkinson's disease (rasagiline, safinamide) and schizophrenia (aripiprazole, brexpiprazole), and more are launched onto the market [60]. These successes give us hope that the synergic effects resulting from complex action might be a great solution to the problems of inefficient AD therapy as well. This strategy indeed allows not only addressing more than one target but also combining disease-modifying and symptomatic components in one molecule [61]. This approach has resulted in the discovery of many multifunctional molecules, the most numerous of which is the combination of cholinesterase inhibitors with other biological targets [62–66]. The most valuable are examples those that combine the pharmacophores responsible for the aggregation of the neurotoxic Aβ protein or the tau protein with other targets [67–70]. It should be emphasized that the design and discovery of a promising multitarget agent with balanced activity and drug-like properties pose a challenge [71,72]. However, considering the potential benefits (multifactorial profile of activities, better patient compliance, lower risk of drug-drug interactions, efficacy, safety), we should continue our efforts to achieve this goal.

The work presented describes the search for new multifunctional compounds targeting both the causes and symptoms of neurodegenerative processes in AD (Fig. 2). To address main causes of the disease, we decided to target protein misfolding by BACE1 enzyme inhibition and Aβ and tau aggregation inhibition. Due to the complexity of the symptoms of AD we focused on the biological targets that alleviate dementia symptoms (BuChE) and neuropsychiatric symptoms (GATs).

2. Results and discussion

2.1. Design

Recently, we presented a series of broad-acting multifunctional anti-AD agents targeting the cholinergic system, amyloidopathy, and tauopathy [73]. Among these hydroxyethylamine derivatives, we highlighted **compound I** as the most interesting multifunctional ligand due to its promising and well-balanced profile of activities, namely inhibition of *eq*BuChE (IC_{50} = 2.92 μM), *h*BuChE (IC_{50} = 5.74 μM), *h*BACE1 (IC_{50} = 41.60 μM), Aβ aggregation (IC_{50} = 3.09 μM) and tau aggregation (53.8% at 10 μM). In the study presented herein we have used **compound I** as a lead structure in the development of first-in-class multifunctional ligands targeting BuChE, BACE1 and GABA transporters with Aβ and tau anti-aggregation properties.

Based on the previous structure-activity relationship (SAR) analysis and molecular modeling studies we have designed a series

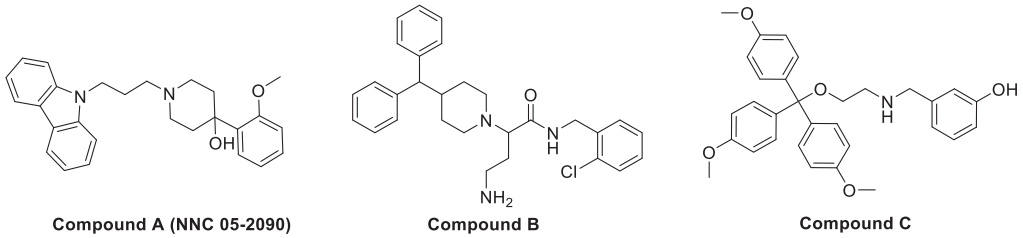

Fig. 1. The structures of selected nonamino acid GATs inhibitors [42–44].

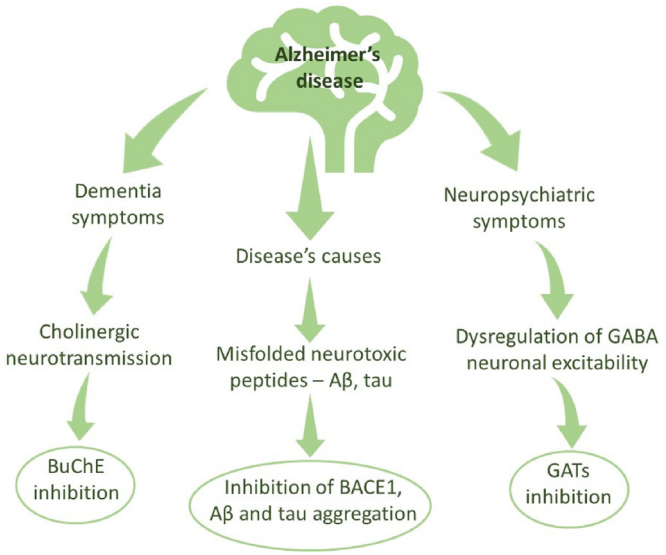

Fig. 2. A strategy for designing multifaceted drugs against AD with possible interventions in dementia symptoms, causes and neuropsychiatric manifestation of disease.

of modifications of **compound I** aiming at improving inhibitory activity of the compounds against BuChE and BACE1. Analysis of docking of **compound I** in the active sites of these enzymes revealed hydrophobic pockets that stay unoccupied by the compound, that could be excellent space for exploration (Fig. 3). Therefore, in **series I** (Fig. 3) an extra benzyl moiety was incorporated into the hydroxyalkylamine core to interact with these hydrophobic pockets. Branching in this fragment can create additional interactions with Tyr71, Phe108 and Trp115 in the S1 pocket of BACE1. This should also ensure a better position of the benzhydryl scaffold in the S2 and S3 pockets and lead to an enhancement in the inhibitory activity toward BACE1. The introduction of an aromatic substituent should improve the fit of the ligand to BuChE through the interaction of the ligand with the free hydrophobic pocket created by Trp231, Phe329 and Phe398, among others. Moreover, due to the structural similarity of the designed molecules to the structures of GABA transporter inhibitors, we decided to examine their activity toward this biological target [74–78].

Further modifications (**series II**) included the replacement of one of the amine moieties with an amide bond placed between the hydroxyethylamine core and the benzhydrylalkyl fragment (Fig. 3). This allows the reduction of one protonated group and localization of a positive charge at only the nitrogen atom of the benzylamine or a corresponding fragment and could result in stabilization of the binding mode in the active site of BuChE and BACE1.

The designed compounds from **series I** and **II** consist of three fragments (Fig. 4). For **fragment A**, we used diphenylmethyl, 2,2-diphenylethyl or 3,3-diphenylpropyl which were connected through an amine (**series I**) or amide (**series II**) group with 1-amino-4-phenylbutan-2-ol-3-yl moiety (**fragment B**). The third fragment (**fragment C**) contained different amino moieties. Due to the valuable influence of branched substituents on the anti-aggregation potency [73], we selected and introduced mainly benzylamines with branched substituents (*tert*-butyl, isopropyl, trifluoromethyl) in various positions of the phenyl ring or with branching on methylene linker with one or two methyl groups. The results of the docking studies indicated that substituents without an aromatic ring could be introduced in place of the benzylamine moiety. Therefore, for numerous derivatives, we replaced the benzylamine fragment (**fragment C**) with various nonaromatic moieties including *tert*-butyl, 2,2-dimethylpropyl, 2,2,2-trifluoroethyl, and cyclopropylmethylene.

Possessing two chiral centers, the designed compounds may take one of four possible configurations: 2*S*,3*R*, 2*S*,3*S*, 2*R*,3*R*, or 2*R*,3*S*. Considering the importance of chirality to biological activity, we decided to assess its impact. We selected and obtained isomers with the 2*S* configuration, which is preferable in numerous BACE1 inhibitors based on hydroxyetylenamine core (e.g., GRL-8234 and GSK188909) [80,81]. We confirmed in molecular modeling studies, that the binding modes of designed compounds were in line with that observed in the crystal structure of a BACE1 complex with active hydroxyetylenamine-based inhibitors [82,83]. The chiral center with a hydroxyl group (position 3) seemed to be much more interesting regarding creating crucial interactions (e.g., with the catalytic dyad), so we decided to focus our exploration here. For unsubstituted benzylamine derivatives (**fragment C**) and for the selected derivatives, we synthesized pairs of diastereoisomers (2*S*,3*R*) and (2*S*,3*S*) and evaluated their biological potencies. Due to the lack of significant differences in biological activity for other designed compounds we obtained just one pure diastereoisomer (2*S*, 3*R* or 2*S*,3*S*).

2.2. Chemistry

Following the chemical synthesis outlined in Scheme 1, we obtained 41 final compounds divided into two groups: amine derivatives (**16**–**27**) and amide derivatives (**28**–**56**). The first step was the nucleophilic substitution of the starting epoxide (2*S*, 3*S* or 2*R*,3*S*) with the appropriate amine under basic conditions (catalytic amount of pyridine). The ring-opening reaction proceeded via the stereospecific S_N2 mechanism and created only one isomer. Next, resulting aminoalcohols **1a**-**15a** were *N*-BOC deprotected to obtain the corresponding 1-substituted 1,3-diamino-4-phenylbutan-2-ol derivatives **1b-15b**. The final compounds were synthesized using one of two alternative methods for **series I** and **series II**. To obtain the amine derivatives (**16**–**27**), we utilized reductive amination of the corresponding amine and 2,2-diphenylacetaldehyde or 3,3-diphenylpropanal using sodium cyanoborohydride in the presence of acetic acid. The last step to obtain the final derivatives of

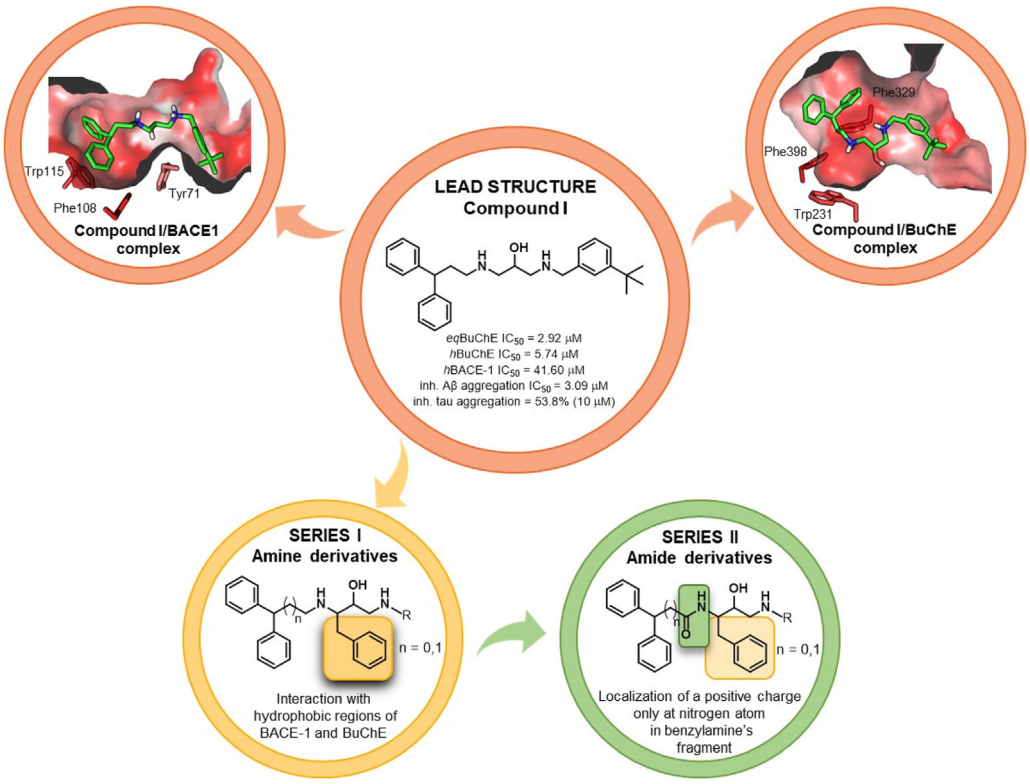

Fig. 3. Design strategy of new multifunctional anti-AD agents – BACE1 and BuChE inhibitors. Binding modes of **compound I** in the active space of BACE1 and BuChE. The aromatic amino acids included in the unoccupied hydrophobic pockets are shown as sticks. The protein surface is presented according to the Eisenberg hydrophobicity scale using a color gradient from white (least hydrophobic) to red (most hydrophobic) [79].

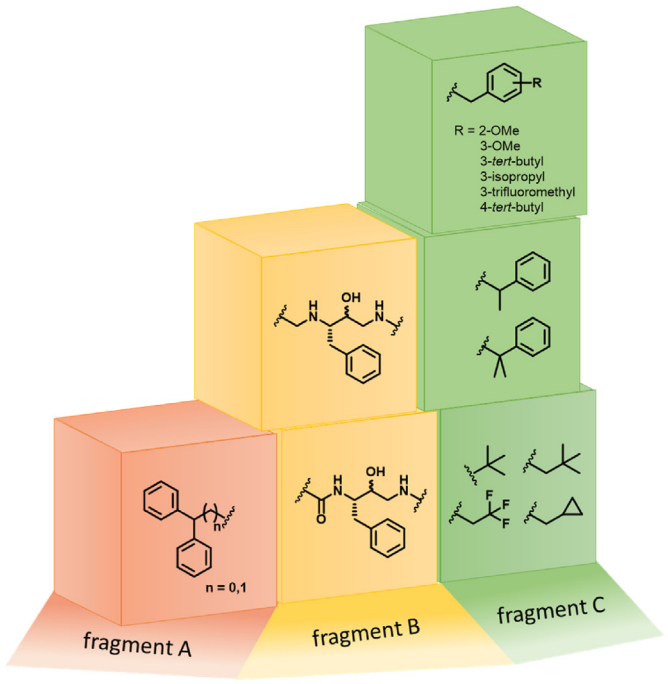

Fig. 4. General structure of the designed compounds.

series II (**28**–**56**) was amidation between the previously obtained primary amines **1b-15b** and 2,2-diphenylacetic acid or 3,3-diphenylpropanoic acid using coupling agents 1-ethyl-3-(3-dimethylaminopropyl)carbodiimide hydrochloride (EDC) or *N*,*N*′-dicyclohexylcarbodiimide (DCC) in the presence of base 4-dimethylaminopyridine (DMAP), which was used as the activator of the coupling reaction, and the addition of hydroxybenzotriazole (HOBt) prevented racemization [84]. All final products were obtained as pure diastereoisomers, which was confirmed by ^{1}H NMR (see Figs. S48 and S49).

2.3. Inhibition of eeAChE, eqBuChE and hBuChE

To evaluate the inhibitory potency of the newly developed compounds against BuChE from equine serum (*eq*BuChE) and human BuChE (*h*BuChE) as well as to check their selectivity over AChE from electric eel (*ee*AChE), we used a method established by Ellman et al. [85]. In the first step, the screening assay was performed, and we chose 10 μM for *ee*AChE and *eq*BuChE and 1 μM for *h*BuChE as the concentration of inhibitor. Then, we determined IC_{50} values for the compounds with the percentage of inhibition against *ee*AChE and *eq*BuChE above 50% and against *h*BuChE above 80%. As reference compounds, we used tacrine and donepezil. The results are presented in Tables 1 and 2.

2.3.1. Series I

Initially, we synthesized and defined the activities of the unsubstituted benzylamine (**fragment C**) compounds, (2*S*,3*R*)-**17** and (2*S*,3*S*)-**18**, which are an exemplary pair of diastereoisomers. We noticed that both derivatives were active, with similar potencies against *h*BuChE and slightly different activities in the case of *eq*BuChE. Therefore, we assumed that it is unnecessary to develop all the pairs of diastereomers; instead it allowed us to choose between either 2*S*, 3*R* or 2*S*, 3*S* derivatives.

All derivatives from **series I** displayed activity against *eq*BuChE

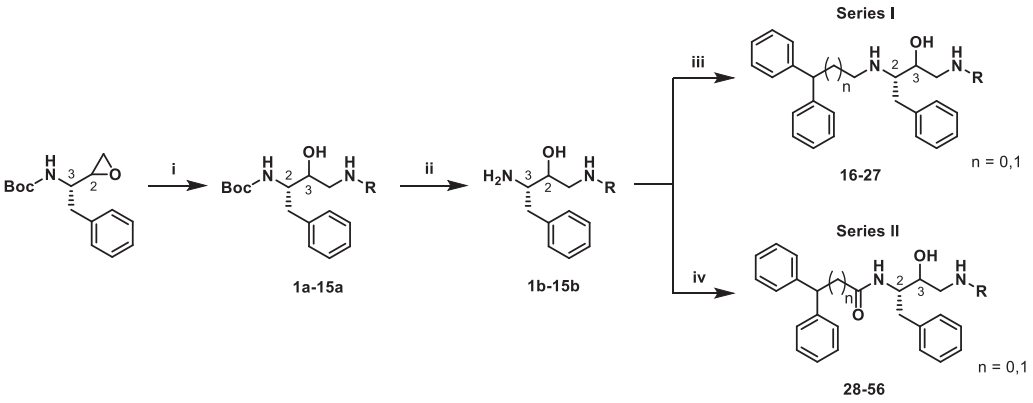

Scheme 1. Reagents and conditions: (i) appropriate amine, pyridine (cat), *n*-propanol/isopropanol, reflux, 16 h; (ii) TFA, DCM, RT, 2 h; (iii) 2,2-diphenylacetaldehyde/3,3-diphenylpropanal, acetic acid, sodium cyanoborohydride, DCM, RT, 24 h; (iv) 2-diphenylacetic acid/3,3-diphenylpropanoic acid, DMAP, HOBt, EDC/DCC, DCM, RT, 24 h.

Table 1
Inhibition of *ee*AChE, *eq*BuChE, *h*BuChE, and *h*BACE1 by compounds in **series I**.

Cmp	R	2,3	n	*ee*AChE	*eq*BuChE	*h*BuChE	*h*BACE1
				IC_{50} [μM]/% inh.[a]	IC_{50} [μM]/% inh.[b]	IC_{50} [μM]/% inh.[c]	IC_{50} [μM]/% inh.[d]
Series I	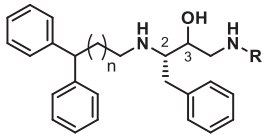						
16		*S,R*	0	<10%	0.95 ± 0.05	0.32 ± 0.02	42% ± 11
17		*S,R*	1	<10%	1.54 ± 0.06	71.7% ± 0.9	55.3% ± 3.8
18		*S,S*	1	<10%	0.65 ± 0.03	0.63 ± 0.02	58.0% ± 8.5
19		*S,S*	0	<10%	0.32 ± 0.01	0.58 ± 0.02	55.2% ± 3.8
20		*S,S*	1	<10%	1.01 ± 0.05	0.80 ± 0.04	65.5% ± 8.5
21	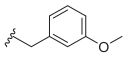	*S,R*	1	<10%	2.04 ± 0.08	55.4% ± 4.7	50.6% ± 1.7
22	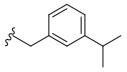	*S,R*	1	25.9% ± 6.5	1.84 ± 0.08	67.4% ± 0.9	6.6 ± 0.4
23		*S,R*	0	<10%	0.95 ± 0.02	0.92 ± 0.04	53.9% ± 7.1
24		*S,R*	1	<10%	0.98 ± 0.02	72.5% ± 0.5	62% ± 10
25		*S,R*	1	<10%	1.60 ± 0.05	53.2% ± 2.9	71.8% ± 3.7
26		*S,S*	1	<10%	0.19 ± 0.01	68.5% ± 0.8	51.3% ± 4.3
27		*S,R*	0	<10%	0.59 ± 0.03	0.19 ± 0.01	63.9% ± 8.0
References							
Compound I				21.8% ± 5.5	2.92 ± 0.10	5.74 ± 0.26	41.6 ± 1.5
Tacrine				0.023 ± 0.0004	0.015 ± 0.0001	0.034 ± 0.0004	nd
Donepezil				0.011 ± 0.0002	1.83 ± 0.04	nd	nd
Inhibitor IV[e]				Nd	nd	nd	0.046 ± 0.01

Values are expressed as the means ± the standard error of the mean (SEM) of at least three experiments (n = 3), each performed in triplicate.
[a] IC_{50} inhibitory concentration of electric eel AChE or percent inhibition at an inhibitor concentration of 10 μM.
[b] IC_{50} inhibitory concentration of BuChE from horse serum or percent inhibition at an inhibitor concentration of 10 μM.
[c] IC_{50} inhibitory concentration of human BuChE or percent inhibition at an inhibitor concentration of 1 μM.
[d] IC_{50} inhibitory concentration of human recombinant BACE1 and substrate (Rh-EVNLDAEFK-quencher) or percent inhibition at an inhibitor concentration of 50 μM.
[e] Calbiochem, Merck, Nottingham, UK. nd; not determined.

with IC_{50} values ranging from 0.19 to 2.04 μM. Since almost all of the compounds inhibited *ee*AChE below 10% at 10 μM (except **22**), they were considered to be highly selective BuChE inhibitors. Among them, we defined **26** as the most potent *eq*BuChE inhibitor with an IC_{50} value of 190 nM. Analyzing the SAR, we observed that a shorter distance between the benzhydryl moiety (**fragment A**) and

Table 2
Inhibition of *ee*AChE, *eq*BuChE, *h*BuChE, and *h*BACE1 by compounds in **series II**.

Cmp	R	2,3	n	*ee*AChE	*eq*BuChE	*h*BuChE	*h*BACE1
				IC_{50} [μM]/% inh.[a]	IC_{50} [μM]/% inh.[b]	IC_{50} [μM]/% inh.[c]	IC_{50} [μM]/% inh.[d]
Series II	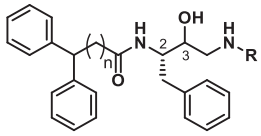						
28		*S,R*	0	<10%	1.51 ± 0.04	34.1% ± 2.2	56.2% ± 9.5
29		*S,S*	0	<10%	0.23 ± 0.01	40.5% ± 1.1	66.1% ± 4.9
30		*S,R*	1	<10%	1.38 ± 0.04	62.3% ± 1.6	35.4 ± 1.6
31		*S,S*	1	<10%	2.94 ± 0.11	67.7% ± 1.8	17.4 ± 0.7
32		*S,S*	0	<10%	0.11 ± 0.01	0.54 ± 0.01	66.2% ± 2.5
33		*S,S*	1	<10%	0.33 ± 0.01	0.35 ± 0.01	23.4 ± 0.9
34	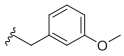	*S,R*	0	<10%	1.55 ± 0.04	56.5% ± 7.0	37.0% ± 9.8
35		*S,R*	1	<10%	1.28 ± 0.04	0.44 ± 0.01	49% ± 11
36	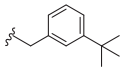	*S,R*	0	2.86 ± 0.14	0.06 ± 0.01	0.02 ± 0.0005	5.9 ± 0.2
37		*S,R*	1	<10%	0.45 ± 0.01	77.3% ± 4.1	6.0 ± 0.2
38	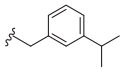	*S,R*	0	5.13 ± 0.22	0.50 ± 0.02	0.08 ± 0.002	66% ± 12
39		*S,S*	0	<10%	0.20 ± 0.01	74.9% ± 0.9	3.4 ± 0.2
40		*S,R*	1	24.0% ± 1.6	0.65 ± 0.02	0.50 ± 0.01	4.6 ± 0.2
41	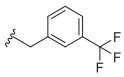	*S,S*	0	<10%	0.39 ± 0.01	0.67 ± 0.02	8.6 ± 0.3
42		*S,S*	1	36.8% ± 9.7	29.5% ± 6.4	<10%	8.3 ± 0.2
43	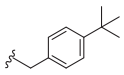	*S,S*	0	<10%	3.44 ± 0.12	0.20 ± 0.003	2.1 ± 0.1
44		*S,S*	1	<10%	0.17 ± 0.01	0.88 ± 0.03	6.2 ± 0.3
45		*S,R*	0	<10%	1.82 ± 0.06	14.5% ± 2.5	61.7% ± 4.9
46		*S,R*	1	<10%	8.86 ± 0.74	36.4% ± 2.7	74.1% ± 6.2
47		*S,R*	0	<10%	45.9% ± 3.1	<10%	76.1% ± 7.7
48		*S,R*	1	<10%	3.23 ± 0.08	13.3% ± 3.8	8.9 ± 0.5
49		*S,S*	0	<10%	0.84 ± 0.02	35.5% ± 8.5	<10%
50		*S,S*	1	<10%	11.8 ± 0.16	<10%	<10%
51		*S,R*	0	<10%	0.10 ± 0.01	0.45 ± 0.01	40.04% ± 4.1
52		*S,R*	1	<10%	2.77 ± 0.07	46.2% ± 4.4	33.6 ± 1.6
53		*S,R*	0	<10%	26.3% ± 5.8	<10%	15.4 ± 1.1
54		*S,R*	1	<10%	19.2% ± 9.9	<10%	24.4% ± 7.3
55		*S,R*	0	<10%	3.21 ± 0.07	12.3% ± 3.6	44.4% ± 6.5
56		*S,R*	1	<10%	3.23 ± 0.07	41.1% ± 3.2	<10%
References							
Compound I				21.8% ± 5.5	2.92 ± 0.10	5.74 ± 0.26	41.6 ± 1.5
Tacrine				0.023 ± 0.0004	0.015 ± 0.0001	0.034 ± 0.0004	nd
Donepezil				0.011 ± 0.0002	1.83 ± 0.04	nd	nd
Inhibitor IV[e]				nd	nd	nd	0.046 ± 0.01

Values are expressed as the means ± the standard error of the mean (SEM) of at least three experiments (n = 3), each performed in triplicate.
[a] IC_{50} inhibitory concentration of electric eel AChE or percent inhibition at an inhibitor concentration of 10 μM.
[b] IC_{50} inhibitory concentration of BuChE from horse serum or percent inhibition at an inhibitor concentration of 10 μM.
[c] IC_{50} inhibitory concentration of human BuChE or percent inhibition at an inhibitor concentration of 1 μM.
[d] IC_{50} inhibitory concentration of human recombinant BACE1 and substrate (Rh-EVNLDAEFK-quencher) or percent inhibition at an inhibitor concentration of 50 μM.
[e] Calbiochem, Merck, Nottingham, UK. nd; not determined.

amine bond slightly improved the inhibitory potency (e.g., **19** *vs* **20**). The introduction of branched, aliphatic moieties instead of the aromatic ring in **fragment C** was the most beneficial for inhibitory activity toward *eq*BuChE (e.g., **26** *vs* **18**).

While testing the inhibitory abilities against *h*BuChE, for six derivatives we established IC_{50} values ranging from 190 to 920 nM. The most active was compound **27** containing a *tert*-butylmethyl moiety in **fragment A**, for which molecular modeling studies were performed (see Supporting Information).

Compared to starting **compound I**, all compounds of **series I** exhibited higher inhibitory potencies toward *eq*BuChE and *h*BuChE. The most active compound toward *eq*BuChE (**26**) is over 15 times more active than **compound I**, while the most potent *h*BuChE inhibitor (**27**) is over 30 times more active than **compound I**. These results clearly confirmed that the introduction of a benzyl moiety into **fragment B** not only allowed retention of selectivity over AChE

but also significantly improved potency toward BuChE.

2.3.2. Series II

Similar to **series I**, the study of compounds of **series II** started with investigating the impact of chirality on biological activity. For compounds with an unsubstituted benzylamine (**fragment C**), we synthesized two pairs of diastereoisomers: (*S,R*)-**28** and (*S,S*)-**29** with a diphenylmethyl substituent and (*S,R*)-**30** and (*S,S*)-**31** with a 2,2-diphenylethyl substituent in **fragment A**. We also obtained a pair of diastereoisomers for 3-isopropyl substituted compounds in **fragment C** ((*S,R*)-**38,** (*S,S*)-**39**). As the observed activity differences did not promote any specific configuration, as previously described, we decided to synthesize compounds in the 2*S*, 3*R* or 2*S*, 3*S* configurations as pure stereoisomers.

While evaluating inhibitory activity against BuChE, most compounds were found to be moderate to potent *eq*BuChE inhibitors with established IC_{50} values ranging from 0.06 to 11.8 μM. Compounds **36** and **51** were the most potent *eq*BuChE inhibitors (IC_{50} values 60 nM and 100 nM, respectively), demonstrating IC_{50} values in the same order of magnitude as tacrine. Almost all active derivatives were revealed as selective inhibitors of *eq*BuChE. Only **36** and **38** exhibited nonselective inhibitory properties against both cholinesterases; however still preferable towards *eq*BuChE.

The SAR analysis for **series II** brought some interesting conclusions that partially coincide with the results of **series I**. Regarding the length of **fragment A**, we found that the benzhydryl directly connected to the amide bond of **fragment B** improved the *eq*BuChE inhibitory properties in most cases (e.g., **36** *vs* **37**), similar to that observed for **series I**. Second, we noticed that the most active compounds contained a benzylamine fragment in their structures (**fragment C**). Unlike in **series I**, here, the substitution of benzylamine (**fragment C**) resulted in an increase in activity in most cases. It is worth emphasizing that the introduction of a 2-methoxy, 3-*tert*-butyl or 3-isopropyl substituent significantly increased activity. In turn, the introduction of one or two methyl groups onto the methylene of the benzylamine clearly impaired anti-BuChE potency. In comparison with compounds of **series I**, the replacement of the benzylamine scaffold with various aliphatic moieties had a totally different result. Generally, such modification did not have a positive impact. However, surprisingly, **51**, which possessed a benzhydryl as **fragment A** and a 2,2-dimethylpropyl substituent as **fragment C** distinguished itself as a potent inhibitor of *eq*BuChE.

Comparing the results for **series I** and **II**, we observed that our hypothesis, that focusing all positive charges on just one nitrogen atom would produce a beneficial effect, was not completely confirmed. Just in cases of the 2-methoxybenzyl, 3-isopropylbenzyl and 2,2-dimethylpropyl derivatives, the introduction of an amide instead of an amine group resulted in an increase in *eq*BuChE inhibitory activity.

Finally, we examined the biological activities against *h*BuChE and for 10 compounds we determined IC_{50} values ranging from 20 to 880 nM. Among them, the most potent was **36**, with a 3-*tert*-butylbenzylamine in **fragment C**, which was also the most potent inhibitor of *eq*BuChE. Additionally, here, we observed the beneficial effect of benzylamine substitution in **fragment C,** especially those with bulky substituents (3- or 4-*tert*-butyl, 3-isopropyl).

2.4. Kinetic studies of eqBuChE inhibition

To determine the mode of BuChE inhibition, we performed kinetic studies of *eq*BuChE with two of the most potent compounds, **36** and **51**. The Lineweaver-Burk and Cornish-Bowden plots (see Fig. S5 and S6) showed that both derivatives were noncompetitive *eq*BuChE inhibitors. The K_m values were not affected by changing the substrate or inhibitor concentrations, whereas the V_{max} values decreased at increasing concentrations of the enzyme inhibitor.

2.5. X-ray crystallography of hBuChE in complex with 51

To examine possible interactions of the obtained compounds with the *h*BuChE, we performed docking studies. Obtained results predicted two significant binding modes for selected compounds: **27** and **51** (see Supporting Information). To answer the bothering question of what binding mode the molecule **51** adopts in the *h*BuChE active site, we decided to conduct crystallographic studies of this complex. To elucidate the binding mode of **51** with *h*BuChE, the crystal structure of this complex was solved at 2.25 Å resolution (Fig. 5). Crystals were obtained by the hanging drop method and then soaked with **51** at a final ligand concentration of 1 mM (1% MeOH). As previously observed for other BuChE inhibitors containing aromatic parts [62,86–88], π-stacking mainly rules the interactions of **51** with *h*BuChE. The *di*-phenyl-acetamide moiety (**fragment A**) engages its benzyl rings in interactions with the aromatic residues that line the active site gorge through π-π interactions. A first benzyl ring fits in the acyl-binding pocket of *h*BuChE and interacts through T-stacking with Trp231 with a centroid distance of 5.2 Å, and, to a lesser extent, with Phe398, with a centroid distance of 6.3 Å. The second benzyl ring interacts with Phe329, with a centroid distance of 4.1 Å, and, to a lesser extent, with Tyr332, with a centroid distance of 4.9 Å, also through π-stacking interactions. The carbonyl of **51** points toward the water molecule that lies in the oxyanion hole between the Oγ atom of the catalytic serine Ser198 and the backbone nitrogen atoms of Gly116 and Gly117. However, the distance between this water molecule and the carbonyl oxygen atom is longer than that of a classical H-bond at 3.5 Å. In the crystallization buffer, the amine functional group bearing the trimethyl moiety (**fragment C**) is likely charged, forming a favorable cation-π interaction with Trp82, with a distance of 4.3 Å in the *h*BuChE choline pocket. The final benzyl ring folds back over the diphenyl moiety and engages an additional π-π interaction with the benzyl ring already engaged with Trp231 and Phe398 with a centroid distance of 5.3 Å. Finally, an additional interaction exists with the hydroxyl group that bridges a water molecule already engaged with Asn83. In this position, the ligand occludes the active site gorge, thus preventing substrate access to the catalytic residues.

Binding mode B of **51** obtained during the *in silico* studies shows many similarities to that observed in this crystal. The most important are undoubtedly the interactions of the 2,2-diphenylethyl fragment with Trp231, Phe398, Phe329, and Tyr332 and the formation of the cation-π bond between the protonated amine and Trp82. The differences between the experimental and predicted *in silico* modes include the formation of T-shaped aromatic intramolecular interactions by the benzyl group and a very significant share of two water molecules that interact with the polar fragments of **51**.

2.6. Inhibition of hBACE1

The second enzyme biological target for the presented compounds is BACE1. We determined the BACE1 inhibitory properties using a FRET (fluorescence resonance energy transfer)-based fluorometric assay [73]. As a substrate for human recombinant BACE1 (*h*BACE1), we used a modified peptide analog of APP with the Swedish mutation. First, we performed the initial assay at a screening concentration of 50 μM. Then, we established IC_{50} values for compounds displaying inhibition percentages above 80% (Tables 1 and 2). We selected inhibitor IV [89] as a reference compound with its established IC_{50} value of 46 nM.

Primarily, the proposed modifications in **series I** were expected

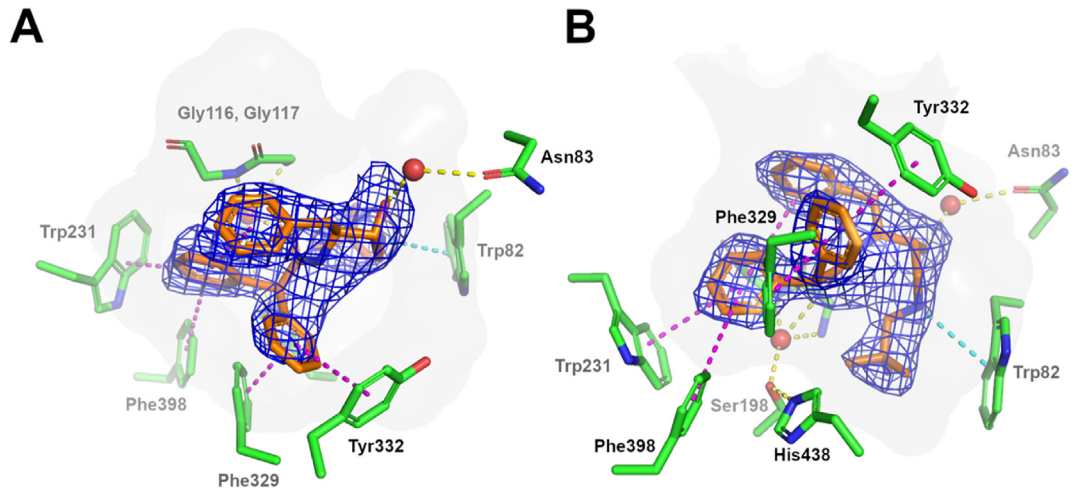

Fig. 5. Close-up view of the 2.25 Å X-ray structure of 51 bound to *h*BuChE. A, top view, B, side view. Critical residues are represented as sticks, with carbon atoms colored green for BuChE or orange for **51**, nitrogen atoms are represented in blue and oxygen atoms appear in red. Water molecules are represented as a red sphere. The gray shape represents the active site gorge, and the blue mesh represents the 3σ-contoured omit map of **51**. Dashed lines represent key interactions, π-interactions are in magenta, H-bonds are in yellow and cation-π interactions are in cyan.

to essentially improve the inhibitory potency against BACE1. Among the tested compounds, the most active was **22**, bearing a 3-isopropylbenzylamine moiety in **fragment C**, which showed an IC_{50} value of 6.6 μM. The remaining compounds of **series I** exhibited inhibitory potencies toward BACE1 ranging from 41.6% to 71.8% at 50 μM. In the preliminary screening test of compounds of **series II**, we selected 14 compounds and established IC_{50} values ranging from 2.1 to 35.4 μM. Among them, **43**, containing a 4-*tert*-butylbenzylamine scaffold as **fragment C**, was the most potent BACE1 inhibitor.

The SAR analysis clearly showed that the introduction of an amide bond was crucial for BACE1 binding and improved the inhibitory potencies in comparison with the compounds of **series I** (e.g., **48** *vs* **25**). Regarding **fragment A**, we observed slightly higher activities for compounds with 2,2-diphenylethyl moieties than those with diphenylmethyl moieties (**40** *vs* **38**). In regard to **fragment C**, we noticed that the benzylamine scaffold substituted by *tert*-butyl, isopropyl, and trifluoromethyl moieties improved the anti-BACE1 potency compared with the unsubstituted derivatives (e.g., **39**, **43** *vs* **29**). This positive effect was not observed for the 2- and 3-methoxy substituents or extra methyl groups at the methylene of benzylamine. On the other hand, we noticed that the replacement of this fragment with an aliphatic moiety decreased the inhibitory ability with the exception of **52** and **53**. Among pairs of diastereoisomers, we did not observe any meaningful differences in the inhibitory activities. For this reason, the configuration of hydroxyl group in position 3 can be considered as not relevant for BACE-1 inhibition.

2.7. Docking studies on hBACE1 for compounds 22 and 43

The results for **series I** indicate that the highest-ranked ligand poses have the assumed binding mode in which the introduced benzyl fragment is arranged in hydrophobic pocket S1. In the example of the most active compound **22** (Fig. 6), we can see that **fragment B** forms a series of hydrogen bonds with the amino acids Asp32, Gly34, Asp221, and Gly223 that are enhanced by the ionic interaction of both protonated amines with Asp221. The extra ring participates in the aromatic CH-π interaction with Tyr71. This contributes to the strong binding of the compound in the vicinity of the catalytic dyad. However, in the case of many molecules, this

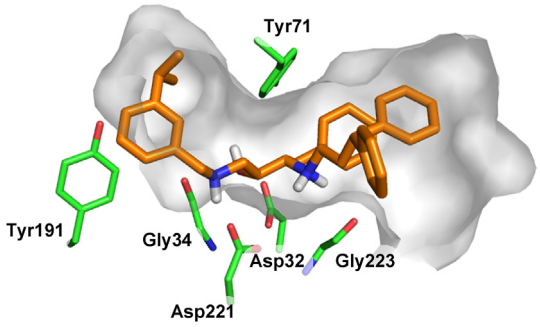

Fig. 6. The docking results of **22** (orange) in BACE1 active site visualized along with the essential amino acids (green). Gray surface represents the boundaries of the active site.

interaction is weakened due to the strong competition of both protonated amines for access to the catalytic dyad. This leads to the occurrence of competing conformations, making the modeling results nonuniform. Among the ten docking repetitions for each compound, the poses compliant with the assumed binding mode were the minority of the obtained conformations. It seems that the key to obtaining the expected results was a good fit of **fragment C** into pockets S1' and S2'. Therefore, with respect to **compound I,** we have improved activity for merely one compound (**22**), while the others, for which **fragment C** did not allow for an optimal fit to the BACE1 active site, exhibited similar or lower potencies.

The binding mode of **43** docked to the BACE1 active site is shown in Fig. 7. It clearly shows that the introduced amide forms two hydrogen bonds with Gly223 and the main chain of the flap (Gln73). Restricting the mobility of this flexible flap promotes the inhibition of enzyme activity. Moreover, limiting the positive charge to the amine in the benzylamine fragment significantly increased the reproducibility of the results for the active derivatives. This indicates a preference for compounds to adopt the expected conformation when binding to BACE1. As seen in the example of compound **43**, adjustment of **fragment C** to pockets S1' and S2' correlates with the strength of the interaction of **fragment B** with the catalytic dyad, an essential grip point for hydroxyethylamine derivatives. As seen in Fig. 7, molecule **43**, with a well-arranged benzylamine substituent, creates many significant

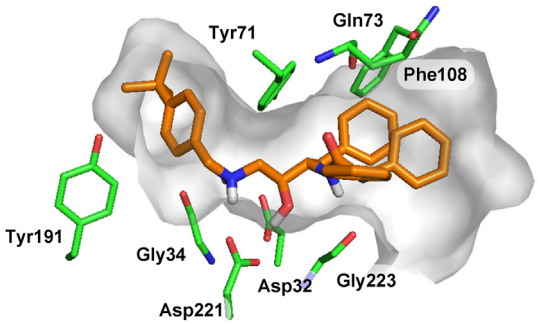

Fig. 7. The docking results of **43** (orange) in BACE1 active site visualized along with the essential amino acids (green). Gray surface represents the boundaries of the active site.

interactions (hydrogen bonds with Asp32, Gly34, Asp221, and Gly223 and an ionic interaction with Asp221) in the vicinity of the BACE1 catalytic site. In addition, its binding is amplified by contacts inside the S1 pocket (Phe108) and with the flap (Tyr71). The docking results of compound **51** with an aliphatic 2,2-dimethylpropane substituent indicate that it cannot bind within the S2' pocket. Furthermore, the nearby Tyr191 was often a steric hindrance for aliphatic variants of **fragment C**. Both effects can explain the observed decline in activity against BACE1 for this group of derivatives.

In summary, the biological evaluation confirmed our molecular modeling studies that branching in hydrophobic space and the introduction of an amide bond would improve the binding mode in the active site of BACE1. Both implemented modifications proved to be necessary to significantly enhance inhibitory activity toward BACE1.

2.8. Inhibitory properties toward GAT subtypes

As mentioned before, cholinergic transmission is impaired during the development of AD, and dysfunction of the GABAergic system is also observed. A possible way to improve this disturbance is through the inhibition of GATs [29,31]. Analyzing the structures of known GAT inhibitors drew our attention to the group of inhibitors possessing general structures and some crucial elements similar to our newly designed compounds. These are two or three aromatic rings (hydrophobic fragments) that are connected through an aliphatic linker to a polar moiety with a protonated nitrogen atom [78]. Because our compounds consist of these three fragments, we performed a biological screening of selected derivatives toward four mouse GAT subtypes (*m*GAT1 to *m*GAT4). We tested 14 compounds with variable length of the alkyl linker in **fragment A**, the substitution on **fragment C,** and the presence of amine or amide bonds. Their inhibitory activities toward the *m*GATs were determined at a screening concentration of 100 μM by [^{3}H] GABA uptake using human embryonic kidney (HEK-293) cells stably expressing mouse GABA transporters. For compounds reducing GABA uptake by at least 50%, IC_{50} values were determined. In addition, IC_{50} values were determined for the inhibition of ($^2H_6$) GABA transport by mass spectrometry (MS) transport assays using COS-7 cells stably expressing *h*GAT-3. The IC_{50} values and percentages of remaining GABA uptake are presented in Table 3.

Studying the obtained results, we noticed that amine derivatives **18** and **27** are moderately potent, nonselective GAT inhibitors, and the replacement of the amine bond by an amide bond resulted in an impairment of biological activity; however, amide derivatives improved the selectivity toward *m*GAT4 (**18** *vs* **31**, **27** *vs* **51**). Considering the influence of the length of the alkyl linker, a longer core was found to be better for potency toward *m*GAT4 without significantly affecting the other *m*GATs (**29** *vs* **31**, **34** *vs* **35**, **45** *vs* **46**, **55** *vs* **56**). Among the tested compounds, we found that unsubstituted **fragment C** derivative **31** was the most active and selective inhibitor of *m*GAT4 (*m*GAT4 $IC_{50} = 5.01$ μM; *h*GAT3 $IC_{50} = 2.95$ μM), and the introduction of a methoxy or *tert*-butyl group slightly decreased the inhibitory potency (**31** *vs* **35**, **36**). An extra methyl group in **fragment C** and replacement with aliphatic moieties also impaired this activity (**29** *vs* **45**, **51**, **53**, **55**; **31** *vs* **46**, **56**). Notably, there was a positive effect from benzylamine substitution on the inhibitory potency toward *m*GATs 1 and 2 in the case of 4-*tert*-butyl substituted compound **36**.

In summary, the obtained preliminary results seem to be very promising but require further development. At present, we have identified the potent and selective *m*GAT4 inhibitor **31** and multifunctional ligands that affect both cholinergic and GABAergic transmission and BACE1 inhibition exemplified by compound **36**. It is noteworthy that **31** is the most potent GAT3 inhibitor known to date among its selective inhibitors [31,77].

2.9. Antiaggregation properties

The processes of Aβ and tau aggregation leading to the formation of neuritic plaques and NFTs are considered the main causes of the development of AD. Since the previously published group of hydroxyethylamine derivatives, including **compound I**, displayed dual antiaggregation properties [73], we evaluated the percent amyloid aggregation inhibition for all synthetized compounds from **series I** and **II** and the inhibitory activity against tau aggregation for a few selected derivatives.

2.9.1. Inhibition of $A\beta_{1\text{-}42}$ aggregation

To determine the inhibition of Aβ aggregation, we performed a fluorometric thioflavin-T (ThT) assay *in vitro* [91] with inhibitors at a concentration of 10 μM. The results are presented in Fig. 8. Except for five compounds (**16**, **28**, **29**, **41**, **52**), the remaining compounds inhibited $A\beta_{1\text{-}42}$ aggregation above 20%. The percentages of inhibition were in the range of 34.7−81.4% and 20.5−74.4% for **series I** and **II**, respectively. Among all derivatives, nine (six from **series I**: **18**, **19**, **21**, **22**, **25**, **27**; three from **series II**: **35**, **46**, **51**) were found to inhibit Aβ aggregation at a level comparable to the well-known reference resveratrol, with the most potent compound **19** displaying an 81.4% inhibitory effect. Analyzing the obtained data, amine bonds were found to be preferable for the inhibition of amyloid aggregation. The introduction of alkyl substituents onto the benzylamine fragment did not significantly influence the level of aggregation. Between aliphatic and aromatic derivatives, no clear structure-activity relationship was observed. However, we noticed some interesting differences between the pairs of 2*S*, 3*R* and 2*S*, 3*S* isomers with 2,2-diphenylethyl moieties in **fragment A** and unsubstituted benzylamines in **fragment C** in both series. In **series I**, we found that the 2*S*, 3*S* isomer (**18**) showed approximately two times stronger inhibition than the 2*S*, 3*R* (**17**), while in **series II**, the 2*S*, 3*R* isomer (**30**) was approximately two times more potent than the 2*S*, 3*S* isomer (**31**). Moreover, analogs with shorter benzhydryl moieties (**16**, **28**, **29**) in **fragment A** in both series showed no significant activity. Remembering the protein nature of Aβ, the impact of compound chirality on antiaggregation activity should not come as a surprise; however, the observed reverse dependencies and subtle structural changes that caused considerable effects on the activity are puzzling and should be explored in future studies. Overall, we should point out that modifications implemented in the lead structure allowed us to retain antiaggregation properties at a level similar to that of **compound I.**

Table 3
Inhibition of GABA transporters by selected compounds.

Cmp	IC_{50} ± SEM [μM]				
	*m*GAT1	*m*GAT2	*m*GAT3	*m*GAT4 / *h*GAT3	*m*GAT1 binding
18	7.59 ± 0.7	5.50 ± 0.5	5.75 ± 1.2	5.50 ± 0.8	30.20
27	26.30	14.13	12.59	9.77 ± 0.7	85.11
29	34.67	34.67	52%	26.91	74%
31	61%	74%	76%	5.01 ± 1.1 2.95 ± 0.9	83%
32	87.10	25.70	69%	19.95	80%
34	61%	61%	67%	33.11	85%
35	67%	41.69	92%	5.89 ± 0.8	65%
36	10.96	19.05	55%	55%	82%
45	77%	60.26	84%	79%	81%
46	59%	51%	69%	55%	66%
51	25.12	72.44	54%	30.90	71%
53	92%	87%	92%	102%	100%
55	51%	85%	54%	74.13	74%
56	39.81	60%	51%	35.48	83%
References					
DDPM-859[a]	64.57	75.86	14.13	1.66 ± 0.1 3.16 ± 0.08	nd
DDPM-1457[a]	39.81	38.02	3.39 ± 0.2	1.35 ± 0.3 1.59 ± 0.04	46.77

Data are given as the mean ± SEM of three independent experiments that were performed in triplicate. The percent result represents the [^{3}H]GABA uptake or NO-711 binding in the presence of 100 μM inhibitor. Data without SEM implies that only one experiment was performed in triplicate. IC_{50} values are from the GABA uptake assays (means ± SEM, n ≥ 3 for values above 10 μM, n = 1 for values between 10 and 100 μM), nd; not determined.
[a] The structures are described in Ref. [90].

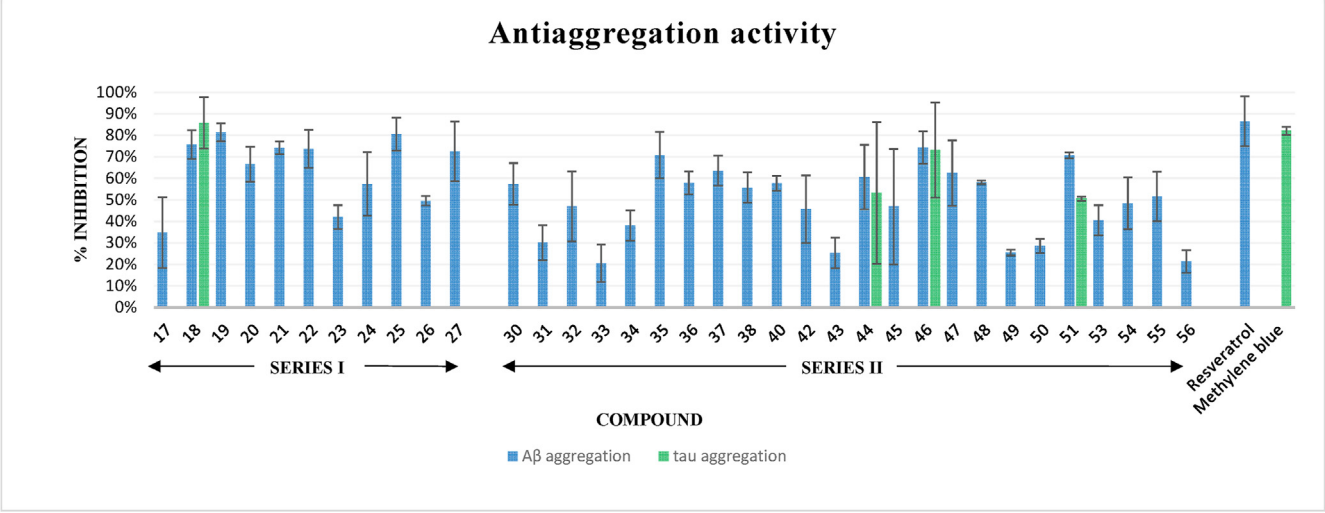

Fig. 8. Effects of the synthesized compounds on $Aβ_{1-42}$ and tau aggregation at the screening concentration 10 μM (compounds with percent inhibition below 20% are not shown, Table S2).

2.9.2. Inhibition of tau aggregation

We selected 5 derivatives (**18**, **36**, **44**, **46**, **51**) with high inhibitory activities against Aβ aggregation to evaluate their ability to inhibit tau aggregation. Therefore, a fluorometric ThT assay was performed using the full-length form of the tau protein (0N4R) at an inhibitor concentration of 10 μM. Two out of five compounds, **46** and **18**, exhibited very high levels of inhibition: 73.1% and 85.8%, respectively (Fig. 8). Nevertheless, we could not specify which fragments are important for this biological property since the most potent derivatives differed greatly in their structure.

2.10. Neurotoxicity

When looking for new anti-AD drugs, both the inhibition of biological targets in the brain and also a lack of neurotoxicity are very important features. To evaluate whether our compounds are safe, we performed an MTT assay with 5 derivatives (**18**, **36**, **44**, **46**, **51**) using murine hippocampal HT22 cells. We determined the cell viability at two different compound concentrations: 10 μM and 30 μM. Fig. 9 presents the results expressed as a percentage of cell viability compared with untreated cells.

The results suggest that the amide derivatives (**36**, **44**, **46**, **51**) were safe at a concentration of 10 μM but strongly decreased cell viability at 30 μM. The observed variability in neurotoxicity at these

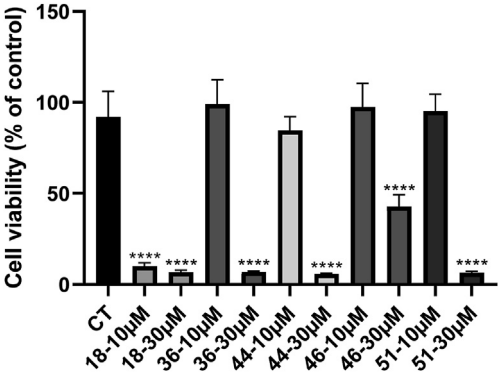

Fig. 9. Murine hippocampal HT22 cell viability by MTT assay. Statistical significance (GraphPad Prism 8.0.1) was evaluated by one-way ANOVA followed by Bonferroni's comparison test (****p < 0.0001 compared with the negative control).

two concentrations 10 μM and 30 μM was significant. Among the tested compounds, we determined that **46** was the safest, which showed 100% cell viability at 10 μM and approximately 50% viability at the higher concentration. Only compound **18** also killed cells at 10 μM, which alerted us to the possible toxicity of the amine derivatives and discouraged greater extension of this series of compounds. Generally, amide compounds can be considered nontoxic at concentrations required for biological activity, and they were the subject of interest for further ADME-tox studies. However, the demonstrated toxicity of tested compounds should be taken under consideration before the further, extended study.

2.11. Hepatotoxicity

Due to the chronic nature of AD, it should be assumed that the therapy will be long-term. It is therefore necessary to determine the toxicity, especially hepatotoxicity, at a very early stage during drug discovery. Consequently, we decided to evaluate the cell viability for three selected amide compounds (**36**, **40**, **51**). The cytotoxic effect was evaluated in *hepatoma* HepG2 cells after 72 h of incubation at four different compound concentrations: 1, 10, 50 and 100 μM. The presented results (Fig. 10) showed a strong hepatotoxic effect for all derivatives at higher concentrations (50 and 100 μM).

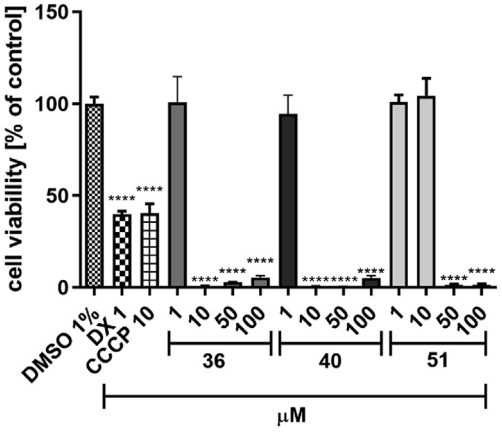

Fig. 10. The effects of the cytostatic drug doxorubicin (DX), the mitochondrial toxin carbonyl cyanide 3-chlorophenyl-hydrazone (CCCP) and **36**, **40**, **51** on *hepatoma* HepG2 cell viability after 72 h of incubation at 37 °C under 5% CO_2. Statistical significance (GraphPad Prism 8.0.1) was evaluated by one-way ANOVA followed by Bonferroni's comparison test (****p < 0.0001 compared with the negative control 1% DMSO in growth media).

However, the compounds proved to be safe at a concentration of 1 μM and aliphatic derivative **51** was safe at 10 μM as well (the concentrations needed for target inhibition). As with the neurotoxicity assessment, the observed variability in hepatotoxicity for compounds **36** and **41** at tested concentrations 1 μM and 10 μM was significant. Clearly, we observed the influence from the number of aromatic rings and the physicochemical properties of the compounds on toxicity. A reduction in the number of aromatic rings and lipophilicity significantly improved the safety, which confirmed that looking for active derivatives with aliphatic moieties in **fragment C** was a very positive step worth continuing. In conclusion, the toxicity properties require further optimization and before undertaking *in vivo* studies, it seems to be reasonable to verify the safety of these compounds using additional concentrations (intermediate concentrations, i.e. 3 μM and 5 μM).

2.12. Metabolic stability

Very often, MTDLs, because of their worse/suboptimal physicochemical properties, have been found to be not drug-like enough in comparison to single-target drugs [92]. It is therefore important to perform ADME-tox studies at an early stage of drug discovery and development to prove their safety and optimal pharmacokinetic parameters. Consequently, we decided to investigate metabolic stability – one of the most critical parameters. In this regard, we determined the structures of probable metabolites *in silico* using MetaSite 6.0.1 software for three selected derivatives with promising biological profiles: **36**, **40**, **51**. The computer predictions demonstrated that the *tert*-butyl moiety and the aliphatic carbons near the nitrogen atom in **fragment C** and at the *para* position in the benzhydryl moiety have the highest probability of metabolism (Fig. S7). Further, *in vitro* experiments with human liver microsomes (HLMs) were performed. We then obtained UPLC spectra of the reaction mixtures after 120 min of incubation. The compounds were mostly metabolically stable (Figs. S8–S13). After incubation, approximately 70% of the parent compounds remained in the mixture (**36**, 79.56%; **40**, 67.89%, and **51**, 79.17% respectively), while the unstable reference drug verapamil displayed 30% retention (Fig. S14). According to the data obtained *in vitro*, the *in silico* predictions and ion fragment analysis we identified prime amines as the most probable metabolites in all three cases (see Supporting Information, Table S3).

To conclude, the synthesized compounds can be considered metabolically stable, and indeed, the main metabolic process for this group of derivatives is *N*-dealkylation in **fragment C** observed in all cases. Additionally, *meta*-substituted compounds can undergo carboxylation or hydroxylation reactions.

2.13. Drug-drug interactions –influence on CYP3A4 and CYP2D6 activity

Elderly patients suffering from AD very often have comorbidities, and they need to take many drugs. This leads to the risk of dangerous drug-drug interactions (DDIs). Most xenobiotics, including drugs, are metabolized by cytochrome P450s, with CYP3A4 and CYP2D6 being the most commonly involved. Influence on these isoforms (induction or inhibition) may suggest potential undesired interactions, and thus, it is important to evaluate whether drug candidates affect cytochromes as early as possible during development. Therefore, we selected 3 derivatives (**36**, **40** and **51**) to examine their influence on CYP3A4 and CYP2D6 activity compared to reference inhibitors (ketoconazole and quinidine). The results are presented on Figs. 11 and 12. All compounds, regardless of whether they contained an aromatic or aliphatic moiety in **fragment C**, inhibited both isoforms at a level comparable to the

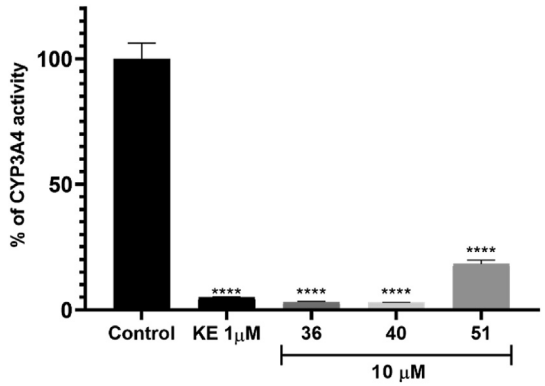

Fig. 11. The influence of **36**, **40**, **51** (10 μM) and the reference inhibitor ketoconazole (KE) on CYP3A4 activity. Statistical significance (****p < 0.0001) was analyzed by GraphPad Prism 8.0.1 software using one-way ANOVA and Bonferroni's multiple comparison posttest. The compounds were examined in triplicate.

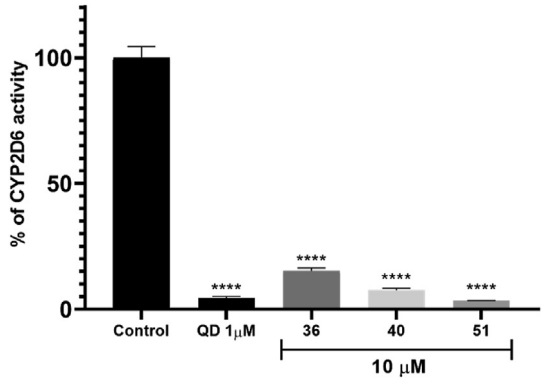

Fig. 12. The influence of **36**, **40**, **51** (10 μM) and the reference inhibitor quinidine (QD) on CYP2D6 activity. Statistical significance (****p < 0.0001) was analyzed by GraphPad Prism 8.0.1 software using one-way ANOVA and Bonferroni's multiple comparison posttest. The compounds were examined in triplicate.

reference compounds at a concentration of 10 μM, and therefore, they showed a high risk of DDIs. Further development of this group of compounds requires the improvement of this property.

3. Conclusions

Multiple factors that influence the development of AD as well as the initiation of changes in the brain many years before the onset of disease symptoms are potential causes of a lack of effective therapy and difficulties in planning and conducting appropriate preclinical and clinical trials. The MTDL strategy applied in this research could be a chance for the discovery of a new medicine and a proper approach to treat this complex disease. With the support of molecular modeling methods, we have implemented rational modifications of the lead structure **compound I** that resulted in a significant improvement in the biological activity of new multidirectional molecules. It should be highlighted that as a result of this work, we obtained two series of hydroxyethylamine derivatives, including interesting compounds with a balanced activity profile affecting both symptoms and causes of AD and molecules with a potent inhibitory effect toward just one target.

Regarding the enzyme BuChE, structural changes in both series greatly ameliorated the level of inhibition. Among amine derivatives**,** the most potent *h*BuChE inhibitor **27** was over 30 times more active (*h*BuChE $IC_{50} = 190$ nM) than **compound I**, whereas in **series II**, inhibitor **36** was the most potent (*h*BuChE $IC_{50} = 20$ nM), showing an IC_{50} that was on the same order of magnitude as the reference tacrine, with some potency against AChE (*ee*AChE $IC_{50} = 2.86$ μM). The obtained crystal structure of the *h*BuChE complex with compound **51**, which is also a strong enzyme inhibitor (*h*BuChE $IC_{50} = 450$ nM), revealed its binding mode to the enzyme and allowed comparison with the analysis of the interactions using the molecular docking method. It should also be noted that for some new derivatives, *h*BACE1 enzyme inhibitory activity significantly increased compared to the lead structure, with the most active compound being **43** (*h*BACE1 $IC_{50} = 2.1$ μM). Moreover, the antiaggregation properties for Aβ and tau protein were retained and remained at a similar level of activity to that displayed by **compound I**.

The crucial achievement of the conducted research is the demonstration of the inhibitory effects of this group of multifunctional compounds on GABA transporters, which led us to discover molecules with unique properties. While the role of the GABAergic system in AD has been shown in various studies, recent data and the proposed GABAergic hypothesis of AD indicate its possibly greater contribution with therapeutic potential from molecules influencing this system. In our study, GAT inhibitory activity was shown for the first time for multifunctional anti-AD agents. To the best of our knowledge, among them, we identified compound **31** as the most potent GAT3 inhibitor (*m*GAT4 $IC_{50} = 5.01$ μM; *h*GAT3 $IC_{50} = 2.95$ μM), with high selectivity against other subtypes.

From the point of view of the strategy of searching for a multifunctional compound against AD, compound **36** is the most interesting and valuable. It exhibits the following activities against the tested molecular targets: *ee*AChE $IC_{50} = 2.86$ μM; *eq*BuChE $IC_{50} = 60$ nM; *h*BuChE $IC_{50} = 20$ nM; *h*BACE1 $IC_{50} = 5.9$ μM; Aβ antiaggregation = 57.9% (at 10 μM); *m*GAT1 $IC_{50} = 10.96$ μM and *m*GAT2 $IC_{50} = 19.05$ μM. It is worth noting that a compound that displays such a broad and complex mechanism of action including the modulation of GATs, potentially affecting the causes and alleviating the symptoms of AD was not so far reported among multitarget agents. The influence on cholinergic and GABAergic transmission and the pathological amyloid pathway make this molecule unique and original. Furthermore, the preliminary results from the *in vitro* preclinical studies of the selected active compounds that determined their potential toxicity, hepatotoxicity, metabolic stability, and drug-drug interactions, are a good indication and a promising starting point for further development of this group of compounds and extended studies *in vivo*.

4. Experimental section

4.1. Chemistry

4.1.1. General methods

All of the reagents were purchased from commercial suppliers and were used without further purification. Tetrahydrofuran (THF) and dichloromethane (DCM) were distilled under nitrogen immediately before use. The drying agent used for THF was sodium/benzophenone ketyl, and for DCM, calcium hydride. Reactions were monitored by thin-layer chromatography carried out on aluminium sheets precoated with silica gel 60 F_{254} (Merck). For the TLC and flash chromatography following solvents were used: dichloromethane (DCM), methanol (MeOH), diethyl ether (Et_2O), chloroform ($CHCl_3$), ethyl acetate (EtOAc), petroleum ether (PET), 25% ammonia–water solution, acetonitrile (CH_3CN). Flash chromatography was performed on Isolera™ Spectra (Biotage) using Merck silica gel 60 (63–200 μm) as a stationary phase. The reverse-phase HPLC purification was performed on LC-4000 Jasco using a Phenomenex Luna C8 (5 μm, 15 × 21.2 mm) column and CH_3CN/H_2O

gradient with 0.1% HCOOH as a mobile phase. The purity of the final compounds was determined using an analytical RPLC-MS on Waters Acquity TQD using an Aquity UPLC BEH C18 column (1.7 μm, 2.1 × 100 mm) at 214 and 254 nm CH_3CN/H_2O gradient with 0.1% HCOOH was used as the mobile phase at a flow rate of 0.3 mL/min. All the compounds showed purity above 95%. ^{1}H NMR and ^{13}C NMR spectra were recorded on Varian Mercury 300 MHz or Jeol 500 MHz. The chemical shifts are reported in ppm and were referenced to residual solvent signals (^{1}H, $CDCl_3$ at 7.26 ppm, DMSO-d_6 at 2.50 ppm; ^{13}C, $CDCl_3$ at 77.2 ppm). Signal multiplicities are represented by the following abbreviations: s (singlet), br. s (broad singlet), br. d (broad doublet), d (doublet), dd (doublet of doublets), ddd (doublet of doublet of doublets), dt (doublet of triplets), t (triplet), td (triplet of doublets), tdd (triplet of doublet of doublets), q (quartet), dq (doublet of quartets), qd (quartet of doublets), and m (multiplet). Mass spectra (MS) were recorded on UPLC-MS/MS system consisting of a Waters ACQUITY UPLC (Waters Corporation, Milford, MA, USA) coupled to a Waters TQD mass spectrometer (electrospray ionization mode ESI-tandem quadrupole).

4.1.2. Procedure for the synthesis of compounds 1a-15a (procedure A)

Tert-butyl ((*S*)-1-((*S*)-oxiran-2-yl)-2-phenylethyl)carbamate or *tert*-butyl ((*S*)-1-((*R*)-oxiran-2-yl)-2-phenylethyl)carbamate (1.0 equiv.), corresponding amine (1, 1.1 or 2 equiv.), and a catalytic amount of pyridine in *n*-propanol, isopropanol or ethanol were refluxed for 16 h. Then, the solvent was evaporated and the resulting residue was purified by flash column chromatography using a mixture of DCM and MeOH (gradient or isocratic purification).

4.1.3. Procedure for the synthesis of compounds 1b–15b (procedure B)

To the solution of appropriate BOC-protected compound (1.0 equiv.) in DCM, TFA (5 mL/1 mmol substrate) was added dropwise. The reaction mixture was stirred at room temperature for 2 h. When the reaction was finished, the solvent and TFA were evaporated under reduced pressure, producing a residue that was then dissolved in ammonia water solution and extracted with DCM. The organic extracts were combined, dried over anhydrous Na_2SO_4, filtered and concentrated under vacuum.

Detailed procedures for the synthesis of intermediates 1a-15a and 1b–15b are described in Supporting Information

4.1.4. Procedure for the synthesis of compounds 16–27 (procedure C)

To the solution of 1-substituted 1,3-diamino-4-phenylbutan-2-ol derivative (1.0 equiv.) in anhydrous DCM (10 mL/1 mmol substrate) 2,2-diphenylacetaldehyde or 3,3-diphenylpropanal (0.8–1.0 equiv.) and acetic acid (1–1.5 equiv.) were added. The reaction mixture was stirred at room temperature for 0.5 h and then sodium cyanoborohydride (1.8–2.5 equiv.) was added portionwise. When the reaction was finished, the reaction mixture was washed with water. The organic phase was then dried over anhydrous Na_2SO_4, filtered and concentrated under vacuum. The crude product was purified by flash column chromatography using a mixture of DCM and MeOH or by HPLC preparative system using an acetonitrile and water mixture.

4.1.4.1. (2R,3S)-1-(benzylamino)-3-((2,2-diphenylethyl)amino)-4-phenylbutan-2-ol (16). The reaction of (2*R*,3*S*)-3-amino-1-(benzylamino)-4-phenylbutan-2-ol (**1b**) (0.200 g, 0.74 mmol) with 2,2-diphenylacetaldehyde (0.145 g, 0.74 mmol) in the presence of acetic acid (0.067 g, 1.11 mmol) and sodium cyanoborohydride (0.093 g, 1.48 mmol) in DCM (5 mL) was performed according to the **procedure C**. Purification: washing reaction mixture with water (3 × 30 mL), flash column chromatography (DCM/MeOH/$NH_{3(aq)}$, 9.5/0.5/0.05 *v/v/v*). Yield: 0.095 g (28.5%), TLC (DCM/MeOH/$NH_{3(aq)}$, 9.5/0.5/0.05 *v/v/v*) R_f = 0.33, MW 450.63, formula: $C_{31}H_{34}N_2O$, MS *m/z* 451.3 ($M + H^+$), ^{1}H NMR (300 MHz, $CDCl_3$) δ ppm 6.97–7.49 (m, 20H), 3.97 (t, J = 7.62 Hz, 1H), 3.69–3.85 (m, 3H), 3.19 (dd, J = 11.72, 6.45 Hz, 1H), 3.08 (dd, J = 11.72, 8.21 Hz, 1H), 2.91 (dt, J = 9.23, 4.47 Hz, 1H), 2.65–2.82 (m, 3H), 2.53 (dd, J = 14.07, 9.38 Hz, 1H), 2.16 (br. s, 3H); ^{13}C NMR (75 MHz, $CDCl_3$) δ ppm 142.9, 142.2, 139.6, 138.4, 128.6, 128.5, 128.5, 128.3, 128.3, 127.9, 127.8, 127.1, 126.5, 126.4, 126.3, 69.6, 62.3, 53.8, 52.7, 51.5, 50.9, 35.6.

4.1.4.2. (2R,3S)-1-(benzylamino)-3-((3,3-diphenylpropyl)amino)-4-phenylbutan-2-ol (17). The reaction of (2*R*,3*S*)-3-amino-1-(benzylamino)-4-phenylbutan-2-ol (**1b**) (0.200 g, 0.74 mmol) with 3,3-diphenylpropanal (0.156 g, 0.74 mmol) in the presence of acetic acid (0.067 g, 1.11 mmol) and sodium cyanoborohydride (0.093 g, 1.48 mmol) in DCM (5 mL) was performed according to the **procedure C**. Purification: washing reaction mixture with water (3 × 30 mL), flash column chromatography (DCM/MeOH/$NH_{3(aq)}$, 9.5/0.5/0.05 *v/v/v*). Yield: 0.061 g (17.7%), TLC (DCM/MeOH/$NH_{3(aq)}$, 9.5/0.5/0.05 *v/v/v*) R_f = 0.26, MW 464.65, formula: $C_{32}H_{36}N_2O$, MS *m/z* 465.4 ($M + H^+$), ^{1}H NMR (300 MHz, $CDCl_3$) δ ppm 7.05–7.36 (m, 20H), 3.70–3.96 (m, 3H), 3.65 (dt, J = 7.03, 4.10 Hz, 1H), 2.37–2.84 (m, 8H), 1.75–2.33 (m, 4H), ^{13}C NMR (75 MHz, $CDCl_3$) δ ppm 144.2, 137.9, 129.2, 129.1, 128.8, 128.8, 128.7, 128.7, 128.5, 128.0, 127.7, 126.6, 126.5, 126.3, 68.5, 62.2, 53.0, 50.3, 48.5, 45.8, 35.3, 35.2.

4.1.4.3. (2S,3S)-1-(benzylamino)-3-((3,3-diphenylpropyl)amino)-4-phenylbutan-2-ol (18). The reaction of (2*S*,3*S*)-3-amino-1-(benzylamino)-4-phenylbutan-2-ol (**2b**) (0.150 g, 0.55 mmol) with 3,3-diphenylpropanal (0.117 g, 0.55 mmol) in the presence of acetic acid (0.050 g, 0.83 mmol) and sodium cyanoborohydride (0.070 g, 1.11 mmol) in DCM (4 mL) was performed according to the **procedure C**. Purification: washing reaction mixture with water (3 × 30 mL), flash column chromatography (DCM/MeOH/$NH_{3(aq)}$, 9.5/0.5/0.05 *v/v/v*). Yield: 0.053 g (20.4%), TLC (DCM/MeOH/$NH_{3(aq)}$, 9.5/0.5/0.05 *v/v/v*) R_f = 0.24, MW 464.65, formula: $C_{32}H_{36}N_2O$, MS *m/z* 465.4 ($M + H^+$), ^{1}H NMR (300 MHz, $CDCl_3$) δ ppm 7.14–7.35 (m, 18H), 7.06–7.13 (m, 2H), 3.93 (t, J = 7.91 Hz, 1H), 3.86 (d, J = 12.89 Hz, 1H), 3.75 (d, J = 13.50 Hz, 1H), 3.48–3.55 (m, 1H), 2.56–2.97 (m, 9H), 2.43 (dt, J = 11.72, 7.33 Hz, 1H), 2.12 (q, J = 7.42 Hz, 2H); ^{13}C NMR (75 MHz, $CDCl_3$) δ ppm 144.5, 144.4, 138.8, 138.4, 129.3, 128.6, 128.5, 128.5, 128.4, 127.7, 127.3, 126.4, 126.3, 69.1, 62.4, 53.5, 52.4, 48.7, 45.7, 36.9, 35.8.

4.1.4.4. (2S,3S)-3-((2,2-diphenylethyl)amino)-1-((2-methoxybenzyl)amino)-4-phenylbutan-2-ol (19). The reaction of (2*S*,3*S*)-3-amino-1-((2-methoxybenzyl)amino)-4-phenylbutan-2-ol (**3b**) (0.150 g, 0.50 mmol) with 2,2-diphenylacetaldehyde (0.098 g, 0.50 mmol) in the presence of acetic acid (0.045 g, 0.75 mmol) and sodium cyanoborohydride (0.057 g, 0.90 mmol) in DCM (4 mL) was performed according to the **procedure C**. Purification: washing reaction mixture with water (3 × 30 mL), flash column chromatography (DCM/MeOH/$NH_{3(aq)}$, 9.5/0.5/0.05 *v/v/v*). Yield: 0.030 g (12.5%), TLC (DCM/MeOH/$NH_{3(aq)}$, 9.5/0.5/0.05 *v/v/v*) R_f = 0.22, MW 480.65, formula: $C_{32}H_{36}N_2O_2$, MS *m/z* 481.4 ($M + H^+$), ^{1}H NMR (300 MHz, $CDCl_3$) δ ppm 7.06–7.39 (m, 17H), 6.83–6.97 (m, 2H), 3.98 (t, J = 7.62 Hz, 1H), 3.77–3.85 (m, 4H), 3.56–3.64 (m, 1H), 3.15–3.48 (m, 5H), 3.04–3.14 (m, 1H), 2.72–2.90 (m, 3H), 2.55–2.71 (m, 2H), ^{13}C NMR (75 MHz, $CDCl_3$) δ ppm 157.6, 142.8, 138.5, 130.3, 129.2, 129.1, 128.7, 128.6, 128.5, 128.0, 127.9, 126.8, 126.6, 126.4, 126.3, 126.1, 125.9, 120.6, 110.4, 68.7, 62.5, 55.3, 52.5, 51.9, 51.7, 48.3, 36.9.

4.1.4.5. (2S,3S)-3-((3,3-diphenylpropyl)amino)-1-((2-methoxybenzyl)amino)-4-phenylbutan-2-ol (20). The reaction of (2*S*,3*S*)-3-amino-1-((2-methoxybenzyl)amino)-4-phenylbutan-2-ol (**3b**) (0.200 g, 0.67 mmol) with 3,3-diphenylpropanal (0.141 g, 0.67 mmol) in the presence of acetic acid (0.060 g, 1.00 mmol) and sodium cyanoborohydride (0.105 g, 1.67 mmol) in DCM (4 mL) was performed according to the **procedure C**. Purification: washing reaction mixture with water (3 × 30 mL), flash column chromatography (DCM/MeOH/$NH_{3(aq)}$, 9.5/0.5/0.05 *v/v/v*). Yield: 0.072 g (21.9%), TLC (DCM/MeOH/$NH_{3(aq)}$, 9.5/0.5/0.05 *v/v/v*) $R_f = 0.38$, MW 494.68, formula: $C_{33}H_{38}N_2O_2$, MS *m/z* 495.2 ($M + H^+$), ^{1}H NMR (300 MHz, $CDCl_3$) δ ppm 7.06–7.33 (m, 17H), 6.81–6.94 (m, 2H), 4.03 (d, $J = 12.89$ Hz, 1H), 3.81–3.95 (m, 4H), 3.80 (s, 3H), 3.66 (br. s, 1H), 3.48 (s, 2H), 3.13 (dd, $J = 12.60$, 3.81 Hz, 1H), 2.56–2.85 (m, 4H), 2.40–2.51 (m, 1H), 1.98–2.10 (m, 2H); ^{13}C NMR (75 MHz, $CDCl_3$) δ ppm 157.6, 144.1, 137.8, 130.9, 130.2, 129.3, 128.7, 128.6, 127.7, 126.6, 126.4, 122.8, 120.9, 110.7, 66.0, 63.6, 55.6, 52.5, 48.8, 48.4, 45.5, 36.3, 35.2.

4.1.4.6. (2R,3S)-3-((3,3-diphenylpropyl)amino)-1-((3-methoxybenzyl)amino)-4-phenylbutan-2-ol (21). The reaction of (2*R*,3*S*)-3-amino-1-((3-methoxybenzyl)amino)-4-phenylbutan-2-ol (**4b**) (0.200 g, 0.67 mmol) with 3,3-diphenylpropanal (0.140 g, 0.67 mmol) in the presence of acetic acid (0.060 g, 1.00 mmol) and sodium cyanoborohydride (0.084 g, 1.33 mmol) in DCM (4 mL) was performed according to the **procedure C**. Purification: washing reaction mixture with water (3 × 30 mL), flash column chromatography (DCM/MeOH/$NH_{3(aq)}$, 9.5/0.5/0.05 *v/v/v*). Yield: 0.070 g (21.2%), TLC (DCM/MeOH/$NH_{3(aq)}$, 9.5/0.5/0.05 *v/v/v*) $R_f = 0.27$, MW 494.68, formula: $C_{33}H_{38}N_2O_2$, MS *m/z* 495.2 ($M + H^+$), ^{1}H NMR (500 MHz, $CDCl_3$) δ ppm 7.77 (br. s, 3H), 7.08–7.26 (m, 14H), 6.97–7.01 (m, 2H), 6.90 (s, 1H), 6.85 (dd, $J = 8.31$, 2.00 Hz, 2H), 4.09 (d, $J = 7.45$ Hz, 1H), 3.95 (d, $J = 13.17$ Hz, 1H), 3.75–3.83 (m, 2H), 3.73 (s, 3H), 3.11–3.17 (m, 1H), 2.76–2.84 (m, 2H), 2.53–2.70 (m, 4H), 2.24 (q, $J = 7.45$ Hz, 2H); ^{13}C NMR (126 MHz, $CDCl_3$) δ ppm 169.4, 160.1, 143.8, 137.2, 130.1, 129.1, 128.8, 128.7, 127.7, 127.7, 126.9, 126.6, 121.7, 114.9, 114.6, 67.8, 62.5, 55.3, 51.4, 49.5, 48.8, 45.7, 33.4.

4.1.4.7. (2R,3S)-3-((3,3-diphenylpropyl)amino)-1-((3-isopropylbenzyl)amino)-4-phenylbutan-2-ol (22). The reaction of (2*R*,3*S*)-3-amino-1-((3-isopropylbenzyl)amino)-4-phenylbutan-2-ol (**6b**) (0.114 g, 0.37 mmol) with 3,3-diphenylpropanal (0.077 g, 0.37 mmol) in the presence of acetic acid (0.033 g, 0.55 mmol) and sodium cyanoborohydride (0.042 g, 0.66 mmol) in DCM (2.5 mL) was performed according to the **procedure C**. Purification: washing reaction mixture with water (3 × 30 mL), flash column chromatography (3–10% MeOH in DCM). Yield: 0.035 g (18.9%), TLC (DCM/MeOH/$NH_{3(aq)}$, 9/1/0.1 *v/v/v*) $R_f = 0.37$, MW 506.73, formula: $C_{35}H_{42}N_2O$, MS *m/z* 507.3 ($M + H^+$), ^{1}H NMR (500 MHz, $CDCl_3$) δ ppm 7.03–7.34 (m, 19H), 3.70–3.93 (m, 3H), 3.66 (dt, $J = 7.88$, 3.79 Hz, 1H), 2.89 (dq, $J = 13.82$, 7.04 Hz, 1H), 2.54–2.84 (m, 5H), 2.15–2.53 (m, 3H), 2.00–2.13 (m, 2H), 1.25 (d, $J = 6.30$ Hz, 6H), two NH not detected; ^{13}C NMR (126 MHz, $CDCl_3$) δ ppm 149.3, 144.6, 138.7, 129.3, 128.7, 128.6, 128.6, 128.5, 127.8, 127.8, 126.6, 126.6, 126.3, 126.3, 125.9, 125.4, 69.1, 61.9, 54.0, 51.1, 48.6, 45.7, 35.8, 35.6, 34.2, 24.1.

4.1.4.8. (2R,3S)-3-((2,2-diphenylethyl)amino)-4-phenyl-1-(((S)-1-phenylethyl)amino)butan-2-ol (23). The reaction of (2*R*,3*S*)-3-amino-4-phenyl-1-(((*S*)-1-phenylethyl)amino)butan-2-ol (**10b**) (0.160 g, 0.56 mmol) with 2,2-diphenylacetaldehyde (0.088 g, 0.45 mmol) in the presence of acetic acid (0.051 g, 0.84 mmol) and sodium cyanoborohydride (0.088 g, 1.66 mmol) in DCM (2.5 mL) was performed according to the **procedure C**. Purification: washing reaction mixture with water (3 × 30 mL), flash column chromatography (3–10% MeOH in DCM), HPLC preparative system (20–90% water in acetonitrile). Yield: 0.038 g (14.6%), TLC (DCM/MeOH/$NH_{3(aq)}$, 9/1/0.1 *v/v/v*) $R_f = 0.36$, MW 464.65, formula: $C_{32}H_{36}N_2O$, MS *m/z* 465.2 ($M + H^+$), ^{1}H NMR (300 MHz, $CDCl_3$) δ ppm 7.00–7.43 (m, 18H), 6.82–6.93 (m, 2H), 4.75 (br. s, 2H), 3.96 (t, $J = 7.62$ Hz, 1H), 3.63–3.85 (m, 2H), 3.10–3.39 (m, 2H), 2.92–3.10 (m, 3H), 2.61 (dd, $J = 12.60$, 4.98 Hz, 1H), 2.43 (dd, $J = 13.48$, 4.69 Hz, 1H), 2.13–2.28 (m, 1H), 1.43 (d, $J = 6.45$ Hz, 2H), 1.24–1.35 (m, 1H), ^{13}C NMR (75 MHz, $CDCl_3$) δ ppm 170.2, 142.6, 142.1, 137.7, 128.9, 128.8, 128.6, 128.5, 128.3, 127.9, 127.7, 127.3, 126.6, 126.5, 68.5, 62.9, 58.1, 53.4, 51.7, 48.0, 36.2, 22.0.

4.1.4.9. (2R,3S)-3-((3,3-diphenylpropyl)amino)-4-phenyl-1-(((S)-1-phenylethyl)amino)butan-2-ol (24). The reaction of (2*R*,3*S*)-3-amino-4-phenyl-1-(((*S*)-1-phenylethyl)amino)butan-2-ol (**10b**) (0.160 g, 0.56 mmol) with 3,3-diphenylpropanal (0.095 g, 0.45 mmol) in the presence of acetic acid (0.051 g, 0.84 mmol) and sodium cyanoborohydride (0.088 g, 1.66 mmol) in DCM (2.5 mL) was performed according to the **procedure C**. Purification: washing reaction mixture with water (3 × 30 mL), flash column chromatography (3–10% MeOH in DCM), HPLC preparative system (20–90% water in acetonitrile). Yield: 0.040 g (14.7%), TLC (DCM/MeOH/$NH_{3(aq)}$, 9/1/0.1 *v/v/v*) $R_f = 0.38$, MW 478.68, formula: $C_{33}H_{38}N_2O$, MS *m/z* 479.3 ($M + H^+$), ^{1}H NMR (300 MHz, $CDCl_3$) δ ppm 7.43–7.51 (m, 2H), 7.30–7.39 (m, 3H), 7.00–7.26 (m, 13H), 6.83 (d, $J = 6.45$ Hz, 2H), 4.74 (d, $J = 9.38$ Hz, 1H), 4.16 (q, $J = 6.84$ Hz, 1H), 3.85–3.95 (m, 1H), 3.40–3.69 (m, 2H), 2.46–3.14 (m, 9H), 2.37 (dd, $J = 12.02$, 10.26 Hz, 1H), 1.74 (d, $J = 7.03$ Hz, 3H); ^{13}C NMR (75 MHz, $CDCl_3$) δ ppm 143.3, 143.2, 135.9, 135.9, 129.3, 128.9, 128.7, 127.9, 127.7, 127.0, 126.5, 126.5, 66.9, 61.9, 59.2, 48.7, 48.6, 45.6, 31.5, 31.4, 20.6.

4.1.4.10. (2R,3S)-3-((3,3-diphenylpropyl)amino)-4-phenyl-1-((2-phenylpropan-2-yl)amino)butan-2-ol (25). The reaction of (2*R*,3*S*)-3-amino-4-phenyl-1-((2-phenylpropan-2-yl)amino)butan-2-ol (**11b**) (0.200 g, 0.67 mmol) with 3,3-diphenylpropanal (0.140 g, 0.67 mmol) in the presence of acetic acid (0.060 g, 1.01 mmol) and sodium cyanoborohydride (0.076 g, 1.21 mmol) in DCM (4 mL) was performed according to the **procedure C**. Purification: washing reaction mixture with water (3 × 30 mL), flash column chromatography (DCM/MeOH/$NH_{3(aq)}$, 9.5/0.5/0.05 *v/v/v*). Yield: 0.074 g (22.4%), TLC (DCM/MeOH/$NH_{3(aq)}$, 9.5/0.5/0.05 *v/v/v*) $R_f = 0.31$, MW 492.71, formula: $C_{34}H_{40}N_2O$, MS *m/z* 493.3 ($M + H^+$), ^{1}H NMR (500 MHz, $CDCl_3$) δ ppm 7.46 (d, $J = 7.45$ Hz, 2H), 7.35 (t, $J = 7.73$ Hz, 2H), 7.06–7.28 (m, 14H), 7.00 (d, $J = 6.87$ Hz, 2H), 3.78 (t, $J = 7.73$ Hz, 1H), 3.64 (dt, $J = 7.30$, 3.51 Hz, 1H), 3.48 (br. s, 3H), 2.82 (td, $J = 6.87$, 4.58 Hz, 1H), 2.58–2.66 (m, 1H), 2.41–2.53 (m, 5H), 1.99–2.13 (m, 2H), 1.57 (d, $J = 10.31$ Hz, 6H); ^{13}C NMR (126 MHz, $CDCl_3$) δ ppm 144.7, 144.6, 138.3, 129.3, 128.7, 128.6, 128.6, 127.9, 127.10 126.5, 126.3, 126.3, 126.1, 69.6, 62.1, 57.1, 48.7, 45.7, 45.5, 35.8, 35.6, 29.1, 28.5.

4.1.4.11. (2S,3S)-1-(tert-butylamino)-3-((3,3-diphenylpropyl)amino)-4-phenylbutan-2-ol (26). The reaction of (2*S*,3*S*)-3-amino-1-(*tert*-butylamino)-4-phenylbutan-2-ol (**12b**) (0.100 g, 0.42 mmol) with 3,3-diphenylpropanal (0.089 g, 0.42 mmol) in the presence of acetic acid (0.038 g, 0.63 mmol) and sodium cyanoborohydride (0.053 g, 0.85 mmol) in DCM (3 mL) was performed according to the **procedure C**. Purification: washing reaction mixture with water (3 × 30 mL), flash column chromatography (3–10% MeOH in DCM). Yield: 0.017 g (9.2%), TLC (DCM/MeOH/$NH_{3(aq)}$, 9/1/0.1 *v/v/v*) $R_f = 0.31$, MW 430.64, formula: $C_{29}H_{38}N_2O$, MS *m/z* 431.5 ($M + H^+$), ^{1}H NMR (300 MHz, $CDCl_3$) δ ppm 7.09–7.32 (m, 15H), 3.94 (t, $J = 7.91$ Hz, 1H), 3.42 (dt, $J = 7.33$, 3.96 Hz, 1H), 2.40–2.85 (m, 10H), 2.12 (q, $J = 7.62$ Hz, 2H), 1.09 (s, 9H); ^{13}C NMR (75 MHz, $CDCl_3$) δ ppm

144.6, 139.0, 129.3, 128.5, 127.7, 126.2, 69.9, 62.3, 50.6, 48.7, 45.8, 45.7, 37.3, 36.2, 28.7.

4.1.4.12. (2R,3S)-3-((2,2-diphenylethyl)amino)-1-(neopentylamino)-4-phenylbutan-2-ol (27). The reaction of (2*R*,3*S*)-3-amino-1-(neopentylamino)-4-phenylbutan-2-ol (**13b**) (0.150 g, 0.60 mmol) with 2,2-diphenylacetaldehyde (0.118 g, 0.60 mmol) in the presence of acetic acid (0.054 g, 0.90 mmol) and sodium cyanoborohydride (0.068 g, 1.08 mmol) in DCM (4 mL) was performed according to the **procedure C**. Purification: washing reaction mixture with water (3 × 30 mL), flash column chromatography (5% MeOH in DCM). Yield: 0.044 g (16.9%), TLC (DCM/MeOH, 9/1 *v/v*) R_f = 0.39, MW 430.64, formula: $C_{29}H_{38}N_2O_2$, MS *m/z* 431.3 ($M + H^+$), ^{1}H NMR (500 MHz, $CDCl_3$) δ ppm 7.12−7.36 (m, 10H), 7.00−7.10 (m, 5H), 3.97 (d, *J* = 19.48 Hz, 2H), 3.34−3.43 (m, 2H), 3.13−3.27 (m, 3H), 3.00−3.09 (m, 1H), 2.75−2.88 (m, 2H), 2.50−2.64 (m, 2H), 1.05 (s, 9H), 0.98 (s, 2H); ^{13}C NMR (126 MHz, $CDCl_3$) δ ppm 129.1, 129.0, 128.9, 128.7, 128.6, 128.0, 127.9, 126.8, 68.1, 63.2, 60.8, 53.3, 52.7, 51.4, 36.7, 31.1, 27.6.

4.1.5. Procedure for the synthesis of compounds 28−56 (procedure D)

To the solution of 2,2-diphenylacetic acid or 3,3-diphenylpropanoic acid (1.0 equiv.) in anhydrous DCM (10 mL/1 mmol substrate) the following reagents in sequence were added: DMAP (0.5 equiv.), HOBt (1.3 equiv.) and EDC or DCC (1.3−2 equiv.). The reaction mixture was stirred at room temperature for 0.5 h and then appropriate 1-substituted 1,3-diamino-4-phenylbutan-2-ol derivative (1.0 equiv.) was added and stirring was overnight continued. When the reaction was finished, the reaction mixture was washed with water. The organic phase was than dried over anhydrous Na_2SO_4, filtered and concentrated under vacuum. The crude product was purified by flash column chromatography using a mixture of DCM and MeOH or by HPLC preparative system using an acetonitrile and water mixture.

4.1.5.1. N-((2S,3R)-4-(benzylamino)-3-hydroxy-1-phenylbutan-2-yl)-2,2-diphenylacetamide (28). The reaction of (2*R*,3*S*)-3-amino-1-(benzylamino)-4-phenylbutan-2-ol (**1b**) (0.200 g, 0.74 mmol) with 2,2-diphenylacetic acid (0.157 g, 0.74 mmol) in the presence of DMAP (0.045 g, 0.37 mmol) and DCC (0.305 g, 1.48 mmol) in DCM (5 mL) was performed according to the **procedure D**. Purification: washing reaction mixture with water (3 × 30 mL), flash column chromatography (5% MeOH in DCM). Yield: 0.103 g (30.0%), TLC (DCM/MeOH, 9/1 *v/v*) R_f = 0.30, MW 464.61, formula: $C_{31}H_{32}N_2O_2$, MS *m/z* 465.4 ($M + H^+$), ^{1}H NMR (500 MHz, $CDCl_3$) δ ppm 7.21−7.37 (m, 14H), 7.01−7.06 (m, 4H), 6.93−6.98 (m, 2H), 5.99 (d, *J* = 9.17 Hz, 1H), 4.82 (s, 1H), 4.22−4.30 (m, 1H), 3.74−3.80 (m, 1H), 3.65−3.73 (m, 1H), 3.55 (td, *J* = 6.01, 3.44 Hz, 1H), 3.25 (br. s, 2H), 2.95 (dd, *J* = 14.32, 4.58 Hz, 1H), 2.69−2.74 (m, 1H), 2.61−2.69 (m, 2H); ^{13}C NMR (126 MHz, $CDCl_3$) δ ppm 172.7, 139.3, 139.1, 139.0, 129.4, 129.1, 129.0, 128.9, 128.8, 128.7, 128.6, 128.6, 127.5, 127.4, 127.2, 126.6, 70.8, 59.3, 54.0, 53.7, 50.6, 36.6.

4.1.5.2. N-((2S,3S)-4-(benzylamino)-3-hydroxy-1-phenylbutan-2-yl)-2,2-diphenylacetamide (29). The reaction of (2*S*,3*S*)-3-amino-1-(benzylamino)-4-phenylbutan-2-ol (**2b**) (0.200 g, 0.74 mmol) with 2,2-diphenylacetic acid (0.157 g, 0.74 mmol) in the presence of DMAP (0.045 g, 0.37 mmol) and DCC (0.305 g, 1.48 mmol) in DCM (5 mL) was performed according to the **procedure D**. Purification: washing reaction mixture with water (3 × 30 mL), flash column chromatography (5% MeOH in DCM). Yield: 0.047 g (13.8%), TLC (DCM/MeOH, 9/1 *v/v*) R_f = 0.35, MW 464.61, formula: $C_{31}H_{32}N_2O_2$, MS *m/z* 465.4 ($M + H^+$), ^{1}H NMR (500 MHz, $CDCl_3$) δ ppm 7.17−7.35 (m, 16H), 7.06−7.13 (m, 4H), 6.01 (d, *J* = 9.17 Hz, 1H), 4.84 (s, 1H), 4.15−4.23 (m, 1H), 3.70 (d, *J* = 13.17 Hz, 1H), 3.64 (d, *J* = 13.75 Hz, 1H), 3.58−3.62 (m, 1H), 2.88 (d, *J* = 8.02 Hz, 2H), 2.64 (dd, *J* = 12.32, 3.72 Hz, 1H), 2.39 (dd, *J* = 12.60, 9.74 Hz, 1H), 1.98 (br. s, 2H); ^{13}C NMR (126 MHz, $CDCl_3$) δ ppm 172.0, 139.3, 139.3, 138.0, 129.5, 128.9, 128.9, 128.8, 128.7, 128.6, 128.6, 128.2, 127.4, 127.3, 127.2, 126.6, 68.9, 59.4, 53.6, 52.5, 51.8, 38.6.

4.1.5.3. N-((2S,3R)-4-(benzylamino)-3-hydroxy-1-phenylbutan-2-yl)-3,3-diphenylpropanamide (30). The reaction of (2*R*,3*S*)-3-amino-1-(benzylamino)-4-phenylbutan-2-ol (**1b**) (0.200 g, 0.74 mmol) with 3,3-diphenylpropanoic acid (0.167 g, 0.74 mmol) in the presence of DMAP (0.045 mg, 0.37 mmol) and DCC (0.305 g, 1.48 mmol) in DCM (5 mL) was performed according to the **procedure D**. Purification: washing reaction mixture with water (3 × 30 mL), flash column chromatography (5% MeOH in DCM). Yield: 0.130 g (36.7%), TLC (DCM/MeOH, 9/1 *v/v*) R_f = 0.30, MW 478.64, formula: $C_{32}H_{34}N_2O_2$, MS *m/z* 479.5 ($M + H^+$),^{1}H NMR (500 MHz, $CDCl_3$) δ ppm 7.33−7.42 (m, 5H), 7.04−7.33 (m, 15H), 6.32 (d, *J* = 8.59 Hz, 1H), 4.48 (dd, *J* = 9.45, 6.59 Hz, 1H), 4.13 (br. s, 2H), 3.95 (qd, *J* = 8.50, 4.30 Hz, 1H), 3.74 (d, *J* = 13.17 Hz, 1H), 3.56 (dt, *J* = 8.02, 4.01 Hz, 1H), 3.49 (d, *J* = 12.60 Hz, 1H), 2.85−2.98 (m, 2H), 2.75−2.84 (m, 3H), 2.28 (dd, *J* = 13.17, 4.58 Hz, 1H); ^{13}C NMR (126 MHz, $CDCl_3$) δ ppm 173.1, 143.4, 143.2, 137.0, 129.8, 129.4, 129.3, 129.2, 128.9, 128.8, 127.9, 127.6, 126.9, 126.8, 126.8, 69.2, 52.5, 52.2, 50.2, 47.3, 42.4, 36.1.

4.1.5.4. N-((2S,3S)-4-(benzylamino)-3-hydroxy-1-phenylbutan-2-yl)-3,3-diphenylpropanamide (31). The reaction of (2*S*,3*S*)-3-amino-1-(benzylamino)-4-phenylbutan-2-ol (**2b**) (0.150 g, 0.55 mmol) with 3,3-diphenylpropanoic acid (0.126 g, 0.55 mmol) in the presence of DMAP (0.034 mg, 0.28 mmol) and DCC (0.231 g, 1.11 mmol) in DCM (4 mL) was performed according to the **procedure D**. Purification: washing reaction mixture with water (3 × 30 mL), flash column chromatography (5−6% MeOH in DCM). Yield: 0.089 g (32.2%), TLC (DCM/MeOH, 9/1 *v/v*) R_f = 0.35, MW 478.64, formula: $C_{32}H_{34}N_2O_2$, MS *m/z* 479.3 ($M + H^+$), ^{1}H NMR (500 MHz, $CDCl_3$) δ ppm 7.13−7.34 (m, 20H), 5.99 (d, *J* = 8.59 Hz, 1H), 4.55 (t, *J* = 8.02 Hz, 1H), 3.89−3.96 (m, 1H), 3.51−3.59 (m, 3H), 2.84−2.94 (m, 2H), 2.83 (br. s, 2H), 2.73 (d, *J* = 7.45 Hz, 2H), 2.31 (dd, *J* = 12.60, 4.01 Hz, 1H), 2.02 (dd, *J* = 12.32, 10.02 Hz, 1H); ^{13}C NMR (126 MHz, $CDCl_3$) δ ppm 171.0, 143.7, 139.2, 138.2, 129.4, 128.7, 128.7, 128.5, 128.2, 128.1, 127.8, 127.5, 126.6, 126.6, 126.5, 67.7, 53.3, 52.1, 51.5, 47.6, 43.3, 38.5.

4.1.5.5. N-((2S,3S)-3-hydroxy-4-((2-methoxybenzyl)amino)-1-phenylbutan-2-yl)-2,2-diphenylacetamide (32). The reaction of (2*S*,3*S*)-3-amino-1-((2-methoxybenzyl)amino)-4-phenylbutan-2-ol (**3b**) (0.120 g, 0.40 mmol) with 2,2-diphenylacetic acid (0.085 g, 0.40 mmol) in the presence of DMAP (0.024 g, 0.20 mmol) and DCC (0.165 g, 0.80 mmol) in DCM (4 mL) was performed according to the **procedure D**. Purification: washing reaction mixture with water (3 × 30 mL), flash column chromatography (5% MeOH in DCM). Yield: 0.092 g (46.3%), TLC (DCM/MeOH, 9/1 *v/v*) R_f = 0.26, MW 494.64, formula: $C_{32}H_{34}N_2O_3$, MS *m/z* 495.3 ($M + H^+$), ^{1}H NMR (500 MHz, $CDCl_3$) δ ppm 7.19−7.32 (m, 12H), 7.09−7.16 (m, 4H), 7.07 (dd, *J* = 7.45, 1.72 Hz, 1H), 6.84−6.92 (m, 2H), 6.13 (d, *J* = 9.17 Hz, 1H), 4.86 (s, 1H), 4.11−4.19 (m, 1H), 3.79 (s, 3H), 3.67 (s, 2H), 3.60−3.66 (m, 1H), 2.90 (d, *J* = 8.02 Hz, 2H), 2.58 (dd, *J* = 12.60, 3.44 Hz, 1 H), 2.34 (dd, *J* = 12.60, 10.31 Hz, 1H), 2.03 (br. s, 2H); ^{13}C NMR (126 MHz, $CDCl_3$) δ ppm 157.8, 155.9, 137.0, 135.5, 129.4, 128.9, 128.8, 128.7, 128.6, 128.1, 128.1, 126.9, 80.1, 72.8, 55.4, 53.6, 48.4, 46.1, 38.7, 28.3.

4.1.5.6. N-((2S,3S)-3-hydroxy-4-((2-methoxybenzyl)amino)-1-phenylbutan-2-yl)-3,3-diphenylpropanamide (33). The reaction of

(2*S*,3*S*)-3-amino-1-((2-methoxybenzyl)amino)-4-phenylbutan-2-ol (**3b**) (0.120 g, 0.40 mmol) with 3,3-diphenylpropanoic acid (0.091 g, 0.40 mmol) in the presence of DMAP (0.024 g, 0.20 mmol) and DCC (0.165 g, 0.80 mmol) in DCM (4 mL) was performed according to the **procedure D**. Purification: washing reaction mixture with water (3 × 30 mL), flash column chromatography (5% MeOH in DCM). Yield: 0.048 g (23.7%), TLC (DCM/MeOH, 9/1 *v/v*) R_f = 0.27, MW 508.66, formula: $C_{33}H_{36}N_2O_3$, MS *m/z* 509.4 ($M + H^+$), ^{1}H NMR (500 MHz, $CDCl_3$) δ ppm 7.11–7.30 (m, 16H), 6.95 (dd, *J* = 7.16, 1.43 Hz, 1H), 6.77–6.84 (m, 2H), 6.32 (d, *J* = 9.17 Hz, 1H), 4.55 (t, *J* = 8.02 Hz, 1H), 3.88–3.95 (m, 1H), 3.73 (s, 3H), 3.50–3.57 (m, 2H), 3.42–3.48 (m, 1H), 2.85–2.97 (m, 2H), 2.77 (dd, *J* = 13.75, 9.16 Hz, 1H), 2.70 (dd, *J* = 13.17, 6.30 Hz, 1H), 2.48 (br. s, 2H), 2.24 (dd, *J* = 12.60, 3.44 Hz, 1H), 2.00 (dd, *J* = 12.32, 10.60 Hz, 1H); ^{13}C NMR (126 MHz, $CDCl_3$) δ ppm 171.1, 157.6, 143.7, 143.7, 138.3, 130.3, 129.5, 128.6, 128.5, 128.1, 127.8, 126.6, 126.5, 126.4, 120.7, 110.5, 67.3, 55.3, 52.3, 51.2, 48.6, 47.6, 43.2, 38.4.

4.1.5.7. N-((2S,3R)-3-hydroxy-4-((3-methoxybenzyl)amino)-1-phenylbutan-2-yl)-2,2-diphenylacetamide (34). The reaction of (2*R*,3*S*)-3-amino-1-((3-methoxybenzyl)amino)-4-phenylbutan-2-ol (**4b**) (0.400 g, 1.33 mmol) with 2,2-diphenylacetic acid (0.282 g, 1.33 mmol) in the presence of DMAP (0.082 g, 0.67 mmol), HOBt (0.234 g, 1.73 mmol) and EDC (0.332 g, 1.73 mmol) in DCM (20 mL) was performed according to the **procedure D**. Purification: washing reaction mixture with water (3 × 30 mL), flash column chromatography (5% MeOH in DCM). Yield: 0.322 g (50.4%), TLC (DCM/MeOH, 9.5/0.5 *v/v*) R_f = 0.24, MW 494.64, formula: $C_{32}H_{34}N_2O_3$, MS *m/z* 495.2 ($M + H^+$), ^{1}H NMR (500 MHz, $CDCl_3$) δ ppm 7.18–7.30 (m, 10H), 7.00–7.07 (m, 4H), 6.94 (dd, *J* = 6.87, 2.86 Hz, 2H), 6.78–6.85 (m, 3H), 6.18 (d, *J* = 8.59 Hz, 1H), 4.81 (s, 1H), 4.24 (dd, *J* = 6.30, 4.01 Hz, 1H), 3.64–3.86 (m, 6H), 3.53–3.63 (m, 2H), 2.93 (dd, *J* = 14.32, 4.58 Hz, 1H), 2.55–2.72 (m, 3H), ^{13}C NMR (126 MHz, $CDCl_3$) δ 172.8, 159.9, 140.2, 139.2, 139.1, 137.7, 129.6, 129.4, 129.1, 129.0, 128.9, 128.8, 128.7, 127.4, 127.2, 126.6, 120.9, 114.1, 113.1, 70.8, 59.2, 55.3, 53.9, 53.5, 50.5, 36.6.

4.1.5.8. N-((2S,3R)-3-hydroxy-4-((3-methoxybenzyl)amino)-1-phenylbutan-2-yl)-3,3-diphenylpropanamide (35). The reaction of (2*R*,3*S*)-3-amino-1-((3-methoxybenzyl)amino)-4-phenylbutan-2-ol (**4b**) (0.400 g, 1.33 mmol) with 3,3-diphenylpropanoic acid (0.301 g, 1.33 mmol) in the presence of DMAP (0.082 g, 0.67 mmol), HOBt (0.234 g, 1.73 mmol) and EDC (0.332 g, 1.73 mmol) in DCM (20 mL) was performed according to the **procedure D**. Purification: washing reaction mixture with water (3 × 30 mL), flash column chromatography (5% MeOH in DCM). Yield: 0.360 g (53.1%), TLC (DCM/MeOH, 9.5/0.5 *v/v*) R_f = 0.27, MW 508.66, formula: $C_{33}H_{36}N_2O_3$, MS *m/z* 509.2 ($M + H^+$), ^{1}H NMR (500 MHz, $CDCl_3$) δ ppm 7.12–7.28 (m, 14H), 7.06 (d, *J* = 6.87 Hz, 2H), 6.79–6.90 (m, 3H), 6.17 (d, *J* = 8.59 Hz, 1H), 4.47 (t, *J* = 8.02 Hz, 1H), 3.99–4.07 (m, 1H), 3.74–3.85 (m, 5H), 3.60–3.65 (m, 1H), 3.50–3.55 (m, 1H), 3.35–3.41 (m, 1H), 2.72–2.88 (m, 4H), 2.53 (dd, *J* = 12.60, 3.44 Hz, 1H), 2.37 (dd, *J* = 12.32, 5.44 Hz, 1H), ^{13}C NMR (126 MHz, $CDCl_3$) δ 171.7, 159.9, 143.6, 143.5, 139.7, 137.6, 129.7, 129.4, 128.7, 128.7, 128.6, 128.0, 127.7, 126.7, 126.6, 126.6, 120.8, 114.3, 113.1, 70.1, 55.3, 53.4, 53.1, 50.5, 47.4, 43.2, 36.4.

4.1.5.9. N-((2S,3R)-4-((3-(tert-butyl)benzyl)amino)-3-hydroxy-1-phenylbutan-2-yl)-2,2-diphenylacetamide (36). The reaction of (2*R*,3*S*)-3-amino-1-((3-(*tert*-butyl)benzyl)amino)-4-phenylbutan-2-ol (**5b**) (0.200 g, 0.61 mmol) with 2,2-diphenylacetic acid (0.130 g, 0.61 mmol) in the presence of DMAP (0.037 g, 0.31 mmol), HOBt (0.107 g, 0.80 mmol) and EDC (0.152 g, 0.80 mmol) in DCM (8 mL) was performed according to the **procedure D**. Purification: washing reaction mixture with water (3 × 10 mL), flash column chromatography (5% MeOH in DCM), HPLC preparative system (20–90% water in acetonitrile). Yield: 0.198 g (62.2%), TLC (DCM/MeOH/$NH_{3(aq)}$, 9/1/0.1 *v/v/v*) R_f = 0.39, MW 520.72, formula: $C_{35}H_{40}N_2O_2$, MS *m/z* 521.3 ($M + H^+$), ^{1}H NMR (500 MHz, $CDCl_3$) δ ppm 7.66 (br. s, 2H), 7.37–7.42 (m, 2H), 7.19–7.30 (m, 11H), 7.13–7.17 (m, 1H), 6.99–7.03 (m, 2H), 6.96 (td, *J* = 4.73, 1.43 Hz, 3H), 6.17 (d, *J* = 8.02 Hz, 1H), 4.78 (s, 1H), 4.19 (qd, *J* = 8.59, 4.01 Hz, 1H), 3.93 (d, *J* = 13.17 Hz, 1H), 3.81 (d, *J* = 12.60 Hz, 2H), 3.10 (dd, *J* = 14.32, 4.01 Hz, 1H), 3.00 (dd, *J* = 12.89, 2.58 Hz, 1H), 2.64–2.75 (m, 2H), 1.30 (s, 9H); ^{13}C NMR (126 MHz, $CDCl_3$) δ ppm 173.3, 169.4, 152.2, 138.9, 138.8, 137.3, 131.3, 129.4, 129.0, 128.9, 128.8, 128.8, 128.7, 127.4, 127.3, 127.2, 126.9, 126.7, 126.2, 69.3, 58.8, 53.3, 52.2, 50.2, 36.0, 34.8, 31.4.

4.1.5.10. N-((2S,3R)-4-((3-(tert-butyl)benzyl)amino)-3-hydroxy-1-phenylbutan-2-yl)-3,3-diphenylpropanamide (37). The reaction of (2*R*,3*S*)-3-amino-1-((3-(*tert*-butyl)benzyl)amino)-4-phenylbutan-2-ol (**5b**) (0.200 g, 0.61 mmol) with 3,3-diphenylpropanoic acid (0.138 g, 0.61 mmol) in the presence of DMAP (0.037 g, 0.31 mmol), HOBt (0.107 g, 0.80 mmol) and EDC (0.152 g, 0.80 mmol) in DCM (8 mL) was performed according to the **procedure D**. Purification: washing reaction mixture with water (3 × 10 mL), flash column chromatography (5% MeOH in DCM). Yield: 0.073 g (22.4%), TLC (DCM/MeOH/$NH_{3(aq)}$, 9/1/0.1 *v/v/v*) R_f = 0.33, MW 534.74, formula: $C_{36}H_{42}N_2O_2$, MS *m/z* 535.3 ($M + H^+$), ^{1}H NMR (500 MHz, $CDCl_3$) δ ppm 7.46 (s, 1H), 7.40 (d, *J* = 8.02 Hz, 1H), 7.32 (t, *J* = 7.73 Hz, 1H), 7.10–7.29 (m, 16H), 6.63 (d, *J* = 7.45 Hz, 1H), 4.50 (dd, *J* = 9.45, 6.59 Hz, 1H), 4.01 (qd, *J* = 8.31, 4.87 Hz, 1H), 3.77 (d, *J* = 13.17 Hz, 1H), 3.56–3.61 (m, 1H), 3.51 (d, *J* = 12.60 Hz, 1H), 2.94–3.02 (m, 2H), 2.87 (dd, J = 14.89, 8.02 Hz, 1H), 2.74–2.83 (m, 2H), 2.31 (dd, *J* = 12.60, 4.58 Hz, 1H), 1.35 (s, 9H), NH, OH not detected; ^{13}C NMR (126 MHz, $CDCl_3$) δ ppm 172.9, 152.1, 143.5, 143.4, 137.6, 129.4, 128.9, 128.8, 128.7, 128.6, 128.1, 127.7, 126.8, 126.8, 126.6, 126.0, 69.7, 53.1, 52.7, 50.5, 47.4, 42.5, 36.2, 34.9, 31.4.

4.1.5.11. N-((2S,3R)-3-hydroxy-4-((3-isopropylbenzyl)amino)-1-phenylbutan-2-yl)-2,2-diphenylacetamide (38). The reaction of (2*R*,3*S*)-3-amino-1-((3-isopropylbenzyl)amino)-4-phenylbutan-2-ol (**6b**) (0.153 g, 0.49 mmol) with 2,2-diphenylacetic acid (0.104 g, 0.49 mmol) in the presence of DMAP (0.030 g, 0.25 mmol), HOBt (0.086 g, 0.64 mmol) and EDC (0.122 g, 0.64 mmol) in DCM (8 mL) was performed according to the **procedure D**. Purification: washing reaction mixture with water (3 × 10 mL), flash column chromatography (5–8% MeOH in DCM), Yield: 0.108 g (43.5%), TLC (DCM/MeOH/$NH_{3(aq)}$, 9/1/0.1 *v/v/v*) R_f = 0.51, MW 506.69, formula: $C_{34}H_{38}N_2O_2$, MS *m/z* 507.7 ($M + H^+$), ^{1}H NMR (500 MHz, $CDCl_3$) δ ppm 7.21–7.31 (m, 10H), 7.15–7.20 (m, 2H), 7.11 (d, *J* = 7.45 Hz, 1H), 7.03 (d, *J* = 7.45 Hz, 4H), 6.93–6.99 (m, 2H), 6.05 (d, *J* = 8.02 Hz, 1H), 4.83 (s, 1H), 4.22–4.30 (m, 1H), 4.22 (br. s, 2H), 3.79 (d, *J* = 13.00 Hz, 1H), 3.70 (d, *J* = 13.00 Hz, 1H), 3.59–3.65 (m, 1H), 2.97 (dd, *J* = 14.03, 4.30 Hz, 1H), 2.90 (dt, *J* = 13.75, 6.87 Hz, 1H), 2.79 (dd, *J* = 12.32, 2.58 Hz, 1H), 2.62–2.71 (m, 2H), 1.25 (d, *J* = 6.87 Hz, 6H); ^{13}C NMR (126 MHz, $CDCl_3$) δ ppm 172.8, 149.4, 139.1, 139.0, 137.6, 129.4, 129.1, 129.0, 128.9, 128.8, 128.7, 127.4, 127.2, 127.0, 126.6, 126.2, 125.8, 70.6, 59.2, 53.8, 53.5, 50.6, 36.4, 34.1, 24.1, 24.1.

4.1.5.12. N-((2S,3S)-3-hydroxy-4-((3-isopropylbenzyl)amino)-1-phenylbutan-2-yl)-2,2-diphenylacetamide (39). The reaction of (2*S*,3*S*)-3-amino-1-((3-isopropylbenzyl)amino)-4-phenylbutan-2-ol (**7b**) (0.090 g, 0.29 mmol) with 2,2-diphenylacetic acid (0.061 g, 0.29 mmol) in the presence of DMAP (0.018 g, 0.14 mmol), HOBt (0.051 g, 0.37 mmol) and EDC (0.072 g, 0.37 mmol) in DCM (5 mL) was performed according to the **procedure D**. Purification: washing reaction mixture with water (3 × 10 mL), flash column chromatography (5% MeOH in DCM), Yield: 0.051 g (35.0%), TLC

(DCM/MeOH, 9/1 *v/v*) $R_f = 0.42$, MW 506.69, formula: $C_{34}H_{38}N_2O_2$, MS *m/z* 507.4 ($M + H^+$), ^1H NMR (500 MHz, $CDCl_3$) δ ppm 7.18–7.31 (m, 12H), 7.13 (t, $J = 7.50$ Hz, 3H), 7.07–7.11 (m, 3H), 7.04 (d, $J = 7.45$ Hz, 1H), 6.00 (d, $J = 8.59$ Hz, 1H), 4.85 (s, 1H), 4.16–4.23 (m, 1H), 3.68 (d, $J = 13.00$ Hz, 1H), 3.57–3.64 (m, 2H), 2.86–2.92 (m, 3H), 2.66 (dd, $J = 12.03$, 4.01 Hz, 1H), 2.39 (dd, $J = 12.32$, 10.02 Hz, 1H), 1.81 (br. s, 2H), 1.25 (d, $J = 6.87$ Hz, 6H); ^{13}C NMR (126 MHz, $CDCl_3$) δ ppm 172.0, 149.3, 139.6, 139.4, 139.3, 138.1, 129.5, 128.9, 128.9, 128.8, 128.7, 128.6, 127.3, 127.2, 126.5, 126.3, 125.6, 125.4, 68.8, 59.4, 53.8, 52.5, 51.9, 38.6, 34.1, 24.1, 24.1.

4.1.5.13. N-((2S,3R)-3-hydroxy-4-((3-isopropylbenzyl)amino)-1-phenylbutan-2-yl)-3,3-diphenylpropanamide (40). The reaction of (2*R*,3*S*)-3-amino-1-((3-isopropylbenzyl)amino)-4-phenylbutan-2-ol (**6b**) (0.150 g, 0.48 mmol) with 3,3-diphenylpropanoic acid (0.109 g, 0.48 mmol) in the presence of DMAP (0.029 g, 0.24 mmol), HOBt (0.084 g, 0.62 mmol) and EDC (0.120 g, 0.62 mmol) in DCM (8 mL) was performed according to the **procedure D**. Purification: washing reaction mixture with water (3 × 10 mL), flash column chromatography (5% MeOH in DCM), Yield: 0.096 g (38.5%), TLC (DCM/MeOH/$NH_{3(aq)}$, 9/1/0.1 *v/v/v*) $R_f = 0.41$, MW 520.72, formula: $C_{35}H_{40}N_2O_2$, MS *m/z* 521.4 ($M + H^+$), ^1H NMR (500 MHz, $CDCl_3$) δ ppm 7.14–7.34 (m, 17H), 7.10 (d, $J = 7.45$ Hz, 2H), 6.21 (d, $J = 8.02$ Hz, 1H), 4.49 (dd, $J = 9.16$, 7.45 Hz, 1H), 4.01–4.09 (m, 1H), 3.75 (d, $J = 13.17$ Hz, 1H), 3.58 (d, $J = 12.60$ Hz, 1H), 3.43–3.48 (m, 1H), 2.78–2.96 (m, 5H), 2.70 (dd, $J = 12.60$, 2.86 Hz, 1H), 2.34 (dd, $J = 12.89$, 4.87 Hz, 1H), 1.27 (dd, $J = 6.87$, 1.72 Hz, 6H), NH, OH not detected; ^{13}C NMR (126 MHz, $CDCl_3$) δ ppm 172.5, 149.7, 143.6, 143.4, 137.5, 129.4, 129.0, 128.8, 128.7, 128.6, 128.0, 127.7, 127.6, 126.8, 126.8, 126.7, 126.7, 69.8, 53.1, 52.8, 50.5, 47.4, 42.7, 36.2, 34.1, 24.1, 24.1.

4.1.5.14. N-((2S,3R)-3-hydroxy-1-phenyl-4-((3-(trifluoromethyl)benzyl)amino)butan-2-yl)-2,2-diphenylacetamide (41). The reaction of (2*R*,3*S*)-3-amino-4-phenyl-1-((3-(trifluoromethyl)benzyl)amino)butan-2-ol (**8b**) (0.338 g, 1.00 mmol) with 2,2-diphenylacetic acid (0.212 g, 1.00 mmol) in the presence of DMAP (0.061 g, 0.50 mmol), HOBt (0.175 g, 1.30 mmol) and EDC (0.249 g, 1.30 mmol) in DCM (10 mL) was performed according to the **procedure D**. Purification: washing reaction mixture with water (3 × 10 mL), flash column chromatography (5–10% MeOH in DCM). Yield: 0.117 g (22.0%), TLC (DCM/MeOH, 9/1 *v/v*) $R_f = 0.5$, MW 532.61, formula: $C_{32}H_{31}F_3N_2O_2$, MS *m/z* 533.3 ($M + H^+$), ^1H NMR (500 MHz, $CDCl_3$) δ ppm 7.50–7.57 (m, 2H), 7.41–7.46 (m, 2H), 7.28–7.31 (m, 4H), 7.21–7.26 (m, 5H), 7.19 (br. d, $J = 6.87$ Hz, 2H), 7.07 (br. d, $J = 6.30$ Hz, 2H), 7.03 (br. d, $J = 6.87$ Hz, 2H), 6.87 (br. d, $J = 4.01$ Hz, 1H), 6.13 (br. d, $J = 9.16$ Hz, 1H), 4.86 (s, 1H), 4.17–4.35 (m, 1H), 3.56–3.79 (m, 4H), 2.85–2.96 (m, 2H), 2.60–2.67 (m, 1H), 2.33–2.55 (m, 1H); ^{13}C NMR (126 MHz, $CDCl_3$) δ ppm 172.2, 140.6, 139.3, 139.2, 137.9, 131.5, 130.9 (q, $J = 32.00$ Hz), 129.5, 129.3, 129.0, 129.0, 128.9, 128.9, 128.8, 128.8, 128.6, 127.4, 127.3, 126.6, 124.8 (q, $J = 3.82$ Hz),124.2 (q, $J = 272.82$ Hz), 124.2 (q, $J = 3.60$ Hz), 69.3, 59.3, 53.2, 52.6, 52.0, 38.4.

4.1.5.15. N-((2S,3R)-3-hydroxy-1-phenyl-4-((3-(trifluoromethyl)benzyl)amino)butan-2-yl)-3,3-diphenylpropanamide (42). The reaction of (2*R*,3*S*)-3-amino-4-phenyl-1-((3-(trifluoromethyl)benzyl)amino)butan-2-ol (**8b**) (0.338 g, 1.00 mmol) with 3,3-diphenylpropanoic acid (0.226 g, 1.00 mmol) in the presence of DMAP (0.061 g, 0.50 mmol), HOBt (0.175 g, 1.30 mmol) and EDC (0.249 g, 1.30 mmol) in DCM (10 mL) was performed according to the **procedure D**. Purification: washing reaction mixture with water (3 × 10 mL), flash column chromatography (5–10% MeOH in DCM). Yield: 0.184 g (33.7%), TLC (DCM/MeOH, 9/1 *v/v*) $R_f = 0.46$, MW 546.63, formula: $C_{33}H_{33}F_3N_2O_2$, MS *m/z* 547.2 ($M + H^+$), ^1H NMR (500 MHz, $CDCl_3$) δ ppm 7.52–7.55 (m, 2H), 7.47–7.49 (m, 1H), 7.45 (d, $J = 8.02$ Hz, 1H), 7.14–7.26 (m, 13H), 7.04 (d, $J = 7.45$ Hz, 2H), 5.72 (br. d, $J = 8.59$ Hz, 1H), 4.48 (t, $J = 8.02$ Hz, 1H), 4.01–4.10 (m, 1H). 3.61–3.72 (m, 2H), 3.20–3.37 (m, 1H), 2.90–3.13 (m, 1H), 2.76–2.81 (m, 4H), 2.41–2.46 (m, 1H), 2.34–2.40 (m, 1H), NH not detected; ^{13}C NMR (126 MHz, $CDCl_3$) δ ppm 171.5, 143.5, 143.5, 140.4, 137.4, 131.7, 130.9 (q, $J = 31.99$ Hz), 129.4, 129.1, 128.7, 128.7, 127.9, 127.7, 126.8, 126.7, 125.1 (q, $J = 4.02$ Hz), 123.9 (q, $J = 272.20$ Hz), 124.2 (q, $J = 3.62$ Hz), 70.3, 53.3, 53.0, 50.5, 47.4, 43.3, 36.3.

4.1.5.16. N-((2S,3S)-4-((4-(tert-butyl)benzyl)amino)-3-hydroxy-1-phenylbutan-2-yl)-2,2-diphenylacetamide (43). The reaction of (2*S*,3*S*)-3-amino-1-((4-(*tert*-butyl)benzyl)amino)-4-phenylbutan-2-ol (**9b**) (0.150 g, 0.46 mmol) with 2,2-diphenylacetic acid (0.098 g, 0.46 mmol) in the presence of DMAP (0.028 g, 0.23 mmol), HOBt (0.081 g, 0.60 mmol) and EDC (0.115 g, 0.60 mmol) in DCM (8 mL) was performed according to the **procedure D**. Purification: washing reaction mixture with water (3 × 10 mL), flash column chromatography (5–10% MeOH in DCM). Yield: 0.129 g (53.9%), TLC (DCM/MeOH, 9.5/0.5 *v/v*) $R_f = 0.24$, MW 520.72, formula: $C_{35}H_{40}N_2O_2$, MS *m/z* 521.5 ($M + H^+$), ^1H NMR (500 MHz, $CDCl_3$) δ ppm 7.34 (d, $J = 8.02$ Hz, 2H), 7.21–7.30 (m, 9H), 7.16–7.20 (m, 4H), 7.05–7.13 (m, 4H), 6.42 (d, $J = 9.17$ Hz, 1H), 4.90 (s, 1H), 4.59 (br. s, 2H), 4.21 (q, $J = 7.45$ Hz, 1H), 3.75–3.82 (m, 1H), 3.67 (d, $J = 13.00$ Hz, 1H), 3.62 (d, $J = 13.00$ Hz, 1H), 2.88 (dd, $J = 7.45$, 4.58 Hz, 2H), 2.64 (dd, $J = 12.20$, 5.00 Hz, 1H), 2.55 (dd, $J = 12.03$, 9.74 Hz, 1H), 1.31 (s, 9H); ^{13}C NMR (126 MHz, $CDCl_3$) δ ppm 172.5, 151.1, 139.4, 139.3, 138.0, 129.5, 129.1, 128.9, 128.8, 128.7, 128.6, 127.3, 127.2, 126.6, 125.8, 68.7, 59.0, 52.8, 52.6, 51.3, 38.2, 34.6, 31.4.

4.1.5.17. N-((2S,3S)-4-((4-(tert-butyl)benzyl)amino)-3-hydroxy-1-phenylbutan-2-yl)-3,3-diphenylpropanamide (44). The reaction of (2*S*,3*S*)-3-amino-1-((4-(*tert*-butyl)benzyl)amino)-4-phenylbutan-2-ol (**9b**) (0.200 g, 0.61 mmol) with 3,3-diphenylpropanoic acid (0.138 g, 0.61 mmol) in the presence of DMAP (0.037 g, 0.31 mmol), HOBt (0.107 g, 0.80 mmol) and EDC (0.152 g, 0.80 mmol) in DCM (8 mL) was performed according to the **procedure D**. Purification: washing reaction mixture with water (3 × 10 mL), flash column chromatography (5% MeOH in DCM). Yield: 0.130 g (39.8%), TLC (DCM/MeOH/$NH_{3(aq)}$, 9/1/0.1 *v/v/v*) $R_f = 0.53$, MW 534.74, formula: $C_{36}H_{42}N_2O_2$, MS *m/z* 535.4 ($M + H^+$), ^1H NMR (300 MHz, $CDCl_3$) δ ppm 7.07–7.41 (m, 19H), 6.76 (d, $J = 8.79$ Hz, 1H), 6.39 (br. s, 2H), 4.59 (dd, $J = 9.38$, 6.45 Hz, 1H), 3.93–4.04 (m, 1H), 3.67–3.81 (m, 2H), 3.48 (d, $J = 12.89$ Hz, 1H), 2.99 (dd, $J = 14.65$, 9.38 Hz, 1H), 2.85 (dd, $J = 14.65$, 6.45 Hz, 1H), 2.72 (d, $J = 7.62$ Hz, 2H), 2.38 (d, $J = 7.03$ Hz, 2H), 1.27 (s, 9H); ^{13}C NMR (126 MHz, $CDCl_3$) δ ppm 171.9, 151.6, 143.7, 143.5, 137.9, 129.4, 128.9, 128.8, 128.7, 128.6, 128.1, 127.8, 126.7, 126.6, 126.6, 125.9, 67.7, 52.3, 52.1, 50.6, 47.5, 42.8, 38.0, 34.7, 31.3.

4.1.5.18. N-((2S,3R)-3-hydroxy-1-phenyl-4-(((S)-1-phenylpropan-2-yl)amino)butan-2-yl)-2,2-diphenylacetamide (45). The reaction of (2*R*,3*S*)-3-amino-4-phenyl-1-(((*S*)-1-phenylethyl)amino)butan-2-ol (**10b**) (0.160 g, 0.56 mmol) with 2,2-diphenylacetic acid (0.119 g, 0.56 mmol) in the presence of DMAP (0.034 g, 0.28 mmol) and DCC (0.232 g, 1.12 mmol) in DCM (5 mL) was performed according to the **procedure D**. Purification: washing reaction mixture with water (3 × 10 mL), flash column chromatography (5% MeOH in DCM). Yield: 0.140 g (50.6%), TLC (DCM/MeOH, 9.5/0.5 *v/v*) $R_f = 0.15$, MW 478.64, formula: $C_{32}H_{34}N_2O_2$, MS *m/z* 479.4 ($M + H^+$), ^1H NMR (500 MHz, $CDCl_3$) δ ppm 7.13–7.43 (m, 15H), 6.86–7.02 (m, 5H), 5.95 (d, $J = 8.59$ Hz, 1H), 4.74–4.82 (m, 1H), 4.26 (tdd, $J = 9.02$, 9.02, 6.59, 5.16 Hz, 1H), 3.65–3.72 (m, 1H), 3.41–3.51 (m, 1H), 2.83–2.90 (m, 1H), 2.52–2.58 (m, 1H), 2.42–2.49 (m, 1H), 1.88–1.96 (m, 1H),

1.68 (dt, J = 14.03, 3.58 Hz, 1H), 1.28–1.41 (m, 3H), 1.04–1.17 (m, 1H), ^{13}C NMR (126 MHz, $CDCl_3$) δ 172.7, 139.1, 137.6, 129.3, 129.1, 129.0, 128.9, 128.8, 128.7, 127.4, 127.3, 127.2, 127.0, 126.8, 126.6, 70.7, 58.8, 53.8, 34.0, 25.7, 25.0, 24.1.

4.1.5.19. N-((2S,3R)-3-hydroxy-1-phenyl-4-(((S)-1-phenylethyl) amino)butan-2-yl)-3,3-diphenylpropanamide (46). The reaction of (2*R*,3*S*)-3-amino-4-phenyl-1-(((*S*)-1-phenylethyl)amino)butan-2-ol (**10b**) (0.160 g, 0.56 mmol) with 3,3-diphenylpropanoic acid (0.127 g, 0.56 mmol) in the presence of DMAP (0.034 g, 0.28 mmol) and ECC (0.216 g, 1.12 mmol) in DCM (5 mL) was performed according to the **procedure D**. Purification: washing reaction mixture with water (3 × 10 mL), flash column chromatography (5% MeOH in DCM). Yield: 0.130 g (47.0%), TLC (DCM/MeOH, 9.5/0.5 *v/v*) R_f = 0.14, MW 492.66, formula: $C_{33}H_{36}N_2O_2$, MS *m/z* 493.7 ($M + H^+$), ^{1}H NMR (300 MHz, $CDCl_3$) δ 7.10–7.40 (m, 18H), 6.97 (dd, J = 1.76, 7.62 Hz, 2H), 5.87 (d, J = 8.79 Hz, 1H), 4.44 (t, J = 7.91 Hz, 1H), 3.99–4.11 (m, 1H), 3.66 (q, J = 6.84 Hz, 1H), 3.19–3.27 (m, 1H), 2.78 (d, J = 8.21 Hz, 2H), 2.72 (dd, J = 7.03, 14.65 Hz, 1H), 2.59 (dd, J = 5.27, 14.07 Hz, 1H), 2.62 (br. s, 2H), 2.43 (dd, J = 3.52, 12.89 Hz, 1H), 2.26 (dd, J = 5.27, 12.89 Hz, 1H), 1.40 (d, J = 6.45 Hz, 3H); ^{13}C NMR (126 MHz, $CDCl_3$) δ 171.3, 143.5, 143.5, 137.3, 129.3, 128.6, 128.6, 128.5, 127.8, 127.6, 127.4, 126.7, 126.6, 126.6, 126.4, 69.8, 58.5, 53.0, 48.8, 47.4, 43.4, 36.3, 23.7.

4.1.5.20. N-((2S,3R)-3-hydroxy-1-phenyl-4-((2-phenylpropan-2-yl) amino)butan-2-yl)-2,2-diphenylacetamide (47). The reaction of (2*R*,3*S*)-3-amino-4-phenyl-1-((2-phenylpropan-2-yl)amino)butan-2-ol (**11b**) (0.160 g, 0.54 mmol) with 2,2-diphenylacetic acid (0.114 g, 0.54 mmol) in the presence of DMAP (0.033 g, 0.27 mmol) and DCC (0.221 g, 1.12 mmol) in DCM (5 mL) was performed according to the **procedure D**. Purification: washing reaction mixture with water (3 × 10 mL), flash column chromatography (5% MeOH in DCM). Yield: 0.092 g (34.8%), TLC (DCM/MeOH, 9.5/0.5 *v/v*) R_f = 0.21, MW 492.66, formula: $C_{33}H_{36}N_2O_2$, MS *m/z* 493.5 ($M + H^+$), ^{1}H NMR (500 MHz, $CDCl_3$) δ ppm 7.16–7.43 (m, 15H), 6.88–7.02 (m, 5H), 4.72–4.83 (m, 3H), 4.17–4.26 (m, 1H), 3.29–3.37 (m, 1H), 2.98 (dd, J = 14.32, 4.01 Hz, 1H), 2.57–2.67 (m, 1H), 2.36 (d, J = 4.01 Hz, 2H), 1.39–1.52 (m, 6H), 1.16–1.38 (br. s, 1H), ^{13}C NMR (126 MHz, $CDCl_3$) δ 172.6, 139.0, 137.5, 129.4, 129.0, 128.9, 128.9, 128.8, 128.7, 128.5, 127.4, 127.3, 126.8, 126.6, 126.1, 100.0, 70.8, 59.3, 53.1, 44.5, 36.5, 29.4, 28.5.

4.1.5.21. N-((2S,3R)-3-hydroxy-1-phenyl-4-((2-phenylpropan-2-yl) amino)butan-2-yl)-3,3-diphenylpropanamide (48). The reaction of (2*R*,3*S*)-3-amino-4-phenyl-1-((2-phenylpropan-2-yl)amino)butan-2-ol (**11b**) (0.160 g, 0.54 mmol) with 3,3-diphenylpropanoic acid (0.121 g, 0.54 mmol) in the presence of DMAP (0.033 g, 0.27 mmol) and DCC (0.221 g, 1.12 mmol) in DCM (5 mL) was performed according to the **procedure D**. Purification: washing reaction mixture with water (3 × 10 mL), flash column chromatography (5% MeOH in DCM). Yield: 0.105 g (38.7%), TLC (DCM/MeOH, 9.5/0.5 *v/v*) R_f = 0.24, MW 506.69, formula: $C_{34}H_{38}N_2O_2$, MS *m/z* 507.6 ($M + H^+$), ^{1}H NMR (500 MHz, $CDCl_3$) δ ppm 6.91–7.50 (m, 20H), 5.70 (d, J = 8.59 Hz, 1H), 4.44 (t, J = 8.02 Hz, 1H), 4.02–4.15 (m, 1H), 3.17 (br. s, 1H), 2.73–2.87 (m, 3H), 2.65 (dd, J = 14.32, 5.16 Hz, 1H), 2.26 (dd, J = 12.60, 2.86 Hz, 1H), 2.14 (dd, J = 12.32, 4.30 Hz, 1H), 1.51 (s, 3H), 1.45 (s, 3H), 1.15–1.37 (m, 2H), ^{13}C NMR (126 MHz, $CDCl_3$) δ 171.5, 143.7, 143.5, 137.4, 129.5, 128.7, 128.6, 128.5, 127.8, 127.7, 127.0, 126.7, 126.7, 126.6, 126.0, 70.0, 56.6, 52.8, 47.5, 44.5, 43.5, 36.1, 29.0, 28.7.

4.1.5.22. N-((2S,3S)-4-(tert-butylamino)-3-hydroxy-1-phenylbutan-2-yl)-2,2-diphenylacetamide (49). The reaction of (2*S*,3*S*)-3-amino-1-(*tert*-butylamino)-4-phenylbutan-2-ol (**12b**) (0.150 g, 0.64 mmol) with 2,2-diphenylacetic acid (0.108 g, 0.51 mmol) in the presence of DMAP (0.039 g, 0.32 mmol), HOBt (0.112 g, 0.83 mmol) and EDC (0.159 g, 0.83 mmol) in DCM (8 mL) was performed according to the **procedure D**. Purification: washing reaction mixture with water (3 × 10 mL), flash column chromatography (5–10% MeOH in DCM), HPLC preparative system (20–90% water in acetonitrile). Yield: 0.061 g (22.4%), TLC (DCM/MeOH/$NH_{3(aq)}$, 9/1/0.1 *v/v/v*) R_f = 0.21, MW 430.59, formula: $C_{28}H_{34}N_2O_2$, MS *m/z* 431.3 ($M + H^+$), ^{1}H NMR (500 MHz, $CDCl_3$) δ ppm 7.18–7.25 (m, 9H), 7.13 (t, J = 6.87 Hz, 4H), 6.96 (br. s, 2H), 6.76 (br. s, 1H), 4.87 (s, 1H), 4.36–4.45 (m, 1H), 4.27 (d, J = 7.45 Hz, 1H), 2.79–3.00 (m, 3H), 2.73 (m, J = 10.31 Hz, 1H), 1.22 (s, 9H), NH, OH not detected; ^{13}C NMR (126 MHz, $CDCl_3$) δ ppm 173.1, 169.5, 139.3, 139.1, 137.6, 129.4, 129.0, 128.6, 128.6, 127.2, 127.0, 126.6, 69.0, 58.6, 56.9, 52.8, 45.1, 38.2, 25.7.

4.1.5.23. N-((2S,3S)-4-(tert-butylamino)-3-hydroxy-1-phenylbutan-2-yl)-3,3-diphenylpropanamide (50). The reaction of (2*S*,3*S*)-3-amino-1-(*tert*-butylamino)-4-phenylbutan-2-ol (**12b**) (0.150 g, 0.64 mmol) with 3,3-diphenylpropanoic acid (0.115 g, 0.51 mmol) in the presence of DMAP (0.039 g, 0.32 mmol), HOBt (0.112 g, 0.83 mmol) and EDC (0.159 g, 0.83 mmol) in DCM (8 mL) was performed according to the **procedure D**. Purification: washing reaction mixture with water (3 × 10 mL), flash column chromatography (5–10% MeOH in DCM), HPLC preparative system (20–90% water in acetonitrile). Yield: 0.041 g (14.6%), TLC (DCM/MeOH/$NH_{3(aq)}$, 9/1/0.1 *v/v/v*) R_f = 0.2, MW 444.62, formula: $C_{29}H_{36}N_2O_2$, MS *m/z* 445.7 ($M + H^+$), ^{1}H NMR (500 MHz, $CDCl_3$) δ ppm 8.43 (br. s, 1H), 7.12–7.30 (m, 14H), 7.04 (d, J = 9.17 Hz, 1H), 6.06 (br. s, 2H), 4.58 (dd, J = 8.88, 6.59 Hz, 1H), 4.17 (q, J = 8.02 Hz, 1H), 3.98 (d, J = 8.02 Hz, 1H), 3.00 (dd, J = 14.89, 9.16 Hz, 1H), 2.83 (dd, J = 14.89, 6.87 Hz, 1H), 2.73–2.80 (m, 2H), 2.58–2.69 (m, 2H), 1.18 (s, 9H); ^{13}C NMR (126 MHz, $CDCl_3$) δ ppm 171.8, 144.0, 143.6, 137.6, 129.2, 128.7, 128.6, 128.6, 127.9, 127.8, 126.7, 126.6, 126.5, 68.2, 56.5, 52.6, 46.9, 44.8, 42.4, 38.3, 25.8.

4.1.5.24. N-((2S,3R)-3-hydroxy-4-(neopentylamino)-1-phenylbutan-2-yl)-2,2-diphenylacetamide (51). The reaction of (2*R*,3*S*)-3-amino-1-(neopentylamino)-4-phenylbutan-2-ol (**13b**) (0.140 g, 0.56 mmol) with 2,2-diphenylacetic acid (0.119 g, 0.56 mmol) in the presence of DMAP (0.034 g, 0.28 mmol) and DCC (0.231 g, 1.12 mmol) in DCM (5 mL) was performed according to the **procedure D**. Purification: washing reaction mixture with water (3 × 30 mL), flash column chromatography (5% MeOH in DCM). Yield: 0.075 g (30.3%), TLC (DCM/MeOH 9.5/0.5 *v/v*) R_f = 0.18, MW 444.62, formula: $C_{29}H_{36}N_2O_2$, MS *m/z* 445.4 ($M + H^+$), ^{1}H NMR (500 MHz, $CDCl_3$) δ ppm 7.20–7.29 (m, 9H), 7.06 (dd, J = 7.45, 2.29 Hz, 2H), 7.03 (dd, J = 7.73, 1.43 Hz, 2H), 6.96–7.00 (m, 2H), 5.94 (d, J = 8.59 Hz, 1H), 4.81 (s, 1H), 4.24–4.31 (m, 1H), 3.54 (td, J = 6.59, 3.44 Hz, 1H), 3.67 (br. s, 2H), 3.06 (dd, J = 14.03, 4.30 Hz, 1H), 2.69–2.79 (m, 3H), 2.40 (d, J = 11.46 Hz, 1H), 2.34 (d, J = 11.46 Hz, 1H), 0.93 (s, 9H); ^{13}C NMR (126 MHz, $CDCl_3$) δ ppm 172.7, 139.1, 139.0, 137.6, 129.5, 129.0, 128.9, 128.8, 128.8, 128.7, 127.4, 127.3, 126.6, 70.4, 62.1, 59.2, 53.5, 52.6, 36.4, 31.5, 27.7.

4.1.5.25. N-((2S,3R)-3-hydroxy-4-(neopentylamino)-1-phenylbutan-2-yl)-3,3-diphenylpropanamide (52). The reaction of (2*R*,3*S*)-3-amino-1-(neopentylamino)-4-phenylbutan-2-ol (**13b**) (0.140 g, 0.56 mmol) with 3,3-diphenylpropanoic acid (0.127 g, 0.56 mmol) in the presence of DMAP (0.034 g, 0.28 mmol) and DCC (0.231 g, 1.12 mmol) in DCM (5 mL) was performed according to the **procedure D**. Purification: washing reaction mixture with water (3 × 30 mL), flash column chromatography (5–8% MeOH in DCM). Yield: 0.128 g (49.8%), TLC (DCM/MeOH, 9/1 *v/v*) R_f = 0.28, MW 458.65, formula: $C_{30}H_{38}N_2O_2$, MS *m/z* 459.6 ($M + H^+$), ^{1}H NMR (500 MHz, $CDCl_3$) δ ppm 7.16–7.30 (m, 13H), 7.11–7.14 (m, 2H), 6.02

(d, J = 8.02 Hz, 1H), 4.51 (dd, J = 9.16, 6.87 Hz, 1H), 4.07–4.16 (m, 1H), 3.33 (ddd, J = 7.73, 4.87, 3.44 Hz, 1H), 2.77–2.93 (m, 4H), 2.53 (dd, J = 12.60, 3.44 Hz, 1H), 2.28–2.35 (m, 2H), 2.14 (d, J = 12.03 Hz, 1H), 0.98 (s, 9H), NH, OH not detected; ^{13}C NMR (126 MHz, $CDCl_3$) δ ppm 171.7, 143.6, 143.5, 137.6, 129.5, 128.7, 128.7, 128.6, 128.0, 127.7, 126.7, 126.6, 126.6, 69.8, 61.9, 53.0, 52.1, 47.4, 43.0, 36.5, 31.4, 27.8.

4.1.5.26. N-((2S,3R)-3-hydroxy-1-phenyl-4-((2,2,2-trifluoroethyl) amino)butan-2-yl)-2,2-diphenylacetamide (53). The reaction of (2*R*,3*S*)-3-amino-4-phenyl-1-((2,2,2-trifluoroethyl)amino)butan-2-ol (**14b**) (0.200 g, 0.76 mmol) with 2,2-diphenylacetic acid (0.129 g, 0.61 mmol) in the presence of DMAP (0.047 mg, 0.38 mmol), HOBt (0.134 g, 1.00 mmol) and EDC (0.190 g, 1.00 mmol) in DCM (8 mL) was performed according to the **procedure D**. Purification: washing reaction mixture with water (3 × 10 mL), flash column chromatography (5% MeOH in DCM). Yield: 0.246 g (70.7%), TLC (DCM/MeOH, 9/1 *v/v*) R_f = 0.6, MW 456.51, formula: $C_{26}H_{27}F_3N_2O_2$, MS *m/z* 457.3 ($M + H^+$), ^{1}H NMR (500 MHz, $CDCl_3$) δ ppm 7.22–7.33 (m, 9H), 7.02–7.08 (m, 4H), 6.93–6.99 (m, 2H), 5.67 (d, J = 8.59 Hz, 1H), 4.84 (s, 1H), 4.18–4.27 (m, 1H), 3.46 (s, 2H), 3.08–3.19 (m, 2H), 3.04 (dd, J = 14.03, 4.30 Hz, 1H), 2.86 (dd, J = 12.32, 3.15 Hz, 1H), 2.65–2.75 (m, 2H), 1.62 (br. s, 1H); ^{13}C NMR (126 MHz, $CDCl_3$) δ ppm 172.9, 139.0, 138.8, 137.4, 129.3, 129.0, 128.9, 128.9, 128.8, 127.5, 127.3, 126.8, 125.7 (q, J = 280.80 Hz), 71.3, 59.3, 53.6, 51.2, 50.8 (q, J = 31.39 Hz), 36.6.

4.1.5.27. N-((2S,3R)-3-hydroxy-1-phenyl-4-((2,2,2-trifluoroethyl) amino)butan-2-yl)-3,3-diphenylpropanamide (54). The reaction of (2*R*,3*S*)-3-amino-4-phenyl-1-((2,2,2-trifluoroethyl)amino)butan-2-ol (**14b**) (0.200 g, 0.76 mmol) with 3,3-diphenylpropanoic acid (0.138 g, 0.61 mmol) in the presence of DMAP (0.047 mg, 0.38 mmol), HOBt (0.134 g, 1.00 mmol) and EDC (0.190 g, 1.00 mmol) in DCM (8 mL) was performed according to the **procedure D**. Purification: washing reaction mixture with water (3 × 10 mL), flash column chromatography (5% MeOH in DCM). Yield: 0.213 g (59.4%), TLC (DCM/MeOH, 9/1 *v/v*) R_f = 0.59, MW 470.54, formula: $C_{27}H_{29}F_3N_2O_2$, MS *m/z* 471.4 ($M + H^+$), ^{1}H NMR (500 MHz, $CDCl_3$) δ ppm 7.17–7.32 (m, 13H), 7.05–7.10 (m, 2H), 5.51 (d, J = 8.59 Hz, 1H), 4.50 (t, J = 7.73 Hz, 1H), 4.05 (dq, J = 8.59, 6.49 Hz, 1H), 3.22–3.28 (m, 1H), 3.12–3.16 (m, 1H), 2.99–3.12 (m, 2H), 2.77–2.83 (m, 3H), 2.47 (d, J = 4.58 Hz, 2H), 1.68 (br. s, 2H); ^{13}C NMR (126 MHz, $CDCl_3$) δ ppm 171.6, 143.5, 143.5, 137.2, 129.4, 128.7, 128.7, 128.7, 128.0, 127.6, 126.8, 126.7, 125.5 (q, J = 278.86 Hz), 70.6, 52.8, 50.9, 50.8 (q, J = 31.40 Hz), 47.5, 43.3, 36.3.

4.1.5.28. N-((2S,3R)-4-((cyclopropylmethyl)amino)-3-hydroxy-1-phenylbutan-2-yl)-2,2-diphenylacetamide (55). The reaction of (2*R*,3*S*)-3-amino-1-((cyclopropylmethyl)amino)-4-phenylbutan-2-ol (**15b**) (0.130 g, 0.56 mmol) with 2,2-diphenylacetic acid (0.119 g, 0.56 mmol) in the presence of DMAP (0.034 g, 0.28 mmol) and DCC (0.231 g, 1.12 mmol) in DCM (10 mL) was performed according to the **procedure D**. Purification: washing reaction mixture with water (3 × 10 mL), flash column chromatography (5% MeOH in DCM). Yield: 0.120 g (48.4%), TLC (DCM/MeOH/$NH_{3(aq)}$, 9.5/0.5/0.05 *v/v/v*) R_f = 0.24, MW 428.58, formula: $C_{28}H_{32}N_2O_2$, MS *m/z* 429.6 ($M + H^+$), ^{1}H NMR (500 MHz, $CDCl_3$) δ ppm 7.16–7.32 (m, 10H), 7.01–7.09 (m, 4H), 6.97 (dd, J = 6.87, 2.86 Hz, 1H), 6.02 (d, J = 8.59 Hz, 1H), 4.81 (s, 1H), 4.24 (td, J = 4.58, 2.29 Hz, 1H), 3.55 (td, J = 6.30, 3.44 Hz, 1H), 3.33 (br. s, 2H), 3.00–3.07 (m, 1H), 2.64–2.78 (m, 3H), 2.49 (dd, J = 12.32, 6.59 Hz, 1H), 2.33 (dd, J = 12.60, 7.45 Hz, 1H), 0.83–0.92 (m, 1H), 0.40–0.51 (m, 2H), 0.05–0.14 (m, 2H), ^{13}C NMR (126 MHz, $CDCl_3$) δ ppm 172.6, 149.5, 139.3, 137.9, 129.4, 129.1, 128.9, 128.8, 128.7, 128.6, 128.5, 127.3, 127.2, 126.5, 106.7, 70.9, 59.2, 54.7, 54.0, 51.3, 39.1, 36.5, 10.7, 3.7, 3.5.

4.1.5.29. N-((2S,3R)-4-((cyclopropylmethyl)amino)-3-hydroxy-1-phenylbutan-2-yl)-3,3-diphenylpropanamide (56). The reaction of (2*R*,3*S*)-3-amino-1-((cyclopropylmethyl)amino)-4-phenylbutan-2-ol (**15b**) (0.350 g, 1.50 mmol) with 3,3-diphenylpropanoic acid (0.338 g, 1.50 mmol) in the presence of DMAP (0.091 g, 0.75 mmol), HOBt (0.262 g, 1.94 mmol) and EDC (0.372 g, 1.94 mmol) in DCM (25 mL) was performed according to the **procedure D**. Purification: washing reaction mixture with water (3 × 30 mL), flash column chromatography (5–10% MeOH in DCM). Yield: 0.380 g (48.4%), TLC (DCM/MeOH/$NH_{3(aq)}$, 9.5/0.5/0.05 *v/v/v*) R_f = 0.28, MW 442.60, formula: $C_{29}H_{34}N_2O_2$, MS *m/z* 443.8 ($M + H^+$), ^{1}H NMR (500 MHz, $CDCl_3$) δ ppm 7.06–7.28 (m, 15H), 6.22 (d, J = 8.59 Hz, 1H), 4.71 (br. s, 1H), 4.48 (dd, J = 9.16, 7.45 Hz, 1H), 4.06 (qd, J = 8.02, 5.16 Hz, 1H), 3.41–3.46 (m, 1H), 2.99 (s, 1H), 2.74–2.92 (m, 4H), 2.61 (dd, J = 12.60, 3.44 Hz, 1H), 2.52 (dd, J = 12.32, 6.59 Hz, 1H), 2.33 (dd, J = 12.60, 5.73 Hz, 1H), 2.09 (dd, J = 12.60, 7.45 Hz, 1H), 0.85–0.99 (m, 1H), 0.41–0.56 (m, 2H), 0.04–0.22 (m, 2H), ^{13}C NMR (126 MHz, $CDCl_3$) δ ppm 173.5, 143.5, 143.2, 137.6, 129.4, 128.8, 128.7, 128.1, 127.6, 126.8, 126.7, 126.6, 69.5, 53.2, 53.0, 50.7, 47.1, 41.9, 36.3, 7.4, 4.5, 4.2.

4.2. Molecular modeling

All 3D structures of compounds were prepared with the appropriate stereoisomerism in CORINA Classic online tool [Molecular Networks GmbH, Germany and Altamira, LLC, USA]. Subsequently, atom types and protonation states were checked and Gasteiger-Marsili charges were assigned using Sybyl-X1.1 [Tripos, St. Louis, MO, USA]. Before docking, *h*BACE1 complex (PDB: 4D8C chain C) and *h*BuChE (PDB: 1P0I chain A) were prepared using PlayMolecule ProteinPrepare web service at pH 7.4 [93]. Molecular docking was performed with GOLD 5.3 [The Cambridge Crystallographic Data Center, Cambridge, UK] based on our previously developed docking algorithms [94,95]. Binding sites were defined as all amino acid residues within 10 Å from NVP-BXD552 (BXD) present in 4D8C complex or 20 Å from glycerol (GOL) present in 1P0I complex. We applied the automatic genetic algorithm settings for very flexible ligands. For each ligand, we received 10 conformations sorted by GoldScore. In the case of docking to 1P0I, chosen water molecules were kept, allowing the program to decide on their participation in ligand binding (toggle option) [95]. Further rescoring of selected ligand poses was carried out using the KDEEP and PRODIGY-LIGAND services [96,97]. The stability of the final complexes was tested by MD simulation using tools available on the PlayMolecule website [98]. Final results were visualized by PyMOL 0.99rc2 [DeLano Scientific LLC, Palo Alto, CA, USA].

4.3. Biological evaluation

All final compounds were tested for known classes of pan assay interference compounds (PAINS). According to SwissADME, none of them contain any structural fragments recognized as PAINS [99].

4.3.1. The in vitro inhibitory activity toward cholinesterases (*eeAChE, eqBuChE, hBuChE*)

The reagents used to perform the experiments and *ee*AChE and *eq*BuChE were purchased from Sigma–Aldrich (Steinheim, Germany); *h*BuChE isolated from human plasma was from Vivonics (Bedford, MA, USA). Ellman's spectrophotometric assay [85], with small modifications, was utilized for testing inhibitory activities of the synthesized compounds against the cholinesterases, according to the protocol described elsewhere [73]. Briefly, 5 U/mL aqueous stock solutions of the enzymes (*ee*AChE, *eq*BuChE, and *h*BuChE) were diluted before use to the final concentrations of 0.384 U/mL. Stock solutions of the tested compounds were prepared in DMSO

and diluted (in demineralized water) prior to use to the desired concentration. At first, the target compound or water or mixture of DMSO/water in appropriate ratio; i.e. blank samples (25 μL) was incubated in 0.1 M phosphate buffer (0.1 M, pH = 8.0, 200 μL) with DTNB (0.0025 M, 20 μL) and the enzyme (20 μL; *ee*AChE, *eq*BuChe or *h*BuChE). The experiments were performed at room temperature (25 °C) for *ee*AChE or *eq*BuChE and 36 °C for the *h*BuChE. Following the 5 min of pre-incubation step, the final reactions were started by adding ATC or BTC solutions (depending on the enzyme used). After the next 5 min, the changes in absorbance were measured at 412 nm, using a microplate reader (EnSpire Multimode; PerkinElmer, Waltham, MA, USA). All the target compounds were tested at the screening concentrations of 10 μM or 1 μM for inhibitory potencies toward animal cholinesterases or human enzyme, respectively. Based on equation 100-(S/B) × 100 (where S and B were the respective enzyme activities with and without the test sample, respectively) the percent of inhibition of each enzyme for each compound was calculated. Compounds with the enzyme inhibitory activities at 10 μM higher than 50% (*ee*AChE or *eq*BuChe), and at 1 μM higher than 80% (*h*BuChE) were further evaluated to obtain IC_{50} values. The IC_{50} values were determined based on the enzymes' inhibitory activities in the seven different concentrations of each compound, resulting in inhibition between 5% and 95%. Calculations were made using nonlinear regression (GraphPad Prism 5; GraphPad Software, San Diego, CA, USA) by plotting the residual enzyme activities against the applied inhibitor concentration. Tacrine and donepezil were used as the reference compounds. All the experiments were performed in triplicate.

4.3.2. The in vitro inhibitory activity toward human recombinant BACE1

BACE1 fluorescence resonance energy transfer (FRET) Assay Kit (Panvera, Madison, WI, USA) was purchased from Life Technologies (Warsaw, Poland) and used according to the protocol described in our previous paper [73]. The 384-well black microplates and a microplate reader (EnSpire Multimode; PerkinElmer, Waltham, MA, USA) were utilized to perform the experiments. The wavelength was optimized for the 553 nm excitation and 576 nm emission. The stock solutions of the target compounds were prepared in DMSO and diluted with assay buffer (50 mM sodium acetate; pH = 4.5) prior to use. The final reaction mixture was composed of BACE1 substrate (Rh-EVNLDAEFK-quencher, based on the Swedish mutant of APP, 10 μL), the tested compound or assay buffer; i.e. blank sample (10 μL) and the enzyme (purified baculovirus-expressed BACE1, 1 U/mL, 10 μL). The reaction mixture was incubated at 25 °C for 60 min, then the stop solution (2.5 M sodium acetate, 10 μL) was added to stop the reaction. The fluorescence signal was read at 576 nm. Based on the [1 − (S60 − S0)/(C60 − C0)] × 100 equation, the percent of BACE1 inhibition was calculated. S0 and S60 were fluorescence intensities of the tested sample (enzyme, substrate, target compound) at the beginning of the reaction and after 60 min respectively; C0 and C60 were analogical fluorescence intensities of the blank sample (enzyme, substrate, buffer). The compounds were screened at a concentration of 50 μM. For the most potent structures (at least 80% of enzyme inhibition) IC_{50} values were determined. The IC_{50} values of the reference and target compounds were determined, based on the BACE1 inhibition results for six diverse concentrations of each compound (resulting in 10%–95% of enzyme inhibition). Nonlinear regression (GraphPad Prism 5, GraphPad Software, San Diego, CA, USA) was used in calculations. The residual enzyme activities were plotted against the applied inhibitor concentration. BACE1 Inhibitor IV (Calbiochem, Merck, Nottingham, UK) was used as the reference compound. All the reactions were performed in triplicate.

4.3.3. Kinetics of eqBuChE inhibition for selected compounds

The most potent *eq*BuChe inhibitors were selected for the kinetic studies. The protocol described above was followed, based on Ellman's method [85]. An aqueous substrate BTC stock solution (0.02125 M) was diluted before use to give six final concentrations in the wells: 0.3, 0.24, 0.18, 0.12, 0.06, and 0.04 mM. Six different concentrations of each inhibitor were prepared, resulting in the percent of enzyme inhibition between 30% and 80%. For each concentration of the target compound, all six BTC solutions were used to perform the assays. V_{max} and K_m values of the Michaelis–Menten kinetics were calculated by nonlinear regression from substrate–velocity curves. Also, Lineweaver-Burk and Cornish-Bowden plots were obtained, both using linear regression in GraphPad Prism 5 (GraphPad Software, San Diego, CA, USA). Each experiment was performed in triplicate.

4.3.4. X-ray crystallography of hBuChE in complex with 51

4.3.4.1. Crystallization. Crystals of *h*BuChE were obtained using recombinant enzyme produced in Chinese ovary cells as described earlier [100] and purified with a BuChE specific affinity chromatography (Hupresin; CHEMFORASE, Rouen, France) followed by size exclusion chromatography (Superdex 200, GE Healthcare) [101]. Crystals were obtained using the hanging drop method at 293 K using a 12 mg/mL protein solution with crystallization buffer (0.1 M MES, pH = 6.5, 2.15 M $(NH_4)_2SO_4$)as crystallization buffer. Compound **51** was initially solubilized in methanol at 0.1 M concentration. Ligand/protein complex was obtained by soaking crystals with a 1 mM **51** solution in crystallization buffer (1% MeOH final concentration). Crystals were cryo-protected in a solution (1 mM **51**, 1% MeOH,0.1 M MES, pH = 6.5, 2.15 M $(NH_4)_2SO_4$, 20% Glycerol) before flash cooling into liquid nitrogen.

4.3.4.2. Structure determination. X-ray diffraction data were collected on the PROXIMA-2A beamline of the SOLEIL Synchrotron (Saint Aubin, France) at 100 K. Images recorded on an EIGER X 9 M (Dectris) detector were processed with XDS [102] using I/sigma>1 and CC1/2 as selection criteria. Data analysis was realized using the Phenix software suite [103]. An initial model was obtained by molecular replacement using Phaser-MR and the *h*BuChE structure (PDB entry 1P0I) devoid of any ligand, glycans or water molecules. Electron density was observed in the active site gorge and allowed unambiguous fitting of **51**. Ligand geometry restraints were processed with Phenix eLBOW [104] using the semi-empirical quantum mechanical method (AM1) and assuming the calculated charged position at pH 6.5 [105]. The model was refined by iterative cycles of model building using *Coot* [106] and refinement using Phenix. refine. *h*BuChE structure in complex with **51** was deposited into the Protein Data Bank under accession number 7AMZ.

4.3.5. Inhibitory properties toward GAT subtypes

The inhibitory activities of obtained compounds toward four subtypes of mGAT were determined at a screening concentration of 100 μM and in the case of sufficient potency characterized in full scale [^{3}H] GABA uptake assays according to a procedure described before [107]. The inhibition of hGAT3 for the most potent compounds was studied in full scale competition experiments as described [108]. MS binding assays for mGAT1 were performed as reported in Ref. [109]. The screening concentration for tested compounds was 100 μM.

4.3.6. Inhibition of Aβ aggregation

To evaluate antiaggregating properties against Aβ amyloid thioflavin-T (ThT) fluorometric assay was performed [91]. The inhibition of $A\beta_{1-42}$ aggregation was measured fluorimetrically as described previously [110]. Briefly, HFIP-pretreated $A\beta_{1-42}$ (Merck

Millipore, Darmstadt, Germany) at 1.5 μM, the test compound (10 μM final concentration) and Thioflavin-T (10 μM final concentration) were incubated at room temperature in 96-well microplate covered with aluminum foil with continuous shaking for 36–48 h. The fluorescence intensity (λ_{ex} = 440 nm; λ_{em} = 490 nm) was measured every 3 min (Synergy™ H4 plate reader, BioTek Instruments, Inc. VT, USA). The assay was run in quadruplicates. To exclude possible interference with the assay readout, absorbance spectra of the compounds were recorded at 10 μM compound concentration, and none of the compounds showed any significant absorbance (>0.05 AU) in the range 400–500 nm.

4.3.7. Inhibition of tau aggregation

Tau aggregation was monitored using ThT fluorometric assay. Tau protein (0N4R) (10 μM) and heparin (5 μM) with or without the tested compounds (10 μM) were dissolved in 30 μL 25 mM PBS (pH 6.8), which were incubated at 37 °C for 72 h. And then the samples were diluted to a final volume of 200 μL PBS (pH 6.8) containing 5 μM ThT. After binding to ThT for 5 min at rt in the dark, the fluorescence signal was measured (excitation wavelength at 440 nm and emission wavelength at 480 nm with a 5 nm slit width) on a monochromator based multimode microplate reader (Tecan Infnite M1000). The fluorescence intensities were recorded, and the percentage of inhibition on aggregation was calculated by the following expression: (1−IFi/IFc) × 100%, in which IFi and IFc were the fluorescence intensities obtained for absorbance in the presence and absence of compounds, respectively, after subtracting the background fluorescence of the ThT solution (5 μM). Methylene blue was used as a reference compound.

4.3.8. Toxicity – MTT assay

For the MTT (3-[4,5-dimethylthiazol-2-yl]-2,5 diphenyl tetrazolium bromide) colorimetric assay [111], HT22 cells, which was an immortalized cell line from hippocampus of mice, were cultured in 96-well plates at the concentration of 1 × 10^5/mL. Cells were cultured in DMEMs with 10% FBS and incubated at 37 °C, 5% CO_2 and then, were incubated with compounds (10 and 30 μM) for 24 h. Then, MTT (5 mg/mL, 10 μL) was added and cells were incubated for more 2 h at 37 °C. The water soluble MTT reagent was converted to an insoluble formazan product by viable cells. Next, the precipitated formazan was dissolved with DMSO= (100 μL). After shaking at room temperature for 10 min, the absorbance was measured through a multi-mode reader (Bio-Tek) at 570 nm. Results were expressed as the percentage of cell viability in comparison with nontreated cells which were considered controls (CT). The statistical significance was analyzed by GraphPad Prism 8 software using one-way ANOVA, followed by Bonferroni's Comparison Test.

4.3.9. In vitro ADME-tox properties

All performed assays and protocols used for determination of ADME-Tox parameters were described previously [112–114]. Statistical significances were analyzed by GraphPad Prism™ 8 software using One-way ANOVA and Bonferroni's Multiple Comparison Post Test. All references used during this study: carbonyl cyanide 3-chlorophenyl-hydrazone (CCCP), doxorubicin (DX), ketoconazole (KE), quinidine (QD) and verapamil (VER) were obtained from Sigma-Aldrich (St. Louis, MO, USA).

4.3.9.1. Hepatotoxicity assays. Hepatotoxicity was estimated using *hepatoma* HepG2 (ATCC® HB-8065™) cell line. The CellTiter 96® AQueous Non-Radioactive Cell Proliferation Assay (MTS) used for estimation of cells viability was purchased from Promega (Madison, WI, USA). The compounds were tested in quadruplicate at four concentrations (1, 10, 50 and 100 μM) and incubated with cells for 72 h. The antiproliferative drug DX in dose 1 μM and mitochondrial toxin CCCP (10 μM) were used as a positive controls.

4.3.9.2. Metabolic stability. The *in silico* prediction of most probable sites of metabolism was done by MetaSite 6.0.1 software (Molecular Discovery Ltd, Hertfordshire, UK). The metabolic pathways determination *in vitro* was performed by 120 min compounds incubation with human liver microsomes (HLMs) purchased from Sigma-Aldrich, St. Louis, MO, USA. The reactions were conducted in 10 mM Tris–HCl buffer (pH 7.4) at 37 °C in the presence of NADPH Regeneration System (Promega, Madison, WI, USA). UPLC/MS analyses were done by Waters ACQUITY TQD system with the TQ Detector (Waters, Milford, USA).

4.3.9.3. Influence on CYP activity. The potential drug-drug interactions were predicted using CYP3A4 and CYP2D6 assays purchased from Promega (Madison, WI, USA). The compounds were tested in triplicate in concentration 10 μM. The study was performed with use of the 1 μM concentration of respective reference CYP inhibitors: KE and QD.

Author contributions

The manuscript was written through contributions of all authors. All authors have given approval to the final version of the manuscript.

Declaration of competing interest

The authors declare that they have no known competing financial interests or personal relationships that could have appeared to influence the work reported in this paper.

Acknowledgments

This work was supported by the National Science Center of Poland (grant UMO-2016/21/B/NZ7/01744) and the European Cooperation in Science and Technology COST Action CA15135 and Slovenian Research Agency – ARRS (grants P1-0208 and L1-8157). Authors would like to thank the SOLEIL synchrotron for long term beamtime access 20181022 (IBS BAG). FC, JD and XB were funded by the French Ministry of Armed Forces (Direction Générale de l'Armement and Service de Santé des Armées, grant NBC-5-C-4210). J.K. acknowledges the support of the Czech Science Foundation (20–29633J).

Appendix A. Supplementary data

Supplementary data to this article can be found online at https://doi.org/10.1016/j.ejmech.2021.113397.

Abbreviations

AD	Alzheimer's disease
ATC	acetylthiocholine
BTC	butyrylthiocholine
DTNB	5,5′-Dithiobis-(2-nitrobenzoic acid)
GATs	GABA transporters
MTDL	multi-target-directed ligands
NFTs	neurofibrillary tangles
PAINS	pan-assay interference compounds

References

[1] F. Zemek, L. Drtinova, E. Nepovimova, V. Sepsova, J. Korabecny, J. Klimes, K. Kuca, Outcomes of Alzheimer's disease therapy with acetylcholinesterase

inhibitors and memantine, Expet Opin. Drug Saf. 13 (2014) 759–774, https://doi.org/10.1517/14740338.2014.914168.
[2] B. Reisberg, R. Doody, A. Stöffler, F. Schmitt, S. Ferris, H.J. Möbius, Memantine in moderate-to-severe alzheimer's disease, N. Engl. J. Med. 348 (2003) 1333–1341, https://doi.org/10.1056/nejmoa013128.
[3] S. Matsunaga, T. Kishi, N. Iwata, Combination therapy with cholinesterase inhibitors and memantine for alzheimer's disease: a systematic review and meta-analysis, Int. J. Neuropsychopharmacol. 18 (2015) 1–11, https://doi.org/10.1093/ijnp/pyu115.
[4] L.K. Huang, S.P. Chao, C.J. Hu, Clinical trials of new drugs for Alzheimer disease, J. Biomed. Sci. 27 (2020) 1–13, https://doi.org/10.1186/s12929-019-0609-7.
[5] A.E. Oxford, E.S. Stewart, T.T. Rohn, Clinical trials in alzheimer's disease: a hurdle in the path of remedy, Int. J. Alzheimer's Dis. 2020 (2020) 1–13, https://doi.org/10.1155/2020/5380346.
[6] S. Bullain, R. Doody, What works and what does not work in Alzheimer's disease? From interventions on risk factors to anti-amyloid trials, J. Neurochem. 155 (2020) 120–136, https://doi.org/10.1111/jnc.15023.
[7] 2020 Alzheimer's disease facts and figures, Alzheimers Dement. 16 (2020) 391–460, https://doi.org/10.1002/alz.12068.
[8] C. Patterson, World Alzheimer Report 2018 the state of the art of dementia research: new frontiers, Alzheimer's Dis. Int. (2018). https://www.alz.co.uk/research/WorldAlzheimerReport2018.pdf. (Accessed 3 November 2020).
[9] K.P. Kepp, Alzheimer's disease due to loss of function: a new synthesis of the available data, Prog. Neurobiol. 143 (2016) 36–60, https://doi.org/10.1016/j.pneurobio.2016.06.004.
[10] M. Goedert, M.G. Spillantini, A century of Alzheimer's disease, Science 314 (2006) 777–781, https://doi.org/10.1126/science.1132814.
[11] A. Sanabria-Castro, I. Alvarado-Echeverría, C. Monge-Bonilla, Molecular pathogenesis of alzheimer's disease: an update, Ann. Neurosci. 24 (2017) 46–54, https://doi.org/10.1159/000464422.
[12] M. Bolós, J.R. Perea, J. Avila, Alzheimer's disease as an inflammatory disease, Biomol. Concepts 8 (2017) 37–43, https://doi.org/10.1515/bmc-2016-0029.
[13] K.P. Kepp, Bioinorganic chemistry of alzheimer ' s disease, Chem. Rev. 112 (2012) 5193–5239, https://doi.org/10.1021/cr300009x.
[14] A. Contestabile, The history of the cholinergic hypothesis, Behav. Brain Res. 221 (2011) 334–340, https://doi.org/10.1016/j.bbr.2009.12.044.
[15] H. Hampel, M.M. Mesulam, A.C. Cuello, M.R. Farlow, E. Giacobini, G.T. Grossberg, A.S. Khachaturian, A. Vergallo, E. Cavedo, P.J. Snyder, Z.S. Khachaturian, The cholinergic system in the pathophysiology and treatment of Alzheimer's disease, Brain 141 (2018) 1917–1933, https://doi.org/10.1093/brain/awy132.
[16] S. Darvesh, D.A. Hopkins, C. Geula, Neurobiology of butyrylcholinesterase, Nat. Rev. Neurosci. 4 (2003) 131–138, https://doi.org/10.1038/nrn1035.
[17] N.H. Greig, T. Utsuki, Q.S. Yu, X. Zhu, H.W. Holloway, T. Perry, B. Lee, D.K. Ingram, D.K. Lahiri, A new therapeutic target in Alzheimer's disease treatment: attention to butyrylcholinesterase, Curr. Med. Res. Opin. 17 (2001) 159–165, https://doi.org/10.1185/03007990152673800.
[18] V. Andrisano, M. Naldi, A. De Simone, M. Bartolini, A patent review of butyrylcholinesterase inhibitors and reactivators 2010–2017, Expert Opin. Ther. Pat. 28 (2018) 455–465, https://doi.org/10.1080/13543776.2018.1476494.
[19] C.G. Lyketsos, M.C. Carrillo, J.M. Ryan, A.S. Khachaturian, P. Trzepacz, J. Amatniek, J. Cedarbaum, R. Brashear, D.S. Miller, Neuropsychiatric symptoms in Alzheimer's disease, Alzheimer's Dementia 7 (2011) 532–539, https://doi.org/10.1016/j.jalz.2011.05.2410.
[20] K.L. Lanctôt, J. Amatniek, S. Ancoli-Israel, S.E. Arnold, C. Ballard, J. Cohen-Mansfield, Z. Ismail, C. Lyketsos, D.S. Miller, E. Musiek, R.S. Osorio, P.B. Rosenberg, A. Satlin, D. Steffens, P. Tariot, L.J. Bain, M.C. Carrillo, J.A. Hendrix, H. Jurgens, B. Boot, Neuropsychiatric signs and symptoms of Alzheimer's disease: new treatment paradigms, Alzheimer's Dement. Transl. Res. Clin. Interv. 3 (2017) 440–449, https://doi.org/10.1016/j.trci.2017.07.001.
[21] J. Cerejeira, L. Lagarto, E.B. Mukaetova-Ladinska, Behavioral and psychological symptoms of dementia, Front. Neurol. (2012) 1–22, https://doi.org/10.3389/fneur.2012.00073. MAY.
[22] A. Lanari, F. Amenta, G. Silvestrelli, D. Tomassoni, L. Parnetti, Neurotransmitter deficits in behavioural and psychological symptoms of Alzheimer's disease, Mech. Ageing Dev. 127 (2006) 158–165, https://doi.org/10.1016/j.mad.2005.09.016.
[23] M. Garcia-Alloza, S.W. Tsang, F.J. Gil-Bea, P.T. Francis, M.K. Lai, B. Marcos, C.P. Chen, M.J. Ramirez, Involvement of the GABAergic system in depressive symptoms of Alzheimer's disease, Neurobiol. Aging 27 (2006) 1110–1117, https://doi.org/10.1016/j.neurobiolaging.2005.06.003.
[24] M.J. Ramirez, M.K.P. Lai, R.M. Tordera, P.T. Francis, Serotonergic therapies for cognitive symptoms in alzheimer's disease: rationale and current status, Drugs 74 (2014) 729–736, https://doi.org/10.1007/s40265-014-0217-5.
[25] M. Solas, E. Puerta, M. Ramirez, Treatment options in Alzheimer's disease: the GABA story, Curr. Pharmaceut. Des. 21 (2015) 4960–4971, https://doi.org/10.2174/1381612821666150914121149.
[26] Y. Li, H. Sun, Z. Chen, H. Xu, G. Bu, H. Zheng, Implications of GABAergic neurotransmission in Alzheimer's disease, Front. Aging Neurosci. 8 (2016) 1–12, https://doi.org/10.3389/fnagi.2016.00031.
[27] K. Govindpani, B.C.F. Guzmán, C. Vinnakota, H.J. Waldvogel, R.L. Faull, A. Kwakowsky, Towards a better understanding of GABAergic remodeling in alzheimer's disease, Int. J. Mol. Sci. 18 (2017) 1813, https://doi.org/10.3390/ijms18081813.
[28] D. Bi, L. Wen, Z. Wu, Y. Shen, GABAergic dysfunction in excitatory and inhibitory (E/I) imbalance drives the pathogenesis of Alzheimer's disease, Alzheimer's Dementia 16 (2020) 1312–1329, https://doi.org/10.1002/alz.12088.
[29] P. Kowalczyk, K. Kulig, GABA system as a target for new drugs, Curr. Med. Chem. 21 (2014) 3294–3309, https://doi.org/10.2174/09298673216661406012021 58.
[30] X. Gong, Y. Shao, B. Li, L. Chen, C. Wang, Y. Chen, γ-aminobutyric acid transporter-1 is involved in anxiety-like behaviors and cognitive function in knockout mice, Exp. Ther. Med. 10 (2015) 653–658, https://doi.org/10.3892/etm.2015.2577.
[31] K. Łątka, J. Jończyk, M. Bajda, γ-Aminobutyric acid transporters as relevant biological target: their function, structure, inhibitors and role in the therapy of different diseases, Int. J. Biol. Macromol. 158 (2020) 750–772, https://doi.org/10.1016/j.ijbiomac.2020.04.126.
[32] L.A. Borden, M.J. Caplan, GABA transporter heterogeneity: pharmacology and cellular localization, Neurochem. Int. 29 (1996) 335–356, https://doi.org/10.1016/0197-0186(95)00158-1.
[33] F. Conti, A. Minelli, M. Melone, GABA transporters in the mammalian cerebral cortex: localization, development and pathological implications, Brain Res. Rev. 45 (2004) 196–212, https://doi.org/10.1016/j.brainresrev.2004.03.003.
[34] T.S. Lee, L.P. Bjørnsen, C. Paz, J.H. Kim, S.S. Spencer, D.D. Spencer, T. Eid, N.C. Lanerolle, GAT1 and GAT3 expression are differently localized in the human epileptogenic hippocampus, Acta Neuropathol. 111 (2006) 351–363, https://doi.org/10.1007/s00401-005-0017-9.
[35] A.S. Kristensen, J. Andersen, T.N. Jorgensen, L. Sorensen, J. Eriksen, C.J. Loland, K. Stromgaard, U. Gether, SLC6 neurotransmitter transporters: structure, function, and regulation, Pharmacol. Rev. 63 (2011) 585–640, https://doi.org/10.1124/pr.108.000869.
[36] A. Minelli, N.C. Brecha, C. Karschin, S. DeBiasi, F. Conti, GAT-1, a high-affinity GABA plasma membrane transporter, is localized to neurons and astroglia in the cerebral cortex, J. Neurosci. 15 (1995) 7734–7746, https://doi.org/10.1523/jneurosci.15-11-07734.1995.
[37] A. Minelli, S. DeBiasi, N.C. Brecha, L.V. Zuccarello, F. Conti, GAT-3, a high-affinity GABA plasma membrane transporter, is localized to astrocytic processes, and it is not confined to the vicinity of GABAergic synapses in the cerebral cortex, J. Neurosci. 16 (1996) 6255–6264, https://doi.org/10.1523/jneurosci.16-19-06255.1996.
[38] A. Scimemi, Structure,function,and plasticity of GABA transporters, Front. Cell. Neurosci. 8 (2014), https://doi.org/10.3389/fncel.2014.00161.
[39] Z. Wu, Z. Guo, M. Gearing, G. Chen, Tonic inhibition in dentate gyrus impairs long-term potentiation and memory in an Alzhiemer' s disease model, Nat. Commun. 5 (2014), https://doi.org/10.1038/ncomms5159.
[40] T.E. Fuhrer, T.H. Palpagama, H.J. Waldvogel, B.J.L. Synek, C. Turner, R.L. Faull, A. Kwakowsky, Impaired expression of GABA transporters in the human Alzheimer's disease hippocampus, subiculum, entorhinal cortex and superior temporal gyrus, Neuroscience 351 (2017) 108–118, https://doi.org/10.1016/j.neuroscience.2017.03.041.
[41] V. Hernandez-Rabaza, A. Cabrera-Pastor, L. Taoro-Gonzalez, A. Gonzalez-Usano, A. Agusti, T. Balzano, M. Llansola, V. Felipo, Neuroinflammation increases GABAergic tone and impairs cognitive and motor function in hyperammonemia by increasing GAT-3 membrane expression. Reversal by sulforaphane by promoting M2 polarization of microglia, J. Neuroinflammation 13 (2016), https://doi.org/10.1186/s12974-016-0549-z.
[42] C. Thomsen, P.O. Sørensen, J. Egebjerg, 1-(3-(9H-Carbazol-9-yl)-1-propyl)-4-(2-methoxyphenyl)-4-piperidinol, a novel subtype selective inhibitor of the mouse type II GABA-transporter, Br. J. Pharmacol. 120 (1997) 983–985, https://doi.org/10.1038/sj.bjp.0700957.
[43] P. Kowalczyk, K. Sałat, G.C. Höfner, M. Mucha, A. Rapacz, A. Podkowa, B. Filipek, K.T. Wanner, K. Kulig, Synthesis, biological evaluation and structure-activity relationship of new GABA uptake inhibitors, derivatives of 4-aminobutanamides, Eur. J. Med. Chem. 83 (2014) 256–273, https://doi.org/10.1016/j.ejmech.2014.06.024.
[44] A. Kragler, G. Höfner, K.T. Wanner, Synthesis and biological evaluation of aminomethylphenol derivatives as inhibitors of the murine GABA transporters mGAT1-mGAT4, Eur. J. Med. Chem. 43 (2008) 2404–2411, https://doi.org/10.1016/j.ejmech.2008.01.005.
[45] J. Cummings, G. Lee, A. Ritter, M. Sabbagh, K. Zhong, Alzheimer's disease drug development pipeline: 2019, Alzheimer's Dement. Transl. Res. Clin. Interv. 5 (2019) 272–293, https://doi.org/10.1016/j.trci.2019.05.008.
[46] E.E. Congdon, E.M. Sigurdsson, Tau-targeting therapies for Alzheimer disease, Nat. Rev. Neurol. 14 (2018) 399–415, https://doi.org/10.1038/s41582-018-0013-z.
[47] A. Morsy, P.C. Trippier, Current and emerging pharmacological targets for the treatment of alzheimer's disease, J. Alzheim. Dis. 72 (2019) S145–S176, https://doi.org/10.3233/JAD-190744.
[48] D.J. Selkoe, Amyloid protein and Alzheimer's disease, Sci. Am. 265 (1991), https://doi.org/10.1038/scientificamerican1191-68.
[49] D. Hardy, J. Selokoe, The amyloid hypothesis of alzheimer 's disease, Amyloid 297 (2002) 353–357.
[50] H. Hampel, R. Vassar, B. De Strooper, J. Hardy, M. Willem, N. Singh, J. Zhou, R. Yan, E. Vanmechelen, A. De Vos, R. Nisticò, M. Corbo, B. Pietro Imbimbo,

J. Streffer, I. Voytyuk, M. Timmers, A.A. Tahami Monfared, M. Irizarry, B. Albala, A. Koyama, N. Watanabe, T. Kimura, L. Yarenis, S. Lista, L. Kramer, A. Vergallo, The β-secretase BACE1 in alzheimer's disease, Biol. Psychiatr. (2020) 1–12, https://doi.org/10.1016/j.biopsych.2020.02.001.

[51] J.R.M. Coimbra, D.F.F. Marques, S.J. Baptista, C.M.F. Pereira, P.I. Moreira, T.C.P. Dinis, A.E. Santos, J.A.R. Salvador, Highlights in BACE1 inhibitors for Alzheimer's disease treatment, Front. Chem. 6 (2018) 1–10, https://doi.org/10.3389/fchem.2018.00178.

[52] B. Das, R. Yan, A close look at BACE1 inhibitors for alzheimer's disease treatment, CNS Drugs 33 (2019) 251–263, https://doi.org/10.1007/s40263-019-00613-7.

[53] B.P. Imbimbo, M. Watling, Investigational BACE inhibitors for the treatment of Alzheimer's disease, Expet Opin. Invest. Drugs 28 (2019) 967–975, https://doi.org/10.1080/13543784.2019.1683160.

[54] M.E. Kennedy, A.W. Stamford, X. Chen, K. Cox, J.N. Cumming, M.F. Dockendorf, M. Egan, L. Ereshefsky, R.A. Hodgson, L.A. Hyde, S. Jhee, H.J. Kleijn, R. Kuvelkar, W. Li, B.A. Mattson, H. Mei, J. Palcza, J.D. Scott, M. Tanen, M.D. Troyer, J.L. Tseng, J.A. Stone, E.M. Parker, M.S. Forman, The BACE1 inhibitor verubecestat (MK-8931) reduces CNS b-Amyloid in animal models and in Alzheimer's disease patients, Sci. Transl. Med. 8 (2016) 1–14, https://doi.org/10.1126/scitranslmed.aad9704.

[55] D. Henley, N. Raghavan, R. Sperling, P. Aisen, R. Raman, G. Romano, Preliminary results of a trial of atabecestat in preclinical alzheimer's disease, N. Engl. J. Med. 380 (2019), https://doi.org/10.1056/NEJMc1813435.

[56] J. Cummings, G. Lee, A. Ritter, M. Sabbagh, K. Zhong, Alzheimer's disease drug development pipeline, Alzheimer's Dementia 6 (2020) (2020), e12050, https://doi.org/10.1002/trc2.12050.

[57] J.L. Cummings, G. Tong, C. Ballard, Treatment combinations for alzheimer's disease: current and future pharmacotherapy options, J. Alzheim. Dis. 67 (2019) 779–794, https://doi.org/10.3233/JAD-180766.

[58] R. Morphy, Z. Rankovic, Designing multiple ligands - medicinal chemistry strategies and challenges, Curr. Pharmaceut. Des. 15 (2009) 587–600, https://doi.org/10.2174/138161209787315594.

[59] M.L. Bolognesi, Polypharmacology in a single Drug : multitarget drugs, Curr. Med. Chem. 20 (2013) 1639–1645, https://doi.org/10.2174/0929867311320130004.

[60] R.R. Ramsay, M.R.P. Nikolic, K. Nikolic, E. Uliassi, M.L. Bolognesi, A perspective on multi - target drug discovery and design for complex diseases, Clin. Transl. Med. 7 (2018) 3, https://doi.org/10.1186/s40169-017-0181-2.

[61] F. Mesiti, D. Chavarria, A. Gaspar, S. Alcaro, F. Borges, The chemistry toolbox of multitarget-directed ligands for Alzheimer's disease, Eur. J. Med. Chem. 181 (2019) 111572, https://doi.org/10.1016/j.ejmech.2019.111572.

[62] K. Chalupova, J. Korabecny, M. Bartolini, B. Monti, D. Lamba, R. Caliandro, A. Pesaresi, X. Brazzolotto, A.J. Gastellier, F. Nachon, J. Pejchal, M. Jarosova, V. Hepnarova, D. Jun, M. Hrabinova, R. Dolezal, J. Zdarova Karasova, M. Mzik, Z. Kristofikova, J. Misik, L. Muckova, P. Jost, O. Soukup, M. Benkova, V. Setnicka, L. Habartova, M. Chvojkova, L. Kleteckova, K. Vales, E. Mezeiova, E. Uliassi, M. Valis, E. Nepovimova, M.L. Bolognesi, K. Kuca, Novel tacrine-tryptophan hybrids: multi-target directed ligands as potential treatment for Alzheimer's disease, Eur. J. Med. Chem. 168 (2019) 491–514, https://doi.org/10.1016/j.ejmech.2019.02.021.

[63] R. Malek, R.L. Arribas, A. Palomino-Antolin, P. Totoson, C. Demougeot, T. Kobrlova, O. Soukup, I. Iriepa, I. Moraleda, D. Diez-Iriepa, J. Godyń, D. Panek, B. Malawska, M. Głuch-Lutwin, B. Mordyl, A. Siwek, F. Chabchoub, J. Marco-Contelles, K. Kiec-Kononowicz, J. Egea, C. De Los Ríos, L. Ismaili, New dual small molecules for alzheimer's disease therapy combining histamine H3 receptor (H3R) antagonism and calcium channels blockade with additional cholinesterase inhibition, J. Med. Chem. 62 (2019) 11416–11422, https://doi.org/10.1021/acs.jmedchem.9b00937.

[64] M. Scheiner, D. Dolles, S. Gunesch, M. Hoffmann, M. Nabissi, O. Marinelli, M. Naldi, M. Bartolini, S. Petralla, E. Poeta, B. Monti, C. Falkeis, M. Vieth, H. Hübner, P. Gmeiner, R. Maitra, T. Maurice, M. Decker, Dual-acting cholinesterase-human cannabinoid receptor 2 ligands show pronounced neuroprotection in vitro and overadditive and disease-modifying neuroprotective effects in vivo, J. Med. Chem. 62 (2019) 9078–9102, https://doi.org/10.1021/acs.jmedchem.9b00623.

[65] C. Rochais, C. Lecoutey, F. Gaven, P. Giannoni, K. Hamidouche, D. Hedou, E. Dubost, D. Genest, S. Yahiaoui, T. Freret, V. Bouet, F. Dauphin, J.S. De Oliveira Santos, C. Ballandonne, S. Corvaisier, A. Malzert-Fréon, R. Legay, M. Boulouard, S. Claeysen, P. Dallemagne, Novel multitarget-directed ligands (MTDLs) with acetylcholinesterase (AChE) inhibitory and serotonergic subtype 4 receptor (5-HT4R) agonist activities as potential agents against alzheimer's disease: the design of donecopride, J. Med. Chem. 58 (2015) 3172–3187, https://doi.org/10.1021/acs.jmedchem.5b00115.

[66] F.J. Pérez-Areales, M. Garrido, E. Aso, M. Bartolini, A. De Simone, A. Espargaró, T. Ginex, R. Sabate, B. Pérez, V. Andrisano, D. Puigoriol-Illamola, M. Pallàs, F.J. Luque, M.I. Loza, J. Brea, I. Ferrer, F. Ciruela, A. Messeguer, D. Muñoz-Torrero, Centrally active multitarget anti-alzheimer agents derived from the antioxidant lead CR-6, J. Med. Chem. 63 (2020) 9360–9390, https://doi.org/10.1021/acs.jmedchem.0c00528.

[67] A. Gandini, M. Bartolini, D. Tedesco, L. Martinez-Gonzalez, C. Roca, N.E. Campillo, J. Zaldivar-Diez, C. Perez, G. Zuccheri, A. Miti, A. Feoli, S. Castellano, S. Petralla, B. Monti, M. Rossi, F. Moda, G. Legname, A. Martinez, M.L. Bolognesi, Tau-centric multitarget approach for alzheimer's disease: development of first-in-class dual glycogen synthase kinase 3β and tau-aggregation inhibitors, J. Med. Chem. 61 (2018) 7640–7656, https://doi.org/10.1021/acs.jmedchem.8b00610.

[68] T. Wichur, A. Więckowska, K. Więckowski, J. Godyń, J. Jończyk, Á.D.R. Valdivieso, D. Panek, A. Pasieka, R. Sabaté, D. Knez, S. Gobec, B. Malawska, 1-Benzylpyrrolidine-3-amine-based BuChE inhibitors with anti-aggregating, antioxidant and metal-chelating properties as multifunctional agents against Alzheimer's disease, Eur. J. Med. Chem. 187 (2020) 111916, https://doi.org/10.1016/j.ejmech.2019.111916.

[69] F.J. Pérez-Areales, O. Di Pietro, A. Espargaró, A. Vallverdú-Queralt, C. Galdeano, I.M. Ragusa, E. Viayna, C. Guillou, M.V. Clos, B. Pérez, R. Sabaté, R.M. Lamuela-Raventós, F.J. Luque, D. Muñoz-Torrero, Shogaol-huprine hybrids: dual antioxidant and anticholinesterase agents with β-amyloid and tau anti-aggregating properties, Bioorg. Med. Chem. 22 (2014) 5298–5307, https://doi.org/10.1016/j.bmc.2014.07.053.

[70] P. Lv, C.L. Xia, N. Wang, Z.Q. Liu, Z.S. Huang, S.L. Huang, Synthesis and evaluation of 1,2,3,4-tetrahydro-1-acridone analogues as potential dual inhibitors for amyloid-beta and tau aggregation, Bioorg. Med. Chem. 26 (2018) 4693–4705, https://doi.org/10.1016/j.bmc.2018.08.007.

[71] J. Zhou, X. Jiang, S. He, H. Jiang, F. Feng, W. Liu, W. Qu, H. Sun, Rational design of multitarget-directed ligands: strategies and emerging paradigms, J. Med. Chem. 62 (2019) 8881–8914, https://doi.org/10.1021/acs.jmedchem.9b00017.

[72] M.L. Bolognesi, Harnessing polypharmacology with medicinal chemistry, ACS Med. Chem. Lett. 10 (2019) 273–275, https://doi.org/10.1021/acsmedchemlett.9b00039.

[73] D. Panek, A. Więckowska, J. Jończyk, J. Godyń, M. Bajda, T. Wichur, A. Pasieka, D. Knez, A. Pišlar, J. Korabecny, O. Soukup, V. Sepsova, R. Sabaté, J. Kos, S. Gobec, B. Malawska, Design, synthesis, and biological evaluation of 1-Benzylamino-2-hydroxyalkyl derivatives as new potential disease-modifying multifunctional anti-alzheimer's agents, ACS Chem. Neurosci. 9 (2018) 1074–1094, https://doi.org/10.1021/acschemneuro.7b00461.

[74] S. Hog, J. Greenwood, K. Madsen, O. Larsson, B. Frolund, A. Schousboe, P. Krogsgaard-Larsen, R. Clausen, Structure-activity relationships of selective GABA uptake inhibitors, Curr. Top. Med. Chem. 6 (2006) 1861–1882, https://doi.org/10.2174/156802606778249801.

[75] R.P. Clausen, K. Madsen, O.M. Larsson, B. Frølund, P. Krogsgaard-Larsen, A. Schousboe, Structure-activity relationship and pharmacology of γ-aminobutyric acid (GABA) transport inhibitors, Adv. Pharmacol. 54 (2006) 265–284, https://doi.org/10.1016/S1054-3589(06)54011-6.

[76] T. Lutz, T. Wein, G. Höfner, K.T. Wanner, Development of highly potent GAT1 inhibitors: synthesis of nipecotic acid derivatives with N-arylalkynyl substituents, ChemMedChem 12 (2017) 362–371, https://doi.org/10.1002/cmdc.201600599.

[77] P. Zaręba, B. Gryzło, G. Mazur, B. Malawska, Development, Recent achievements and current directions of research into GABA uptake inhibitors, Curr. Med. Chem. 26 (2019), https://doi.org/10.2174/0929867325666191010120236.

[78] K. Łątka, J. Jończyk, M. Bajda, Structure modeling of γ-aminobutyric acid transporters – molecular basics of ligand selectivity, Int. J. Biol. Macromol. 158 (2020) 1380–1389, https://doi.org/10.1016/j.ijbiomac.2020.04.263.

[79] D. Eisenberg, E. Schwarz, M. Komaromy, R. Wall, Analysis of membrane and surface protein sequences with the hydrophobic moment plot, J. Mol. Biol. 179 (1984) 125–142, https://doi.org/10.1016/0022-2836(84)90309-7.

[80] I. Hussain, J. Hawkins, D. Harrison, C. Hille, G. Wayne, L. Cutler, T. Buck, D. Walter, E. Demont, C. Howes, A. Naylor, P. Jeffrey, M.I. Gonzalez, C. Dingwall, A. Michel, S. Redshaw, J.B. Davis, Oral administration of a potent and selective non-peptidic BACE-1 inhibitor decreases β-cleavage of amyloid precursor protein and amyloid-β production in vivo, J. Neurochem. 100 (2007) 802–809, https://doi.org/10.1111/j.1471-4159.2006.04260.x.

[81] A.K. Ghosh, N. Kumaragurubaran, L. Hong, S. Kulkarni, X. Xu, H.B. Miller, D. Srinivasa Reddy, V. Weerasena, R. Turner, W. Chang, G. Koelsch, J. Tang, Potent memapsin 2 (β-secretase) inhibitors: design, synthesis, protein-ligand X-ray structure, and in vivo evaluation, Bioorg. Med. Chem. Lett 18 (2008) 1031–1036, https://doi.org/10.1016/j.bmcl.2007.12.028.

[82] H. Rueeger, R. Lueoend, O. Rogel, J.M. Rondeau, H. Möbitz, R. MacHauer, L. Jacobson, M. Staufenbiel, S. Desrayaud, U. Neumann, Discovery of cyclic sulfone hydroxyethylamines as potent and selective β-site APP-cleaving enzyme 1 (BACE1) inhibitors: structure-based design and in vivo reduction of amyloid β-peptides, J. Med. Chem. 55 (2012) 3364–3386, https://doi.org/10.1021/jm300069y.

[83] Y. Xu, M.J. Li, H. Greenblatt, W. Chen, A. Paz, O. Dym, Y. Peleg, T. Chen, X. Shen, J. He, H. Jiang, I. Silman, J.L. Sussman, Flexibility of the flap in the active site of BACE1 as revealed by crystal structures and molecular dynamics simulations, Acta Crystallogr. Sect. D Biol. Crystallogr. 68 (2012) 13–25, https://doi.org/10.1107/S0907444911047251.

[84] G.C. Windridge, E.C. Jorgensen, 1-Hydroxybenzotriazole as a racemization-suppressing reagent for the incorporation of im-Benzyl-L-histidine into peptides, J. Am. Chem. Soc. 93 (1971) 6318–6319, https://doi.org/10.1021/ja00752a081.

[85] G.L. Ellman, K.D. Courtney, V. Andres, R.M. Featherstone, A new and rapid colorimetric determination of acetylcholinesterase activity, Biochem. Pharmacol. 7 (1961) 88–95, https://doi.org/10.1016/0006-2952(61)90145-9.

[86] A. Meden, D. Knez, N. Malikowska-Racia, X. Brazzolotto, F. Nachon, J. Svete, K. Sałat, U. Grošelj, S. Gobec, Structure-activity relationship study of

tryptophan-based butyrylcholinesterase inhibitors, Eur. J. Med. Chem. 208 (2020) 112766, https://doi.org/10.1016/j.ejmech.2020.112766.
[87] D. Knez, N. Coquelle, A. Pišlar, S. Žakelj, M. Jukič, M. Sova, J. Mravljak, F. Nachon, X. Brazzolotto, J. Kos, J.P. Colletier, S. Gobec, Multi-target-directed ligands for treating Alzheimer's disease: butyrylcholinesterase inhibitors displaying antioxidant and neuroprotective activities, Eur. J. Med. Chem. 156 (2018) 598–617, https://doi.org/10.1016/j.ejmech.2018.07.033.
[88] S.N. Dighe, G.S. Deora, E. De La Mora, F. Nachon, S. Chan, M.O. Parat, X. Brazzolotto, B.P. Ross, Discovery and structure-activity relationships of a highly selective butyrylcholinesterase inhibitor by Structure-based virtual screening, J. Med. Chem. 59 (2016) 7683–7689, https://doi.org/10.1021/acs.jmedchem.6b00356.
[89] S.J. Stachel, C.A. Coburn, T.G. Steele, K.G. Jones, E.F. Loutzenhiser, A.R. Gregro, H.A. Rajapakse, M.T. Lai, M.C. Crouthamel, M. Xu, K. Tugusheva, J.E. Lineberger, B.L. Pietrak, A.S. Espeseth, X.P. Shi, E. Chen-Dodson, M.K. Holloway, S. Munshi, A.J. Simon, L. Kuo, J.P. Vacca, Structure-based design of potent and selective cell-permeable inhibitors of human β-secretase (BACE-1), J. Med. Chem. 47 (2004) 6447–6450, https://doi.org/10.1021/jm049379g.
[90] J. Pabel, M. Faust, C. Prehn, B. Wörlein, L. Allmendinger, G. Höfner, K.T. Wanner, Development of an (S)-1-{2-[Tris(4-methoxyphenyl)methoxy] ethyl}piperidine-3-carboxylic acid [(S)-SNAP-5114] carba analogue inhibitor for murine γ-aminobutyric acid transporter Type4, ChemMedChem 7 (2012) 1245–1255, https://doi.org/10.1002/cmdc.201200126.
[91] H. Levine, Thioflavine T interaction with synthetic Alzheimer's disease β-amyloid peptides: detection of amyloid aggregation in solution, Protein Sci. 2 (1993) 404–410, https://doi.org/10.1002/pro.5560020312.
[92] R. Morphy, Z. Rankovic, The physicochemical challenges of designing multiple ligands, J. Med. Chem. 49 (2006) 4961–4970, https://doi.org/10.1021/jm0603015.
[93] G. Martínez-Rosell, T. Giorgino, G. De Fabritiis, PlayMolecule ProteinPrepare: a web application for protein preparation for molecular dynamics simulations, J. Chem. Inf. Model. 57 (2017) 1511–1516, https://doi.org/10.1021/acs.jcim.7b00190.
[94] M. Bajda, J. Jończyk, B. Malawska, S. Filipek, Application of computational methods for the design of BACE-1 inhibitors: validation of in Silico modelling, Int. J. Mol. Sci. 15 (2013) 5128–5139, https://doi.org/10.3390/ijms15035128.
[95] M. Bajda, A. Więckowska, M. Hebda, N. Guzior, C.A. Sotriffer, B. Malawska, Structure-based search for new inhibitors of cholinesterases, Int. J. Mol. Sci. 14 (2013) 5608–5632, https://doi.org/10.3390/ijms14035608.
[96] J. Jiménez, M. Škalič, G. Martínez-Rosell, G. De Fabritiis, KDEEP: protein-ligand absolute binding affinity prediction via 3D-convolutional neural Networks, J. Chem. Inf. Model. 58 (2018) 287–296, https://doi.org/10.1021/acs.jcim.7b00650.
[97] A. Vangone, J. Schaarschmidt, P. Koukos, C. Geng, N. Citro, M.E. Trellet, L.C. Xue, A.M.J.J. Bonvin, Large-scale prediction of binding affinity in protein-small ligand complexes: the PRODIGY-LIG web server, Bioinformatics 35 (2019) 1585–1587, https://doi.org/10.1093/bioinformatics/bty816.
[98] S. Doerr, M.J. Harvey, F. Noé, G. De Fabritiis, HTMD: high-throughput molecular dynamics for molecular discovery, J. Chem. Theor. Comput. 12 (2016) 1845–1852, https://doi.org/10.1021/acs.jctc.6b00049.
[99] A. Daina, O. Michielin, V. Zoete, SwissADME: a free web tool to evaluate pharmacokinetics, drug-likeness and medicinal chemistry friendliness of small molecules, Sci. Rep. 7 (2017) 42717, https://doi.org/10.1038/srep42717.
[100] F. Nachon, Y. Nicolet, N. Viguié, P. Masson, J.C. Fontecilla-Camps, O. Lockridge, Engineering of a monomeric and low-glycosylated form of human butyrylcholinesterase: expression, purification, characterization and crystallization, Eur. J. Biochem. 269 (2002) 630–637, https://doi.org/10.1046/j.0014-2956.2001.02692.x.
[101] X. Brazzolotto, M. Wandhammer, C. Ronco, M. Trovaslet, L. Jean, O. Lockridge, P.Y. Renard, F. Nachon, Human butyrylcholinesterase produced in insect cells: huprine-based affinity purification and crystal structure, FEBS J. 279 (2012) 2905–2916, https://doi.org/10.1111/j.1742-4658.2012.08672.x.
[102] W. Kabsch, XDS, Acta Crystallogr. Sect. D Biol. Crystallogr. 66 (2010) 125–132, https://doi.org/10.1107/S0907444909047337.
[103] P.D. Adams, P.V. Afonine, G. Bunkóczi, V.B. Chen, I.W. Davis, N. Echols, J.J. Headd, L.W. Hung, G.J. Kapral, R.W. Grosse-Kunstleve, A.J. McCoy, N.W. Moriarty, R. Oeffner, R.J. Read, D.C. Richardson, J.S. Richardson, T.C. Terwilliger, P.H. Zwart, PHENIX: a comprehensive Python-based system for macromolecular structure solution, Acta Crystallogr. Sect. D Biol. Crystallogr. 66 (2010) 213–221, https://doi.org/10.1107/S0907444909052925.
[104] N.W. Moriarty, R.W. Grosse-Kunstleve, P.D. Adams, Electronic ligand builder and optimization workbench (eLBOW): a tool for ligand coordinate and restraint generation, Acta Crystallogr. Sect. D Biol. Crystallogr. 65 (2009) 1074–1080, https://doi.org/10.1107/S0907444909029436.
[105] MarvinSketch (Version 6.2.2), ChemAxon Ltd., 2014.
[106] P. Emsley, B. Lohkamp, W.G. Scott, K. Cowtan, Features and development of Coot, Acta Crystallogr. Sect. D Biol. Crystallogr. 66 (2010) 486–501, https://doi.org/10.1107/S0907444910007493.
[107] A. Kragler, G. Höfner, K.T. Wanner, Novel parent structures for inhibitors of the murine GABA transporters mGAT3 and mGAT4, Eur. J. Pharmacol. 519 (2005) 43–47, https://doi.org/10.1016/j.ejphar.2005.06.053.
[108] S. Schmitt, G. Höfner, K.T. Wanner, Application of MS transport assays to the four human γ-aminobutyric acid transporters, ChemMedChem 10 (2015) 1498–1510, https://doi.org/10.1002/cmdc.201500254.
[109] C. Zepperitz, G. Höfner, K.T. Wanner, MS-binding assays: kinetic, saturation, and competitive experiments based on quantitation of bound marker as exemplified by the GABA transporter mGAT1, ChemMedChem 1 (2006) 208–217, https://doi.org/10.1002/cmdc.200500038.
[110] M. Hebda, M. Bajda, A. Wieckowska, N. Szałłaj, A. Pasieka, D. Panek, J. Godyń, T. Wichur, D. Knez, S. Gobec, B. Malawska, Synthesis, molecular modelling and biological evaluation of novel heterodimeric, multiple ligands targeting cholinesterases and amyloid Beta, Molecules 21 (2016) 410, https://doi.org/10.3390/molecules21040410.
[111] M.V. Berridge, A.S. Tan, Characterization of the cellular reduction of 3-(4,5-dimethylthiazol-2- yl)-2,5-diphenyltetrazolium bromide (MTT): subcellular localization, substrate dependence, and involvement of mitochondrial electron transport in MTT reduction, Arch. Biochem. Biophys. 303 (1993) 474–482, https://doi.org/10.1006/abbi.1993.1311.
[112] G. Latacz, A. Lubelska, M. Jastrzębska-Więsek, A. Partyka, M.A. Marć, G. Satała, D. Wilczyńska, M. Kotańska, M. Więcek, K. Kamińska, A. Wesołowska, K. Kieć-Kononowicz, J. Handzlik, The 1,3,5-triazine derivatives as innovative chemical family of 5-HT6 serotonin receptor agents with therapeutic perspectives for cognitive impairment, Int. J. Mol. Sci. 20 (2019) 1–21, https://doi.org/10.3390/ijms20143420.
[113] A. Lubelska, G. Latacz, M. Jastrzębska-Więsek, M. Kotańska, R. Kurczab, A. Partyka, M.A. Mańc, D. Wilczyńska, A. Doroz-Płonka, D. Łazewska, A. Wesołowska, K. Kieć-Kononowicz, J. Handzlik, Are the hydantoin-1,3,5-triazine 5-HT6R ligands a hope to a find new procognitive and anti-obesity drug? Considerations based on primary in vivo assays and ADME-tox profile in vitro, Molecules 24 (2019) 4472, https://doi.org/10.3390/molecules24244472.
[114] G. Latacz, A.S. Hogendorf, A. Hogendorf, A. Lubelska, J.M. Wierońska, M. Woźniak, P. Cieślik, K. Kieć-Kononowicz, J. Handzlik, A.J. Bojarski, Search for a 5-CT alternative. In vitro and in vivo evaluation of novel pharmacological tools: 3-(1-alkyl-1H-imidazole-5-yl)-1H-indole-5-carboxamides, low-basicity 5-HT7 receptor agonists, Medchemcomm 9 (2018) 1882–1890, https://doi.org/10.1039/c8md00313k.